

---

# SCUOLA DI SCIENZE

Dipartimento di Chimica Industriale “Toso Montanari”

Corso di Laurea Magistrale in

## Chimica Industriale

Curriculum: Advanced Spectroscopy in Chemistry

Classe LM-71 - Scienze e Tecnologie per la Chimica Industriale

### **PM and material decay: Analysis of dry depositions on horizontal and vertical surrogate surfaces through a Deposition Box system.**

CANDIDATE

**Laura Guenoden**

SUPERVISOR

**Prof.ssa Elena BERNARDI**

CO-SUPERVISORS

**Prof. Ivano VASSURA**

**Dr.ssa Simona RAFFO**

EXTERNAL REVIEWER

**Prof. Wiesław Łasocha**

---

**Academic Year 2016/2017**

---

## **ABSTRACT:**

Airborne Particulate Matter (PM), can get removed from the atmosphere through wet and dry mechanisms, and physically/chemically interact with materials and induce premature decay. The effect of dry depositions is a complex issue, especially for outdoor materials, because of the difficulties to collect atmospheric deposits repeatable in terms of mass and homogeneously distributed on the entire investigated substrate. In this work, to overcome these problems by eliminating the variability induced by outdoor removal mechanisms (e.g. winds and rainfalls), a new sampling system called 'Deposition Box', was used for PM sampling. Four surrogate materials (Cellulose Acetate, Regenerated Cellulose, Cellulose Nitrate and Aluminum) with different surfaces features were exposed in the urban-marine site of Rimini (Italy), in vertical and horizontal orientations. Homogeneous and reproducible PM deposits were obtained and different analytical techniques (IC, AAS, TOC, VP-SEM-EDX, Vis-Spectrophotometry) were employed to characterize their mass, dimension and composition. Results allowed to discriminate the mechanisms responsible of the dry deposition of atmospheric particles on surfaces with different nature and orientation and to determine which chemical species, and in which amount, tend to preferentially deposit on them.

This work demonstrated that "Deposition Box" can represent an affordable tool to study dry deposition fluxes on materials and results obtained will be fundamental in order to extend this kind of exposure to actual building and heritage materials, to investigate the PM contribution in their decay.

## TABLE OF CONTENT

1. INTRODUCTION & AIM OF THE WORK	1
1.1. Atmosphere and its role in outdoor material decay	1
1.2. Key concepts in Particulate Matter	3
1.3. Studies of interaction between particles and materials	6
1.4. Aim of the work	7
2. EXPERIMENTAL	9
2.1. Exposure Device: the “Deposition Box”	9
2.2. Preliminary exposure	12
2.3. Exposure campaign	14
2.3.1. Selection and preparation of substrates to expose	15
2.3.2. Exposure of the substrates	20
2.4. Analyses of the exposed substrates	23
2.4.1. Samples treatment	23
2.4.2. Ion Chromatography (IC)	26
2.4.3. Atomic Absorption Spectroscopy (AAS)	30
2.4.4. Total Organic Carbon (TOC)	35
2.4.5 Variable-Pressure Scanning Electron Microscopy and Energy Dispersive X-ray Spectroscopy (VP-SEM-EDX)	38
2.4.6. Colour measurements	42

<b>3. RESULTS &amp; DISCUSSION</b>	<b>46</b>
<b>3.1. Preliminary exposure</b>	<b>46</b>
3.1.1. PM deposition	46
3.1.2. Ion Chromatography (IC)	48
3.1.3. Metal Analysis by Atomic Absorption Spectroscopy (AAS)	51
3.1.4. General remarks	53
<b>3.2. The main campaign</b>	<b>55</b>
3.2.1. Visual observations	55
3.2.2. Colour measurements	58
3.2.3. PM deposition	64
3.2.4. Deposition rates	67
3.2.5. SEM-EDX analysis	69
3.2.6. Treatment of SEM images by Image J	77
3.2.7. Ionic composition of the PM soluble-fraction	82
3.2.8. Metals analysis	89
3.2.9. TOC results	94
<b>4. CONCLUSION</b>	<b>95</b>
<b>5. BIBLIOGRAPHY</b>	<b>98</b>
<b>APPENDICES</b>	<b>104</b>
Appendix A: Atmospheric data	104
Appendix B: Weight % of identified elements in SEM-EDX analysis	107
Appendix C: Relative amounts of considered ions for analysed substrates during the main campaign	108

# 1. INTRODUCTION AND AIM OF THE WORK

## 1.1. Atmosphere and its role in outdoor material decay.

Since the beginning of life, Humans feel the need to leave traces, either by painting the walls of caves like in the famous Cave of Lascaux, by creating sculptures as the ones originating from the Ancient Greek art or by building impressive monuments. The common examples of human creations that easily come to mind are the majestic Pyramids of Gizeh in Egypt. They are fascinating because they have been built thousands of years ago and are still here to be observed nowadays. However, those pyramids share a common point with each human creation such as any sculpture, tool, electronic device or ornamental object. All of them are submitted to the atmospheric corrosion and get soiling and degrading over time.

Atmospheric corrosion is defined as the interaction between a material and its surrounding atmosphere. Any object is submitted to this phenomenon: metallic surfaces, calcareous stones, glasses, polymers or surfaces covered by paints. The atmosphere is divided into four different layers, characterized by variations in temperature and pressure with altitude. A portion of the troposphere, the lowest layer, is called the boundary layer and is directly influenced by the Earth's surface. This boundary layer is an important player in pollutant dispersion and chemistry [1].

Decay is an inevitable process even in an uncontaminated atmosphere as all environmental factors influence the decay mechanisms of materials and all of them have to be considered.

The environment decay factors involved in the atmospheric corrosion can be classified based on their interactions with the surfaces exposed to the atmosphere [2]:

- the physical factors action is due to pure mechanical mechanisms, like thermal shock, wind erosion, dissolution and crystallization of salts,
- the chemical factors produce damages through chemical and/or physical-chemical mechanisms. This is the case for acids pollutants, oxidants, chelating agents or solubilizers,
- microorganisms (bacteria, archaea and fungi), but also lichens and insect pests are also involved in the damages caused to objects of cultural heritage, because of their biodeteriorative potential.

The decay phenomena observed on the exposed artefacts results in the combination of these different types of factors, making their understanding harder. In general, the first stage of atmospheric corrosion consists of the formation of layers on the surface because of its interaction with the atmosphere, which causes damage to the original material [3, 4].

Among all the possible factors, wind, rainfall, variation of temperature and humidity and pollutants play a crucial role to establish the main mechanisms in action and the rate of the decay of most of the exposed surfaces.

The atmosphere and its composition differs according to the localisation and the environment. Indeed, an urban environment where lots of cars or engines needed fuel to operate are used tend to contain more particles originating from anthropogenic sources than a rural environment with few machines. Four different environments are distinguished [4]: rural, marine, urban and industrial, which present different characteristic compositions. The chemical species identified as atmospheric gases or as constituents of atmospheric particles may then be present in different quantities according to the type of environment and not all the chemical species have the same effects on all the materials.

Nowadays one of pollutants object of more scientific and public attention due to its sanitary effects is Particulate Matter (PM), that can play also an important role in the soiling and decay of materials. The degradation effect of particles and of the substances they vehiculate can be dependent on the characteristics of the surface the particle is deposited on. As an example, nickel is more sensitive to the influence of sulfur compounds present in the atmosphere than aluminum [5]. The atmospheric particles size, their concentration [6] and the positioning of the surface submitted to the atmosphere can be determinant in the rate of soiling and these aspects were studied in previous works [7, 8, 9]. However, it is important to deepen the study of PM deposition processes and effects with respect to outdoor materials to have a good understanding of their involvement in corrosion.

## 1.2. Key concepts in Particulate Matter.

The study of atmospheric corrosion is a recent science as it is less than a century old. W. H. J. Vernon in the beginning of the 1920's started the systematic experiments in atmospheric corrosion [4]. More precisely, atmospheric chemistry has been recognised as a specific field since the 1970's and has undergone rapid development. Pollutant contained and diffused in the atmosphere are important data to analyse, because they have major impact in various fields like climate change, air and health quality, and materials corrosion.

Among them is airborne particulate matter (PM), a complex mixture gathering organic and inorganic substances of different origins and chemical compositions. The particles have irregular shapes but for convenience their aerodynamic behaviour is often described by assimilating them to idealised spheres, according to the aerodynamic diameter.

The sources of emission of particles can be classified in different ways. First of all, particles can be emitted directly, from a primary source or indirectly, by undergoing transformation processes from gases. Also, sources can be classified as natural sources and anthropogenic sources, which are presented in Figure 1.1. We observe that sea spray, with breaking ocean waves, and mineral dust, produced by the windblown surface soil and influenced by emissions of gases, are the main natural sources. In contrary, the principal anthropogenic sources of particles correspond to biomass burning, vehicles traffic, construction activity and industrial processes. These particles have more local impacts, when on a global scale the natural sources of directly emitted particles are more important. Usually PM is divided into two main groups based on their aerodynamic diameter (calculated by assuming particle as a sphere with unit density and the same settling velocity as the real particle): (i) the coarse fraction in which are the larger particles, with size ranging from 2.5 to 10  $\mu\text{m}$  ( $\text{PM}_{2.5}$  -  $\text{PM}_{10}$ ). Those particles mainly contain earth crust materials and primary dust from roads and industries; (ii) the fine fraction corresponding to the smaller particles with size up to 2.5  $\mu\text{m}$ , mainly containing the secondarily formed aerosols, combustion particles and recondensed organic and metal vapours. The particles smaller than 0.1  $\mu\text{m}$  are called ultrafine particles. Most of the total airborne PM mass is usually made up of fine particles ranging from 0.1 to 2.5  $\mu\text{m}$  and secondarily of particles bigger than 2.5  $\mu\text{m}$  [10].

Different chemical fractions of PM have been identified and are associated with specific fractions of PM. First of all, there is the water-soluble inorganic fraction, containing water-soluble compounds like nitrates, sulphates, chlorides and ammonium salts. Chlorides are known to be mainly found in coarse particles [11], when nitrates are mainly present in the fine fraction of PM [4, 12]. Studies shown that PM precise composition may vary according to the seasons. For example, the work done by Perrone et al. [13] shows that the PM concentrations in Milan were higher during winter than during summer, being



influenced by seasonal meteorology: pollutants are more dispersed thanks to the higher wind speed. The water-soluble fraction also present oxalates [14], and some organic compounds [15]. The organic fraction of PM contains several kinds of compounds, as aliphatic hydrocarbons, polycyclic aromatic hydrocarbons, diterpenoids, fatty acids or phthalates which were identified in damaged layers [16]. Finally, carbonaceous particles are another relevant constituent of PM. They are often associated with transition and heavy metals like Fe, Mn, Zn, Cu, Cr, Pb, or Ni [17].

PM and other pollutants can be removed from the atmosphere and get transferred to the surface of buildings or artefacts through the wet and dry deposition processes. On the one hand, wet depositions take place during rainy events, i.e. rain, snow or fog, and encompass processes by which airborne pollutants are transferred in an aqueous form: the rain-out (pollutant is included in the droplets developing within a cloud) and wash-out (take-up of pollution by precipitation as it falls from the cloud) processes. On the other hand, dry deposition occurs without any precipitation and denotes the direct transfer of gas and particulates [16]. Aerosol dry deposition on surfaces results from the combination of several processes such as Brownian diffusion, impaction and interception due to the turbulent motions, gravitational sedimentation, thermophoresis, diffusiophoresis, electrostatic attraction, etc. [6, 18].

Figure 1.1. Natural sources (a) and anthropogenic sources (b) for atmospheric particles [4].

(a) Global Natural Emissions of Aerosols (A) and Aerosol Precursors (P) in the year 2000 (Tg year <sup>-1</sup> ).		
	Minimum	Maximum
Sea spray (A)	1400	6800
Mineral dust (A)	1000	4000
Terrestrial primary biological aerosol (A)	50	1000
Dimethylsulfide (P)	10	40
Biogenic volatile organic compounds (P)	20	380
Monoterpenes (P)	30	120
Isoprene (P)	410	600
(b) Global Anthropogenic emissions of Aerosols (A) and Aerosol Precursors (P) in the Year 2000 (Tg year <sup>-1</sup> or TgS year <sup>-1</sup> for SO <sub>2</sub> ).		
	Minimum	Maximum
Biomass burning aerosols (A)	29.0	85.3
Soot (A)	3.6	6.0
Marine primary organic aerosols (A)	6.3	15.3
Nonmethane volatile organic compounds (P)	98.2	157.9
SO <sub>2</sub> (P)	43.3	77.9
NH <sub>3</sub> (P)	34.5	49.6

### 1.3. Studies of interaction between particles and materials.

Two different approaches may be employed to study the interactions between atmospheric particles and materials. The empirical method consists in the direct analysis of monuments and decayed layers, which allow the evaluation of the complexity of the decay phenomena. The modellistic approach permits to develop and establish mathematic relationships between some environmental

parameters and the effects in terms of material decay. Moreover, scientists can focus their work by performing field studies [19, 20], where materials are directly exposed to the atmosphere, or laboratory studies [21, 22], where materials are selected and submitted to precise protocol in order to simulate one or few factors involved in premature weathering and understanding their mechanisms. Of course, field and laboratory studies can be performed in a same work [2, 23]. In both cases, either real artefacts can be exposed, or surrogate materials, which can simulate precise characteristics of objects submitted to the atmospheric degradation. Working with substrates allows to focus on precise aspects of surfaces and to better understand which feature is involved in the decay process.

#### 1.4. Aim of the work.

This master thesis work is part of a project that aims to better understand the role of particulate matter in building and heritage materials decay. The specific objective was to analyse PM depositions occurring on surrogate materials exposed outdoor with different orientation.

In order to perform field studies by isolating the dry deposition process and eliminating the variability induced by removal mechanisms, such as rain and wind, a new sampling system called Deposition Box was used. Four surrogate materials with different porosities and surface features were exposed in the urban-marine site of Rimini (Italy). Two different conditions of exposure were investigated by analysing samples exposed both in horizontal and in vertical positions.

Colour measurements were performed on surrogate materials before and after the exposure to evaluate the surface soiling due to PM deposition. Morphological and dimensional characterizations of the deposited particles were

performed by SEM-EDX analyses. Beside the mass, the water-soluble fraction of PM was also characterized by Ion Chromatography (IC) and the PM metal content was analysed by Atomic Absorption Spectroscopy (AAS).

## 2. EXPERIMENTAL

The main processes by which particulate matter (PM) can be removed from the atmosphere and get deposited on monuments are the wet and dry deposition processes. Atmospheric particles and pollutants play a role and can have an impact on the corrosion and the decay of indoor and outdoor-exposed materials. As described in the introduction, the atmospheric corrosion is the result of the interaction between a material and its surrounding atmospheric environment.

In this work we decided to focus on the dry deposition mechanisms and effects, as they are less studied and understood than the wet deposition ones. To do so, we used an exposure system recently developed by the group of Prof. Bolzacchini (UniMIB) [2] for studying ambient dry depositions and their effects on heritage materials. The device, named “Deposition Box”, permits to collect ambient PM, originating only from dry deposition, on any kind of substrate and with low construction and operating costs.

### 2.1 Exposure Device: the “Deposition Box”

The “Deposition Box” (“DepBox”) is made by a 50 x 50 x 20 cm box covered by a pitched roof. The overall dimension of the DepBox, including the roof, is 70 x 70 x 55 cm. In Figure 2.1 is presented a general scheme of the device. A steel exposure grid is placed inside the box for positioning the samples. A fan is housed at the bottom of the box in order to ensure a continuous air flux and to standardize the air exchange ratio through the exposure floor. The air flow is schematized by the blue arrows in Figure 2.1.

The fan (Figure 2.2) is a Sunon DR MagLev DC fan 17 x 17 x 8 mm, maximum current 160 mA, supply voltage 5 V dc and 20 000 rpm with air flow of 1.5 m<sup>3</sup>h<sup>-1</sup>. The fan is connected to a power adapter to provide current at 220 V. With the given fan specifications the calculated air exchange ratio is 7 min<sup>-1</sup>. The distance between the exposure grid and the bottom of the box is 150 mm. The DepBox rests on 4 pins of 20 mm in height which ensure the correct operation space for the fan discharge.

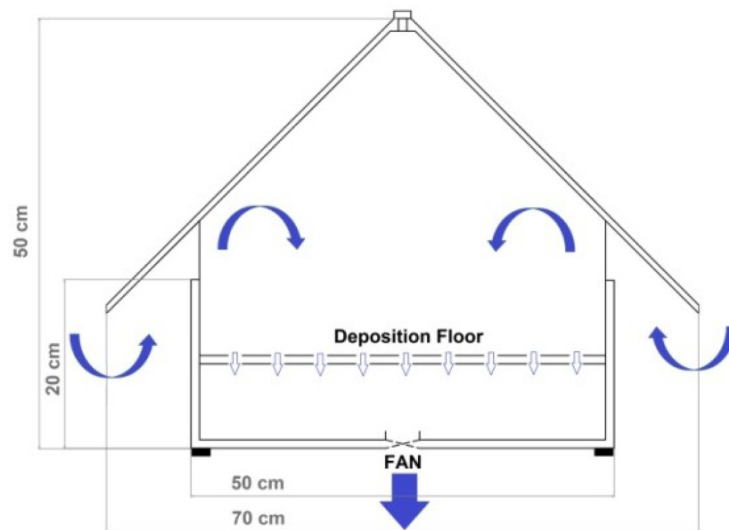


Figure 2.1. Scheme of the DepBox device.



Figure 2.2. Picture of the fan placed at the bottom of the box.

The external structure of the DepBox is made of white polypropylene (PP) and is shown in Figure 2.3. This polymer was chosen as it is supposed to be inert at environmental conditions. The white color is useful to avoid overheating within the structure in conditions of high temperature or high solar radiation. The roof is secured by a threaded fastener and can be easily removed to inspect and substitute the specimens housed on the exposure floor. Materials like stone, metal or polymeric specimens can be housed directly on the exposure grid. Filters or materials used as surrogate surfaces can be inserted in special filter holders as described in the section 2.3.1 ' Selection and preparation of substrates to expose'.



*Figure 2.3. Picture of the external feature of the DepBox.*

## 2.2 Preliminary exposure

A preliminary exposure has been performed in order to obtain information to properly plan the actual campaign of exposure. Specifically, the aim of the preliminary test was to verify (i) the capability of our exposure device not only to isolate the dry depositions, but also to discriminate between depositions on horizontal and vertical surfaces, (ii) the reproducibility among substrates exposed in a box and between two boxes and finally (iii) to determine the better operating conditions and time of exposure to collect a suitable amount of deposit.

Three different materials were exposed for 36 days, during December 2016 and January 2017 in two DepBoxes (see section 2.1) placed on the roof of the laboratory (around 5 meters high) close to the city center of Rimini (Italy) and at about 2,7 km from the sea (see Figure 2.4), to be submitted to the same atmospheric conditions.

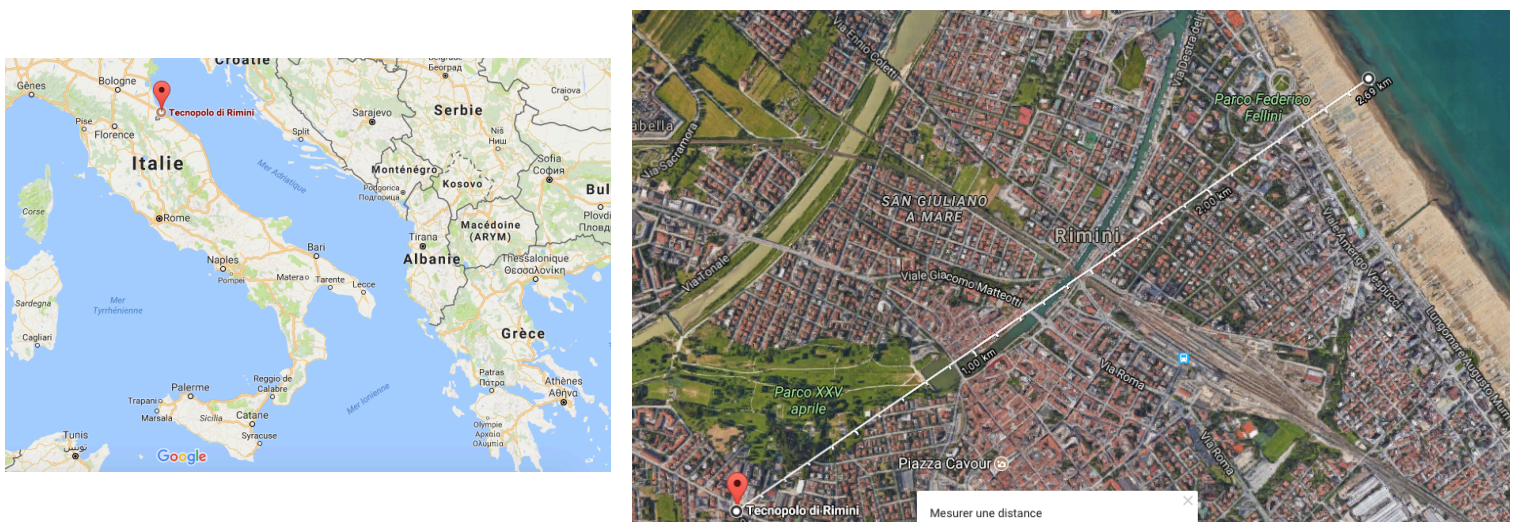


Figure 2.4. The exposure site in the city of Rimini, in the North of Italy.



Two types of cellulose nitrate membrane filters from different brands (Albet - 0.2 m and Whatman - 0.45 m) and some glass slides (20 x 20 mm) were placed in the boxes following the schemes reported in Figure 2.5. Membrane filters were placed in filter holders (section 2.3.1), while glass slide were exposed without any support.

Before and after the exposure the substrates were conditioned and weighted. After the exposure main anions, cations and metals contained in the collected deposits were analysed by following the procedures described in detail in section 2.4 'Analyses of the exposed substrates'.

The general conclusions drawn after preliminary test (which results are detailed in the results section 3.1, 'Preliminary exposure'), were that the Deposition Boxes have been confirmed to be efficient tools to avoid the wet deposition process and focus on the dry deposition process. About a month seems to be the minimum time of exposure to collect deposit suitable to be analysed. The reproducibility inter and intra DepBoxes is good and allows us to increase the number of different substrates for the actual campaign of exposure. Furthermore the devices seems to be able to differentiate the deposition processes on horizontally and vertically oriented substrates. Horizontal substrates seem to keep more and bigger particles (the so-called coarse fraction), while the vertical ones tend to collect less particles of smaller size (the fine fraction). This is suggested also by the analyses of macro ions and metals, as on the horizontal and vertical substrates are mainly present species characteristic of coarse and fine fractions respectively [24, 25, 26, 27]. However, it is important to remember that composition of PM can significantly vary depending on sources of pollution and the sites where

sampling was performed. Given these results, the actual exposure campaign was planned.

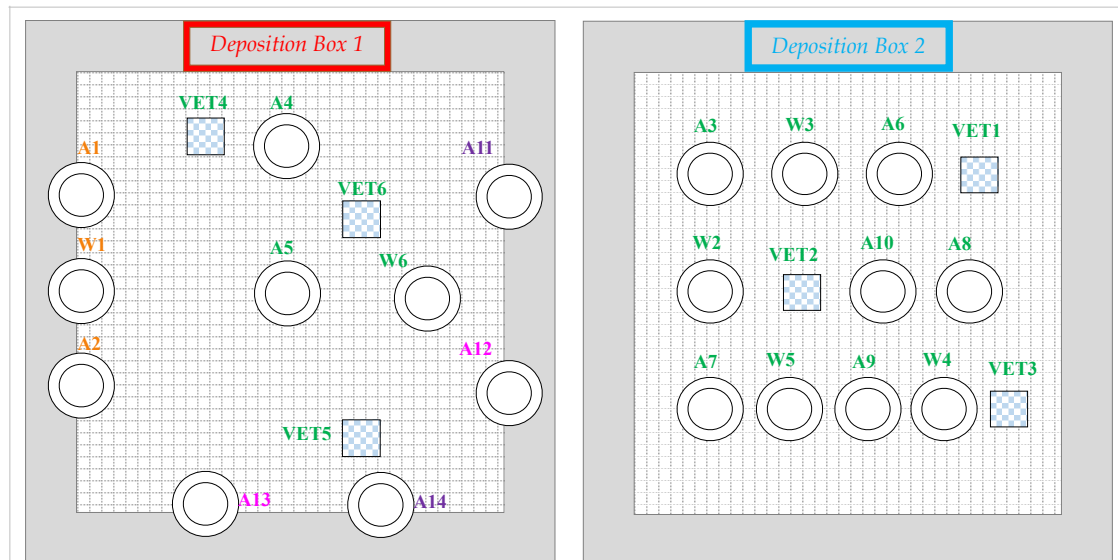


Figure 2.5a. Disposition of materials in the DepBox 1 during the preliminary test.

Figure 2.5b. Disposition of materials in the DepBox 2 during the preliminary test.

VET = glass pieces;  
A = Albet filter, cellulose nitrate, 0.20  $\mu$  porosity;  
W = Whatman filter, cellulose nitrate, 0.45  $\mu$  porosity.

green = material directly on the grid;  
orange = material on vertical position, suspended by nylon threads;  
pink = material on horizontal position, suspended, face up;  
violet = material on horizontal position, suspended, face down.

### 2.3 Exposure campaign

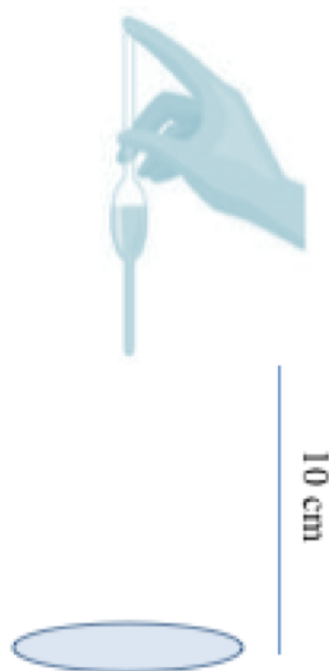
After having obtained the necessary operational information through the preliminary tests, we started to plan the exposure campaign. The first thing to evaluate was the materials to expose.

### 2.3.1 Selection and preparation of substrates to expose

It was decided to expose different surrogated substrates showing different properties that can characterize also materials found in cultural heritage such as metallic or porous materials.

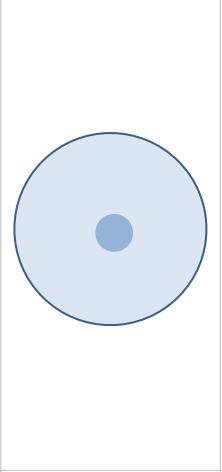
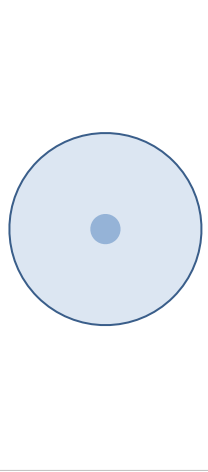
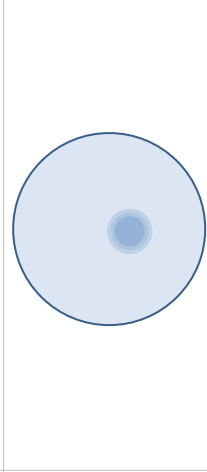
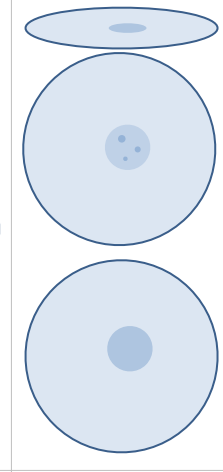
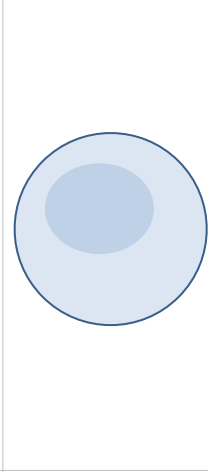
Hydrophilicity/hydrophobicity being one interesting property, some tests have been realised in order to choose between the available filters.

A Pasteur pipette was used to drop a single droplet of MilliQ ( $R > 18.2 \text{ M}\cdot\text{cm}$ ) water on different membrane filters available with different composition and porosity. The drop was released at 10 cm from the surface, as presented in Figure 2.6, and we waited for 1 minute before measuring the size of the wet surface area. Table 2.1 resumes the observations and figures obtained.



*Figure 2.6. Operating conditions for the hydrophilicity tests.*

Table 2.1. Results of the hydrophilicity test.

					
<b>Material</b>	MCE (Mixed Cellulose Ester) - SKC	Cellulose nitrate - Albet	Cellulose nitrate - Whatman	Cellulose acetate - Sartorius	Regenerated cellulose - Schleicher
<b>Porosity (µm)</b>	0.8	0.2	0.45	0.45	0.45
<b>Observations</b>	Water absorbed. Wet area Ø 2 cm.	Water absorbed. Wet area Ø 1.2 cm.	Water absorbed. Total wet area Ø 1.8 cm.	Water not absorbed at the beginning. Then total wet area Ø 1.8 cm.	Water quickly absorbed and spread. Wet area Ø 3.2 cm.

Considering the results of the hydrophilicity/hydrophobicity test and the filters at our disposal, we decided to expose 5 different types of substrates:

- two cellulose nitrate filters with different porosities: 0.2 µm and 0.45 µm,
- cellulose acetate filters with porosity 0.45 µm,
- regenerated cellulose filters with porosity 0.45 µm,
- aluminum foils, conductive and not porous,

in order to compare substrate with: metallic/not metallic nature, same composition and different porosities, same porosity and different compositions, and same porosity and different hydrophilicities.

We exposed in total 40 samples (8 per substrate), divided between the two DepBoxes we have.

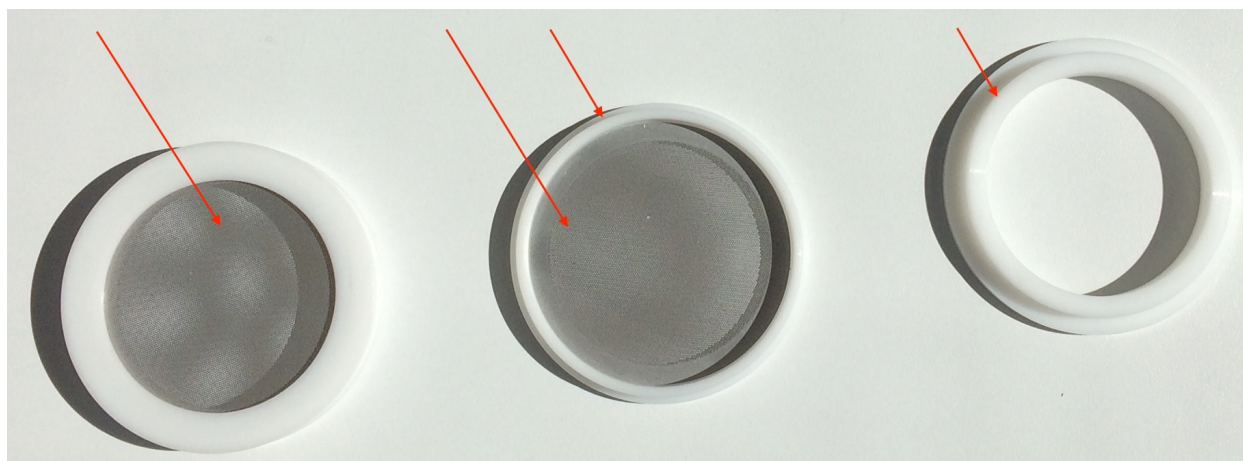
The samples were labelled (with a code representing their composition and a progressive number) and prepared for the exposure. Membrane filters were placed in a desiccator for 24 hours before any treatment. This allows to condition the substrates and stabilize their weight, as the humidity is controlled. Then each filter was weighted at least 3 times, using an analytical KERN 770 balance which a sensitivity of 0.1 mg. The substrates were stored inside the desiccator and placed into special sample holders just before the beginning of the exposure. Filter holders made of PTFE and usually used for PM sampling were used as sample holders; their structure is shown in Figure 2.7.

The filter is placed inside with deposition face up.

Grid on which is placed the filter.

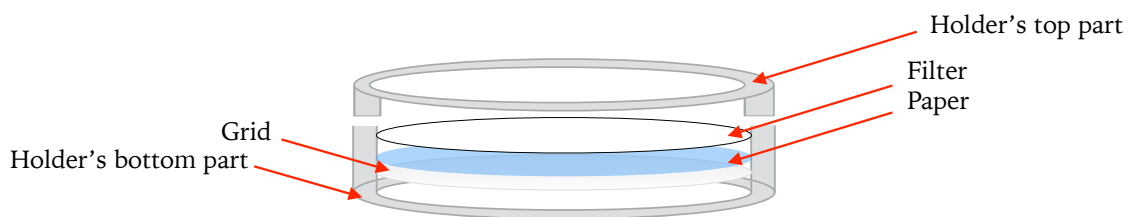
Upper part of the filter holder.

Bottom part of the filter holder.



*Figure 2.7. PTFE filter holder (on the left) and its single parts.*

A special paper, used by the producing companies to protect the filters from any contamination, was placed between the grid and the filter (Figure 2.8) in order to have only one face on which the deposition of PM can occur.

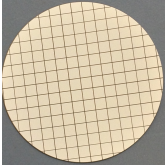
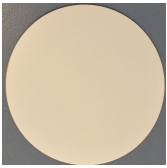
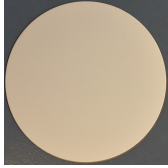
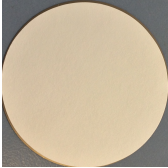
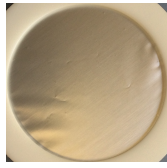


*Figure 2.8. Scheme of a filter inside the filter holder.*

For aluminum foils, a specific procedure was followed. Before the exposure, aluminum foils have been washed with MilliQ and acetone, and dried into an oven. The foils, protected on the back with the special paper, have then been placed inside the sample holders (Fig. 2.7-2.8) and their weights were determined using the analytical KERN 770 balance after being conditioned 24 hours in a desiccator. Obtaining a plane and not crumpled surface was the harder part, but once inserted in the sample holders the foils cannot be deformed. This is why we determined their weights making the difference between the filled sample holder and the empty sample holder (holder, grid and paper).

In Table 2.2 pictures and resume characteristics of each material are shown.

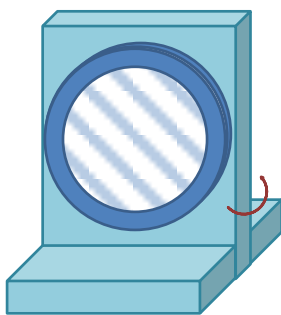
Table 2.2. Filters & their characteristics.

Picture					
Material	Cellulose nitrate - Albet	Cellulose nitrate - Whatman	Cellulose acetate - Sartorius	Regenerated cellulose - Schleicher	Aluminum
Label	CNA	CNW	CA	RC	A
Porosity ( $\mu\text{m}$ )	0.2	0.45	0.45	0.45	/
Hydrophilicity	++	++	+	++++	++/-
Features	low porosity, hydrophilic	high porosity, hydrophilic	high porosity, low hydrophilic	high porosity, very hydrophilic, less smooth surface	can simulate metal behaviour
Exposed Area, $A_T$ ( $\text{cm}^2$ )	11.95	11.95	11.95	11.95	11.95
Number of exposed samples	8	8	8	8	8

### 2.3.2 Exposure of the substrates

The exposure of the chosen substrates started at the beginning of April (April the 10<sup>th</sup>) and last for 63 days. The substrates were exposed to the marine-urban atmosphere of Rimini, at the same exposure site as the one used for the preliminary tests and described in section 2.2 ‘Preliminary Exposure’. Having verified the reproducibility between the DepBoxes through the preliminary tests, we used the two DepBoxes at our disposal in order to expose the maximum number of sample possible per type of substrate and to obtain statistically relevant information. As previously explained, we decided to expose 5 different substrates, presenting different features. For each substrate a total of 8 samples were exposed: 4 in horizontal position, by directly placing the sample holder on the deposition grid, and 4 in vertical position. Each vertical sample was disposed back-to-back to another one as presented in Figure 2.9.

Each DepBox contained 10 horizontal and 10 vertical filter holders, so a total of 40 samples were exposed.



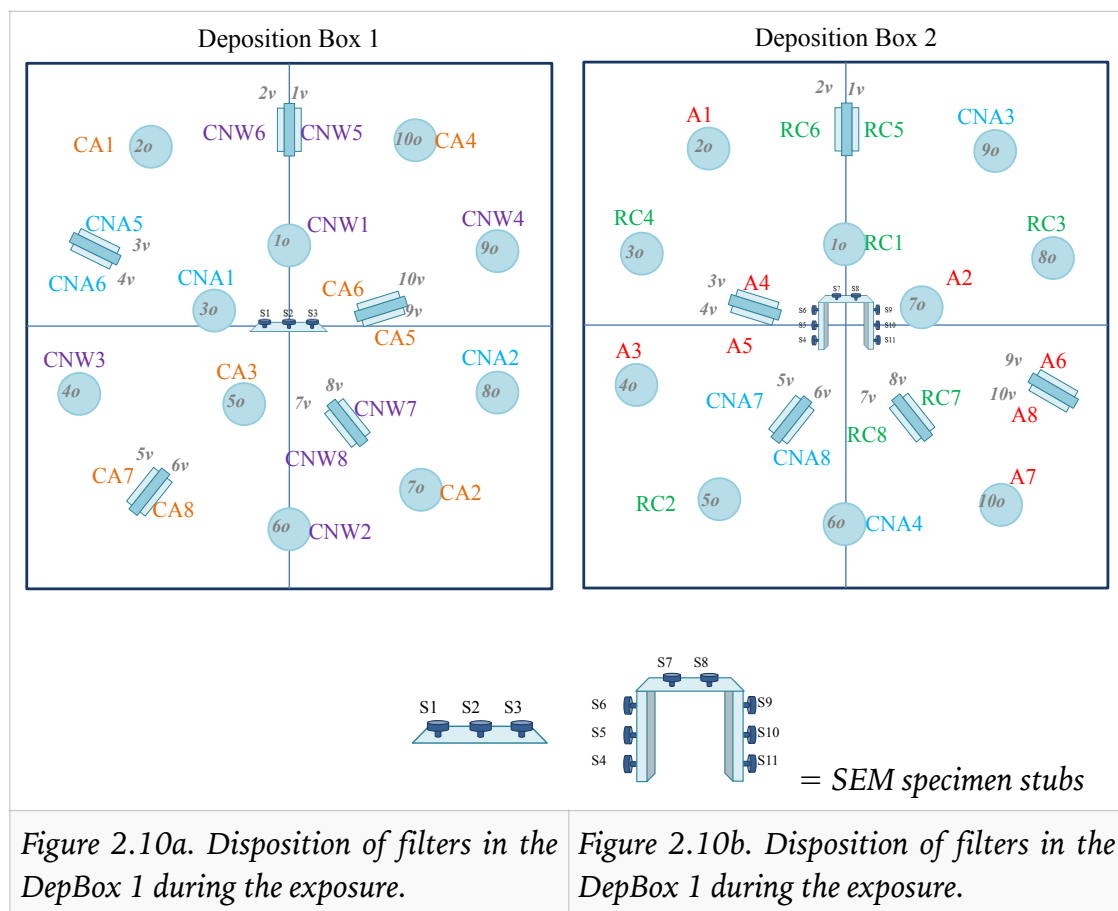
*Figure 2.9. Disposition of sample holders in vertical position (scheme & picture).*



Table 2.3. Position and label of exposed samples.

Substrate	Label	DepBox	Orientation	Substrate	Label	Depbox	Orientation
Cellulose Acetate (Sartorius) 0.45 $\mu\text{m}$	CA 1o	1	horizontal	Regenerated Cellulose (Schleicher) 0.45 $\mu\text{m}$	RC 1o	2	horizontal
	CA 2o	1	horizontal		RC 2o	2	horizontal
	CA 3o	1	horizontal		RC 3o	2	horizontal
	CA 4o	1	horizontal		RC 4o	2	horizontal
	CA 5v	1	vertical		RC 5v	2	vertical
	CA 6v	1	vertical		RC 6v	2	vertical
	CA 7v	1	vertical		RC 7v	2	vertical
	CA 8v	1	vertical		RC 8v	2	vertical
Cellulose Nitrate (Whatman) 0.45 $\mu\text{m}$	CNW 1o	1	horizontal	Cellulose Nitrate (Albet) 0.2 $\mu\text{m}$	CNA 1o	1	horizontal
	CNW 2o	1	horizontal		CNA 2o	1	horizontal
	CNW 3o	1	horizontal		CNA 3o	2	horizontal
	CNW 4o	1	horizontal		CNA 4o	2	horizontal
	CNW 5v	1	vertical		CNA 5v	1	vertical
	CNW 6v	1	vertical		CNA 6v	1	vertical
	CNW 7v	1	vertical		CNA 7v	2	vertical
	CNW 8v	1	vertical		CNA 8v	2	vertical
Aluminum	A1o	2	horizontal				
	A2o	2	horizontal				
	A3o	2	horizontal				
	A4v	2	vertical				
	A5v	2	vertical				
	A6v	2	vertical				
	A7o	2	horizontal				
	A8v	2	vertical				

The Cellulose Nitrate - Albet (CNA) filters were divided between the two DepBoxes to confirm the reproducibility of the boxes already verified during the preliminary test (see section 4.1 Preliminary exposure). Inside a same DepBox, the position of samples was precisely chosen in order to avoid interferences among them and to maximise the observations and comparisons to make. As presented in Figure 2.10, the samples are disposed on two ‘circles’, the inner one and the outer one, and samples belonging to the same type of substrate were spread in different areas of the DepBox so as to cover all possible conditions and to make the sampling more representative.



In addition to filters and Al foils, we also exposed some stubs covered with carbon adhesive discs, to directly collect particles on a substrate suitable for performing Scanning Electron Microscopy (SEM). These stubs were 11 in total

and placed in the center of the DepBoxes: 3 were disposed horizontally in the first DepBox and 8 were disposed both horizontally and vertically in the second DepBox (Figure 2.10).

## 2.4 Analyses of the exposed substrates

Different analytical techniques were employed in order to study particles that deposited during the exposure campaign, with the final aim to better understand how the dry deposition process can affect the decay of materials.

### 2.4.1 Samples treatment

After removing the samples (i.e. the exposed substrates) from the DepBoxes, all of them were placed into a desiccator for an entire day in order to condition them before a new weighting session. The 40 samples were weighed 3 times using the analytical balance and the corresponding amount of deposited PM was determined.

Samples were then divided in groups according to the different analyses to perform.

For a same kind of substrate, the samples were divided as follow (Figure 2.11):

- 3 horizontal and 3 vertical samples (so a total of 6 samples) were used to perform the main ion analysis by Ion Chromatography (IC) and the metal determination by Atomic Absorption Spectroscopy (AAS),
- 1 horizontal sample and 1 vertical sample (so a total of 2 samples) were selected to perform in sequence: Colour measurements, Scanning Electron Microscopy (SEM) and Total Organic Carbon (TOC) analyses.

- Blank (i.e. not exposed) substrates were also analysed through all the above mentioned techniques.

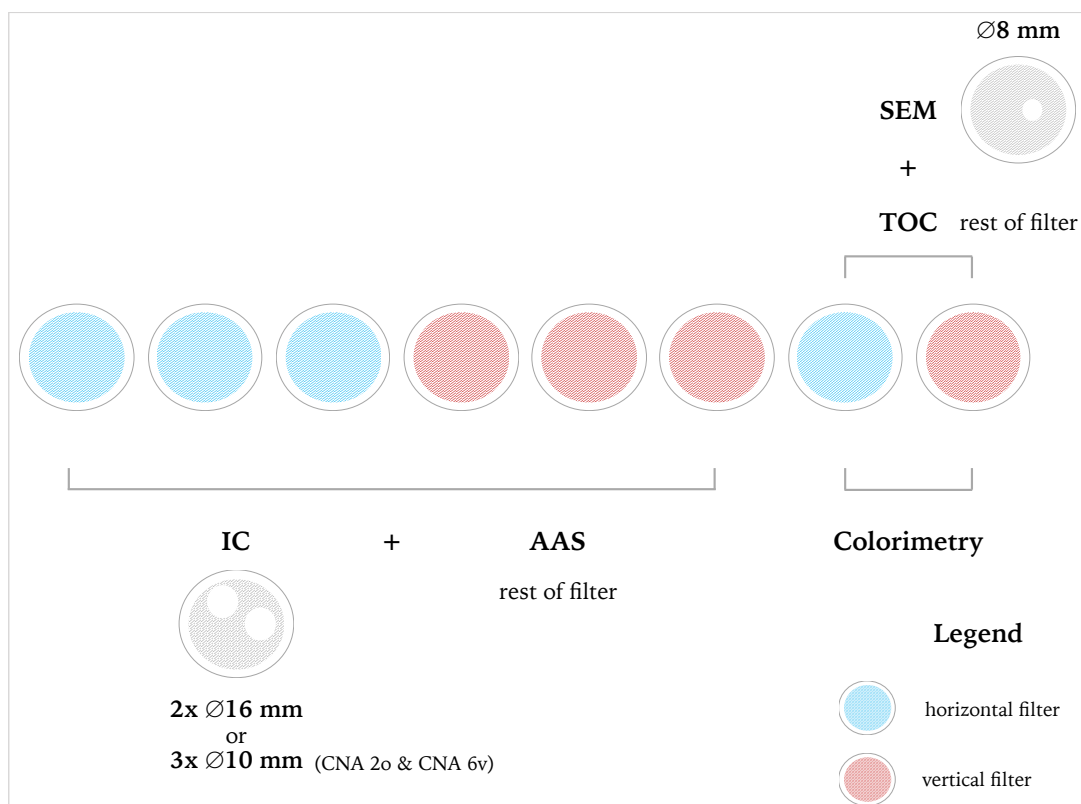


*Figure 2.11. Scheme resuming the separation of samples for analyses.*

On samples selected for IC, 2 spots of 16 mm diameter were collected from the whole substrate and placed into a flask filled with 5 mL of milliQ water. The flask is put in an ultrasonic bath for 30 min to speed up the particulates dissolution process. The two spots are then carefully removed from the liquid phase and the filtration of the latter made using a syringe and a syringe filter made of cellulose acetate with a porosity of 0.45  $\mu\text{m}$ .

The rest of the filter was used for AAS. In this case, the extraction process is performed through an Anton Paar Multiwave 3000 Microwave digestion system, which permits to digest completely the substrate. The cut sample is placed inside a teflon vessel, and 1 mL of hydrogen peroxide ( $\text{H}_2\text{O}_2$ ) and 4 mL of ultrapure nitric acid ( $\text{HNO}_3$ ) are added. The vessels are carefully closed and put

inside the digester. The digestion process is made according to the thermal program suggested by the UNI EN 14902 method. Once the thermal program finishes, the obtain liquid is transferred in a 25 mL flask filled with milliQ water. Between each extraction, a cleaning phase has to be conducted by filling the teflon vessels with 2 mL of nitric acid in order to avoid any contamination. Figure 2.12 schematizes the whole procedure that was followed.

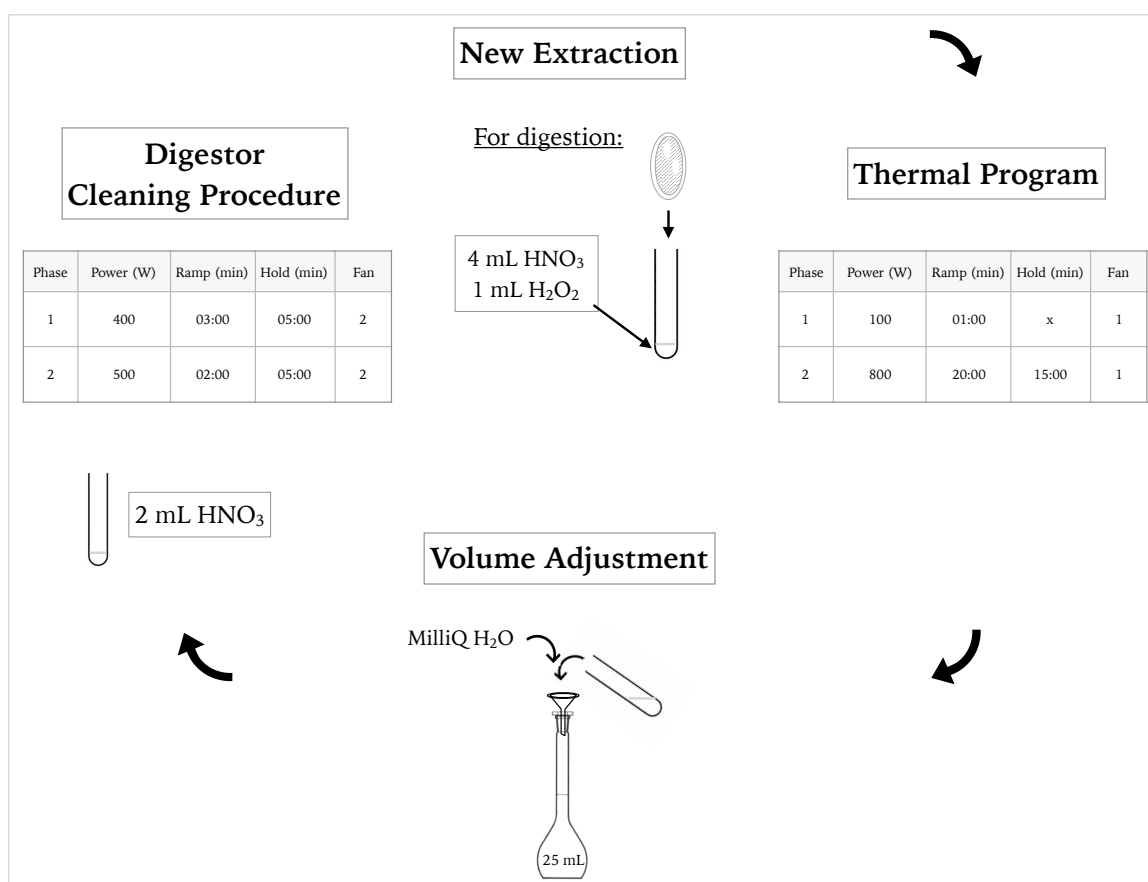


Figure 2.12. Extraction steps of samples using the Microwave 3000 digester.

The extraction method of samples selected for TOC is similar to the one employed for IC. The difference is that here 20 mL are employed for the extraction.

Colorimetry and SEM analyses were performed without any specific pretreatment, to visualize specific characteristics of the surfaces as they were.

Specifically, colorimetry was performed to determine precisely how the deposition of PM affects the appearance of substrates. In consequence, this kind of analyses were applied before performing any other analysis.

#### 2.4.2 Ion Chromatography (IC)

Ion Chromatography is an analytical technique used for the separation, determination and quantification of ionic compounds. The separation process is achieved with the help of two phases: a mobile phase, called eluent, flows through the solid stationary phase and carries the components of a mixture with it. Ion-exchange between the mobile and the stationary phases is the leading principle [28]. Given an eluent, components that display stronger interactions with the stationary phase are carried slower through the column than components with weaker interactions. This difference in rates results in the separation of several components in a complex solution.

The IC system employed depends on the nature of the ionic compounds to be analysed. On one hand, Cation Exchange Chromatography (CEC) allows the determination of cations with the stationary phase displaying negatively charged functional groups. On the other hand, the stationary phase of Anion Exchange Chromatography (AEC) displays positively charged functional groups interacting with anions coming from the analyte.

The IC system is schematically represented in Figure 2.13 and consists in the following parts:

- the pump: the high-pressure pump generates a specific flow rate of mobile phase and permits the entrance of the eluent in the column. The flow rate is expressed in milliliters per minute (mL/min).

- the sample injector: the injector introduces the liquid sample into the flow of the mobile phase. The multiport valve (called loop) introduces an exact volume of sample, decreasing systematic errors during the injection. The sample injection system is connected to the mobile phase tube.
- the guard column: this column protects the separation column from contamination.
- the separation column: the column corresponds to the stationary phase in which the separation occurs. Different stationary phases are used according to the ionic compounds to separate.
- the suppressor: this supplementary column is usually placed in AEC after the separation column. It decreases the background conductivity of the eluent and optimize the signal-to-noise ratio.
- the detector: the detector, usually conductivity or UV/VIS detector, is capable of detecting the different molecules eluted from the column. It measures the amount of conductive or absorbing component passing through it, allowing a quantitative analysis of the sample components. The detector provides an output to a computer.
- the computer: the computer, through a suitable software, controls all the modules of the IC instrument. It receives also the signal from the detector, and allows to determine the retention times of the different components and their relative amounts. The resulting graphs with the counts measurement and retention times are called chromatograms.

In this work a Metrohm 761 Compact IC equipped with a conductivity detector was used for the analysis of water soluble ions.

- Cations ( $\text{NH}_4^+$ ,  $\text{Na}^+$ ,  $\text{Ca}^{2+}$ ,  $\text{Mg}^{2+}$ ,  $\text{K}^+$ ) were separated on a Metrosep C2/150 column (150x4mm) with an eluent phase of tartaric acid 1mM and dipicolinic acid 4 mM, at a flow rate of 1.5 mL.min<sup>-1</sup>.

- Anions ( $\text{Cl}^-$ ,  $\text{NO}_2^-$ ,  $\text{NO}_3^-$ ,  $\text{SO}_4^{2-}$ ), were separated on a Metrosep A sup 4 column (250x4mm), followed by a suppressor, with an eluent phase of  $\text{Na}_2\text{CO}_3$  1.8 mM,  $\text{NaHCO}_3$  1.7 mM and acetone 2%, at a flow rate of 1.5  $\text{mL}\cdot\text{min}^{-1}$ .

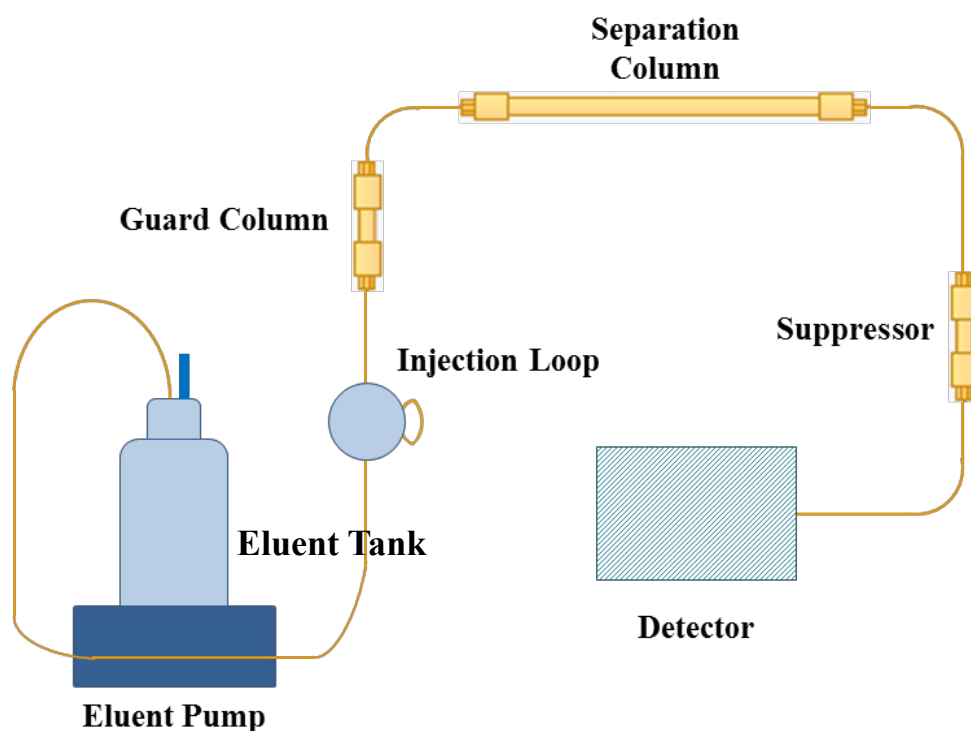


Figure 2.13. IC equipment for the determination of anions. The equipment for cations determination does not involve a suppressor [23].

The ion concentrations were determined by external standard method, using standard solutions reported in Table 2.4 to build calibration curves.



Table 2.4. Composition of the standards solutions for IC.

Ions concentration (ppm)	$Cl^-$	$NO_2^-$	$NO_3^-$	$SO_4^{2-}$	
<b>AEC analysis — Standards</b>					
1A	40	2	10	20	
2A	20	1	5	10	
3A	10	0.5	2.5	5	
4A	4	0.2	1	1	
5A	1	0.05	0.4	0.5	
6A	0.04	0.01	0.05	0.1	
<b>CEC analysis — Standards</b>					
Ions concentration (ppm)	$Na^+$	$NH_4^+$	$K^+$	$Ca^{2+}$	$Mg^{2+}$
1C	20	20	10	20	20
2C	10	10	5	10	10
3C	5	5	2.5	5	5
4C	2	2	1	2	2
5C	0.5	0.5	0.25	0.5	0.5
6C	0.2	0.2	0.1	0.2	0.2

Limits of Quantification (LoQ) for the investigated ions are given in Table 2.5.

Table 2.5. Limit of Quantification for the soluble ions analysed [29].

Cations	LoQ (mg/L)	Anions	LoQ (mg/L)
$NH_4^+$	0.02	$Cl^-$	0.08
$Na^+$	0.02	$NO_2^-$	0.01
$Ca^{2+}$	0.05	$NO_3^-$	0.1
$Mg^{2+}$	0.05	$SO_4^{2-}$	0.1
$K^+$	0.05		

### 2.4.3 Atomic Absorption Spectroscopy (AAS)

Atomic Absorption Spectroscopy is an analytical technique useful for the qualitative and quantitative determination of chemical elements in different matrices. The principle of the technique is based on the property of atoms to absorb light at specific wavelengths [30]. One or more electrons in the outer shell of an atom can be promoted to higher energy orbitals by absorbing a defined quantity of energy. It promotes the atom transition from the fundamental configuration to the excited state, energetically less stable. The amount of energy, and thus the wavelength according to the Planck-Einstein relation<sup>1</sup>, is specific to a particular electron transition in a particular element.

When light passes through a sample, a part is thus absorbed. The remaining part goes out from the sample and can be determined. This is the absorption, and absorbance is the quantity measured. The absorption spectrum of an element consists of a series of lines at specific wavelengths. Each line corresponds to an energetic transition, and the identification of the corresponding wavelength allows characterizing the element. Furthermore, the amount of absorbed light depends on the number of atoms undergoing the transition, which allows the element quantification<sup>2</sup>.

The absorbance is defined as:

$$A = -\log T = \log (I_0/I)$$

---

<sup>1</sup>  $E = hc/\lambda$  with  $E$  = energy of a photon (J),  
 $h$  = Planck constant ( $6.63 \times 10^{-34}$  J.s),  
 $c$  = speed of light ( $3.00 \times 10^8$  m.s<sup>-1</sup>),  
 $\lambda$  = wavelength (m).

<sup>2</sup> More information about AAS can be found in: J. C. Van Loon, « Analytical Atomic absorption spectroscopy: Selected Methods », Academic Press, 1980.

With  $A$  = absorbance

$T$  = transmittance

$I_0$  = intensity of light emitted by the light source

$I$  = intensity of light not absorbed passing through the sample

Atomic absorption follows a law analogous to the Lambert-Beer law defined for molecular absorption, so, at a specific wavelength, absorbance can be related to the concentration of the analyte as follow:

$$A = \epsilon * l * N$$

With  $\epsilon$  = spectral atomic absorption coefficient

$l$  = optical path

$N$  = total number of free atoms

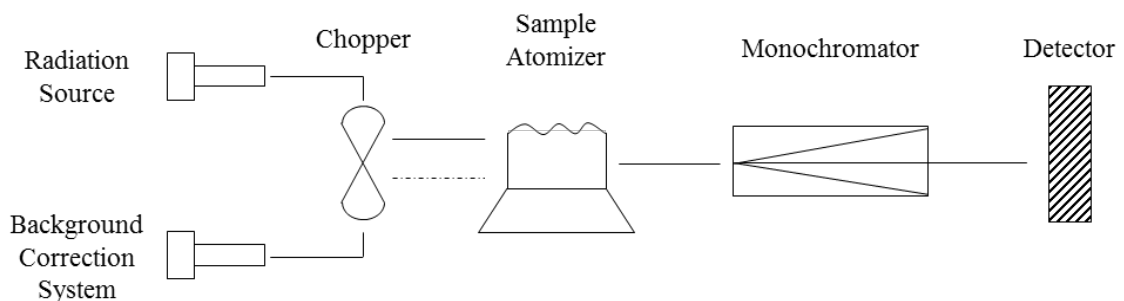


*Figure 2.14. Scheme of an Atomic Absorption Spectrometer.*

The Atomic Absorption Spectrometer is schematized in Figure 2.14 and consists in the following parts:

- the radiation source: the radiation source has to emit wavelengths that can be absorbed by the element we want to analyse. Two different types of 'line sources' are commonly used (Figures 2.15): the Hollow Cathode Lamp

(HCL) and the Electrodeless Discharge Lamp (EDL). The HCL consists of a glass cylinder filled with inert gas at low pressure (commonly argon) in which a little plate of the element of interest is placed. The gas ions are accelerated by applying a difference of electric potential, and collide with the cathode, causing the ejection of surface metal atoms (sputtering). These atoms tend to return to the ground state by emitting radiation with the wavelength characteristic of the element. The EDL is a ceramic tube filled with low pressure argon, in which a quartz bulb containing the element to be analysed and surrounded by a radiofrequencies (RF) generator is placed. The energy vaporizes the element and excites atoms that emit their characteristic spectrum to return in the ground state. Both types of lamp have been used according to the element we analysed.

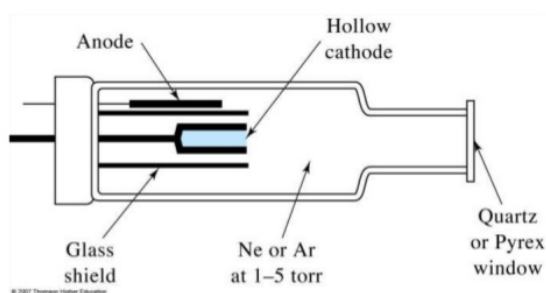


Figure 2.15a. Hollow Cathode Lamp scheme.

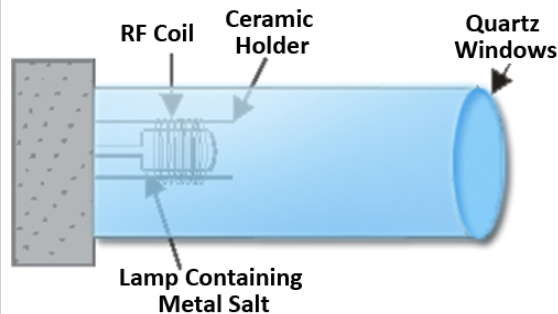


Figure 2.15b. Electrodeless Discharge Lamp scheme.

- the background correction system: in order to correct the background signal in atomic absorption, a continuum source of radiation, such as deuterium lamp emitting from 190 to 320 nm, can be used. The vaporized sample is submitted to the light originating from the radiation source giving the total absorbance (analyte + background), and also to the radiation of the continuum source giving an estimate of the background absorbance. The subtraction of the background signal from the total absorbance gives the corrected absorption arising only from the analyte. Another possibility for background correction is to take advantage of the so called “Zeeman effect”, in fact when an atom is placed in a magnetic field and its absorption is

observed in polarised light, the normal single line is split into three components  $-\sigma$ ,  $\pi$  and  $+\sigma$  displaced symmetrically about the normal position, while liquid droplets or solid particles show no Zeeman splitting. In a Zeeman system a polariser is present and the combined atomic and background absorption is measured while magnetic field is off; when the magnetic field is on, the detector measures only the background absorption as the  $\pi$  component is removed by the polarizer. The difference between the two is the Zeeman corrected atomic absorption signal.

- the sample atomizer: in order to determine and quantify elements with AAS, atomization of the sample is required. Two systems are commonly used: the flame atomizer and the electro-thermal atomizer. As we only used the later, we are only going to describe it briefly. A graphite furnace, which is a cylindrical graphite tube equipped with a platform and an injection hole, is used for the atomization of the sample. A known amount of analyte is deposited on the platform and submitted to a thermal program (solvent evaporation, incineration, atomization, cleaning) which permits the atomization of the sample.
- the optical devices and the monochromator: a system of lenses guides the radiation that passes through the sample to a monochromator. Its function is to isolate the spectral line of the desired analyte, and it comprises an entrance slit, a dispersion device and finally an exit slit.
- the detector: in AAS, Photomultiplier (PM) is the most used detector because of its high sensitivity. The light signal received is converted into an electrical signal and amplified.
- the computer: the computer, through a specific software, controls all the modules of the AAS instrument. It receives also the signal from the detector, both the background absorbance and the total absorbance, and allows to make the correction of the absorption spectra.

As for Ion Chromatography, the element concentrations from the particulate matters were determined by external standard method: calibration curves are built by analysing standards of known concentration of the metal of interest. In this work, a Perkin Elmer PinAAcle900z Atomic Absorption Spectrometer with electro-thermal atomizer was used for metal determination (Cu, Cr, Cd, Pb, Al, Fe and Mn). The instrument condition, the graphite furnace temperature programs and the Limits of Detection (LoD) for each analysed metal are listed in Table 2.6. Limits of Detection (LoD) were determined as the metal concentrations corresponding to 3 times the standard deviation of 20 replicates of a blank solution [23].

*Table 2.6. Operating conditions for AAS analyses.*

Analyte	Step	T (°C)	Ramp time (s)	Hold time (s)	Internal gas flow (mL.min <sup>-1</sup> )	gas type	$\lambda$ (nm)	slit (nm)	LoD ( $\mu\text{g/L}$ )
Cu	1	100	1	30	250	Argon	324.7	0.7	0.3
	2	130	15	40	250	Argon			
	3	600	10	20	250	Argon			
	4	2000	0	5	-	-			
	5	2450	1	3	250	Argon			
Cr	1	100	1	30	250	Argon	357.9	0.7	0.2
	2	130	15	40	250	Argon			
	3	800	10	10	250	Argon			
	4	2300	0	5	-	-			
	5	2450	1	3	250	Argon			
Cd	1	110	1	30	250	Argon	228.8	0.7	0.02
	2	130	15	30	250	Argon			
	3	500	10	20	250	Argon			
	4	1500	0	3	-	-			
	5	2450	1	3	250	Argon			

*follows...*

...continues

Pb	1	110	1	30	250	Argon	283.3	0.7	0.4
	2	130	15	40	250	Argon			
	3	900	15	20	250	Argon			
	4	2100	0	5	-	-			
	5	2450	1	5	250	Argon			
Al	1	110	1	30	250	Argon	309.3	0.7	0.2
	2	130	15	40	250	Argon			
	3	600	10	20	250	Argon			
	4	2300	0	5	-	-			
	5	2450	1	3	250	Argon			
Fe	1	100	5	20	250	Argon	248.3	1.8	0.8
	2	140	15	15	250	Argon			
	3	1400	10	20	250	Argon			
	4	2400	0	5	-	-			
	5	2600	1	3	250	Argon			
Mn	1	100	1	30	250	Argon	279.5	0.2	0.2
	2	130	15	40	250	Argon			
	3	600	10	20	250	Argon			
	4	1900	0	5	-	-			
	5	2450	1	3	250	Argon			

#### 2.4.4 Total Organic Carbon (TOC)

In PM that can deposit on outdoor-exposed material, carbon is usually present in compounds deriving from weathering of the parent material, decomposition of plant and animal matter, and natural or anthropogenic activities (e.g. combustion, traffic, solvent use, ...). Carbon can be present

under two different forms: inorganic carbon (IC) and organic carbon (OC). Collectively, the two forms of carbon are referred as Total Carbon (TC) and the relationship between them is expressed as:

$$TC = TOC + TIC$$

where

TOC = Total Organic Carbon

TIC = Total Inorganic Carbon

During this work, TOC measurements were performed through the TC-IC Method, by using a SHIAMADZU TOC-L CPN analyser. In TC-IC Method, TOC is calculated as the difference between the TC and the TIC values<sup>3</sup>.

- TC analysis:

The sample is introduced into the TC combustion tube, filled with an oxidation catalyst, and heated to 680°C. This thermal process burns the sample and as a result, the TC components in the sample are converted to carbon dioxide (CO<sub>2</sub>). Pure air, used as carrier gas, flows at a rate of 150 mL/min to the combustion tube, and carries the sample combustion products to an electronic dehumidifier where the gas is cooled and dehydrated. The combustion products are then carried through a halogen scrubber to remove chlorine and other halogens. Finally, the sample production products are delivered into the cell of a non-dispersive infrared (NDIR) gas analyser, where CO<sub>2</sub> is detected. The NDIR outputs an analog detection signal that forms a peak, which area is measured by a software.

---

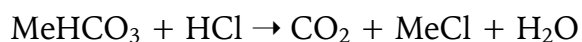
<sup>3</sup> Other methods for TOC determination are explained in: « PC-Controlled Total Organic Carbon Analyzer, TOC-VCPH/CPN & TOC-Control V Software, User Manual » from SHIAMADZU company. available at: [http://www.ecs.umass.edu/eve/facilities/equipment/TOC/TOCV/TOC-V\\_CP\\_Users\\_Manual\\_E.pdf](http://www.ecs.umass.edu/eve/facilities/equipment/TOC/TOCV/TOC-V_CP_Users_Manual_E.pdf) (Access 10/07/2017).



The TC concentration from the sample is determined by external standard method: a calibration curve is built by analysing various concentrations of a TC standard solution.

- IC analysis

The IC measured by TOC analysis mainly consists of the carbon contained in carbonates, and in CO<sub>2</sub> dissolved in water. Acidifying the sample with a small amount of hydrochloric acid (HCl) allows to obtain a pH less than 3, and all carbonates are converted to CO<sub>2</sub> by the following reactions:



CO<sub>2</sub> and dissolved CO<sub>2</sub> in the sample are volatilized by bubbling pure air or nitrogen gas through the sample. The analysis was performed using the IC reaction vessel (H type instrument). The TOC-L IC reactor kit is used to sparge the IC reaction solution (acidified reaction liquid) with carrier gas. Sample is injected into the IC reaction vessel and the IC in the sample is converted to CO<sub>2</sub>, which is volatilized by the sparging process and detected by the NDIR.

Figure 2.16 resumes the TC-IC method for the TOC determination.

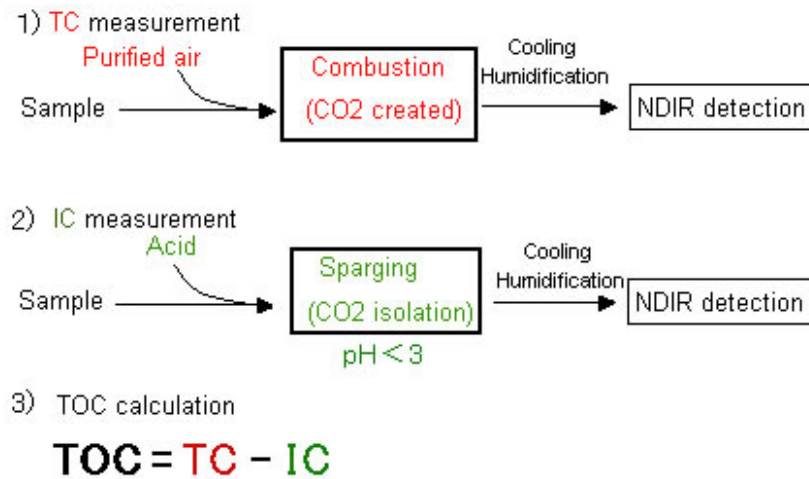


Figure 2.16. Schematic diagram of TOC measurement [31].

#### 2.4.5 Variable-Pressure Scanning Electron Microscopy and Energy Dispersive X-ray Spectroscopy (VP-SEM-EDX)

Scanning Electron Microscopy (SEM) is a powerful analytical technique that permits the observation of the surface morphology of a sample and gives some information about its composition. The leading principle in SEM is the interaction between an electron beam and the sample surface<sup>4</sup>. When the beam hits the sample, some electrons are ejected from it. Different signals are then emitted: X-Rays, Auger electrons, Cathodeluminescence, Backscattered electrons (BSE) and Secondary electrons (SE). BSE corresponds to an elastic scattering. Some of the primary electrons emitted from the electron beam are backscattered after the collision with the sample and detected. SE corresponds to an inelastic scattering, and the beam transfers a certain amount of energy to the atom it interacts with. This produces the expulsion of a secondary electron from the sample. Both BSE and SE are the most common signals used in SEM.

<sup>4</sup> The principle of SEM is explained in: C.E. Lyman, D.E. Newbury, J.I. Goldstein, D.B. Williams, A.D. Romig, J.T. Armstrong, P. Echlin, C.E. Fiori, D.C. Joy, E. Lifshin and Klaus-Ruediger Peters, Scanning Electron Microscopy, X-Ray Microanalysis and Analytical Electron Microscopy: A Laboratory Workbook, Plenum Press. New York, N.Y., 1990.

Due to the interaction of the sample with the primary electrons, many atoms are left in an excited state. When these atoms return to a lower energy state, they emit Auger electrons or X-Rays that can give information on the chemical composition of the sample, using a specific detector. An Energy Dispersive X-ray spectroscopy (EDX) probe was used in our case. The different signals that can be observed in SEM are illustrated in Figure 2.17 and the different explained emissions are reported in Figure 2.18.

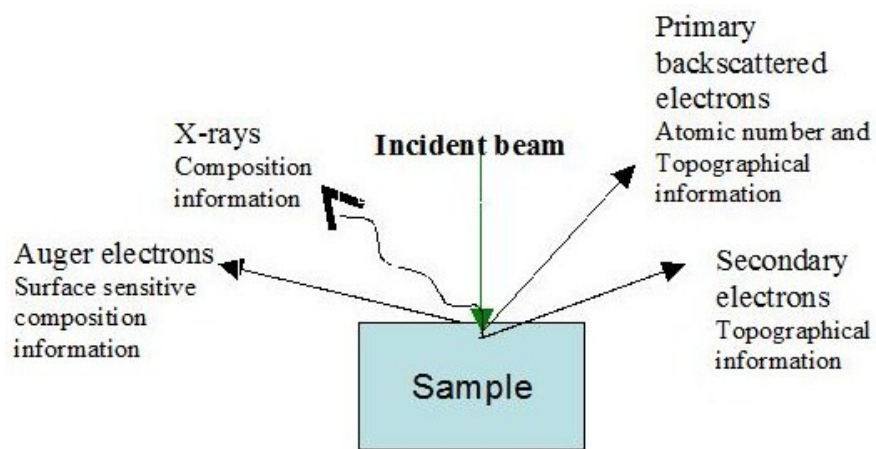


Figure 2.17. Signals emitted during SEM analysis [32].

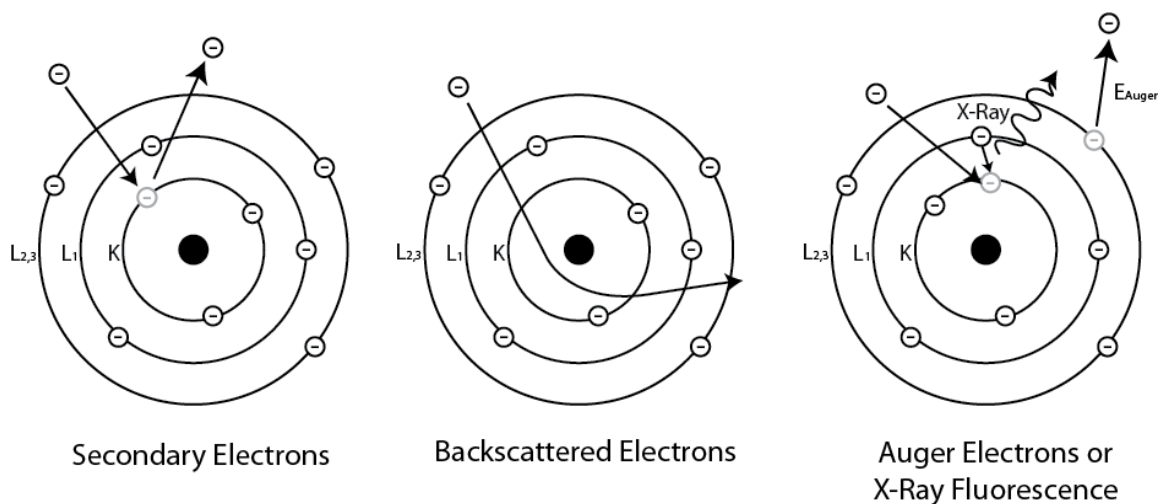


Figure 2.18. Electron detected during SEM analysis [33].

The Scanning Electron Microscope is schematized in Figure 2.19 and consists of the following parts<sup>5</sup>:

- the electron column: this is where the electron beam is generated. An electron gun is placed at the top of the column, and the electrons can be produced in thermal emission or field emission. When the electrons are generated they are oriented to hit the sample. They pass through the column with the help of lenses and some magnetic coils deflect the beam to scan the desired area of the sample.
- the specimen stage: the sample is placed at the end of the electron column on a mobile sample holder. If a non-conducting sample is analysed, the accumulation of static electric charges is observed, which deteriorates the image information. Thus, a metal coating can be applied to avoid this effect.
- the detectors: different detectors collect the different signals produced when the beam hits the sample surface. An Everhart-Thornley detector catches the SE when a solid state detector is used for the BSE.
- the vacuum system: the SEM has to be maintained under normalised vacuum conditions. The electrons are produced under high temperatures (~2700-2800 K) and the vacuum prevents the electron beam's filament from being oxidized.

The instrument used during the analysis was a variable pressure scanning electron microscope (VP-SEM) ZEISS EP EVO 50 with secondary (SE) and back scattered (BSE) electrons detectors. The samples were analysed using BSE and SE signals, with the electron beam focused at 8.5 mm from the surface. Different magnifications (88 x, 500 x, 1 000 x and 2 000 x) were applied according to what was observed. An EDS X-ray detector Oxford Instruments

---

<sup>5</sup> The information about SEM microscope come from: Brandon Cheney, « Introduction to Scanning Electron Microscopy », Senior Project in Material Engineering Department, San Jose State University. [Online]. Available at: [http://www.sjsu.edu/people/anastasia.micheals/courses/MatE143/s1/SEM\\_GUIDE.pdf](http://www.sjsu.edu/people/anastasia.micheals/courses/MatE143/s1/SEM_GUIDE.pdf) (Acces 16/05/2017).

INCA ENERGY 350 was used to obtain chemical informations from the samples, by applying an accelerating voltage of 20 keV.

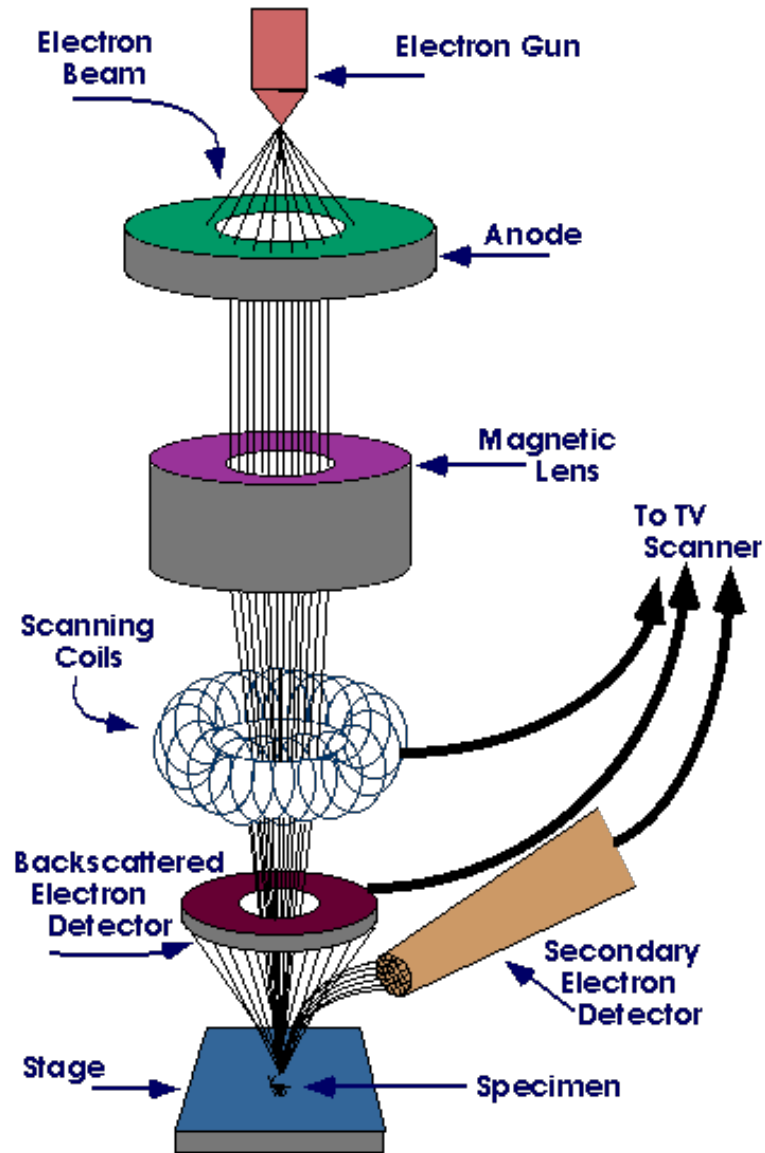


Figure 2.19. Diagram of a Scanning Electron Microscope [34].

#### 2.4.6 Colour measurements

Information about the evolution of the color of a material exposed to the atmosphere are interesting as they express some direct observable aesthetical effects of pollution and deposition of atmospheric particles. In general visual changes of the materials can be consequence of soiling, due to the accumulation of PM (as in this case), and/or of chemical-physical changes of the exposed surfaces due to decay processes, so evaluating color changes can provide useful information about these phenomena. The changes of color can be hard to detect by the naked eye and further information can be obtained through spectrophotometric color measurements.

The color changes of our substrates and thus the corresponding soiling can be measured as the difference between the color of the samples after and before exposure. Different color spaces were elaborated but one of the frequently used is the CIE  $L^*a^*b^*$  color system. This color space is a cartesian coordinate system in which a single point depicts one color. Three coordinates are defined:

- $L^*$ , corresponding to the lightness, moving from black (0) to white (100);
- $a^*$ , corresponding to the color changes moving from green ( $-a^*$ ) to red ( $+a^*$ );
- $b^*$ , corresponding to the colors changes moving from blue ( $-b^*$ ) to yellow ( $+b^*$ ).

The Figure 2.20 presents the graphical representation of this system.

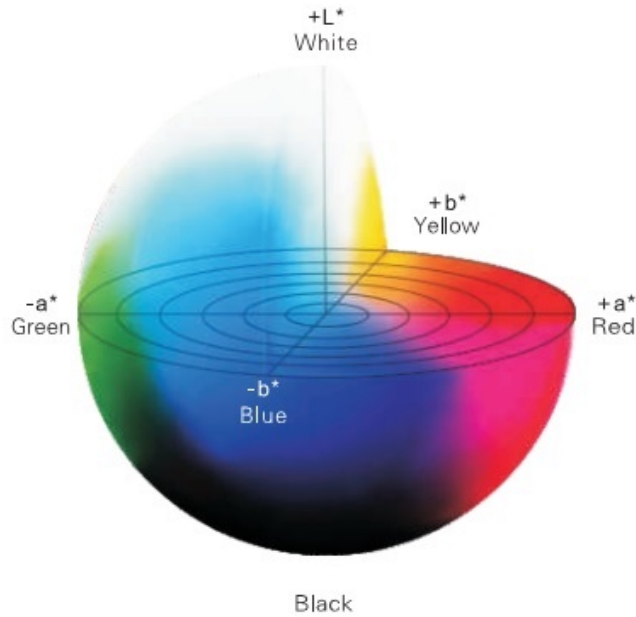


Figure 2.20. CIE  $L^*a^*b^*$  space. The  $L^*$  coordinate moves from 0 to 100.

The difference between two colors, and thus the change that can be observed is expressed as Euclidian distance:

$$\Delta E = \sqrt{(\Delta L^*)^2 + (\Delta a^*)^2 + (\Delta b^*)^2}$$

The threshold of perceptibility of a color variation is not easy to determine, and the tolerances are not standardized and can vary also because of the characteristic of the original surface. As an example,  $\Delta E \leq 3$  is the value commonly used in the field of cultural heritage [35]. This means that for a E value equal to or less than 3, ones consider that no change of color occurred. When the change is determined as perceptible, we have to look more in details to understand and make an interpretation of the color changes. This is why we also have to consider  $\Delta L^*$ ,  $\Delta a^*$  and  $\Delta b^*$  separately.

When light beam hits the surface of a material, different phenomena occur. One part of the light is absorbed and the rest is reflected and then can be detected. Two types or reflection happen:

- the specular reflection. The light is reflected in a single direction. This occurs more strongly on shiny and glossy surfaces. It makes an object appear more saturated and vivid in color.
- the diffuse reflection. In this case, the light is scattered in various directions. This occurs more strongly on rough and irregular surfaces making the object appear less saturated and duller in color.

The Figure 2.21 presents both types of phenomena.

When performing the analysis, we can decide if we want to include or not the specular radiations. The Specular Component Included (SCI) radiation mode includes both the specular and diffused reflected light. The Specular Component Excluded (SCE) radiation mode excludes any specular reflected light and permits to measure the appearance of an object's color in a way closer to the human perception.

If a glossy surface is analysed, we expect it to be very reflecting and we can see a noticeable difference between SCI and SCE. In contrary if a mat surface is analysed we would observe almost the same values for SCI and SCE. In general, bare metals have a high reflectance and thus we observe a more marked difference between the SCI and the SCE results.



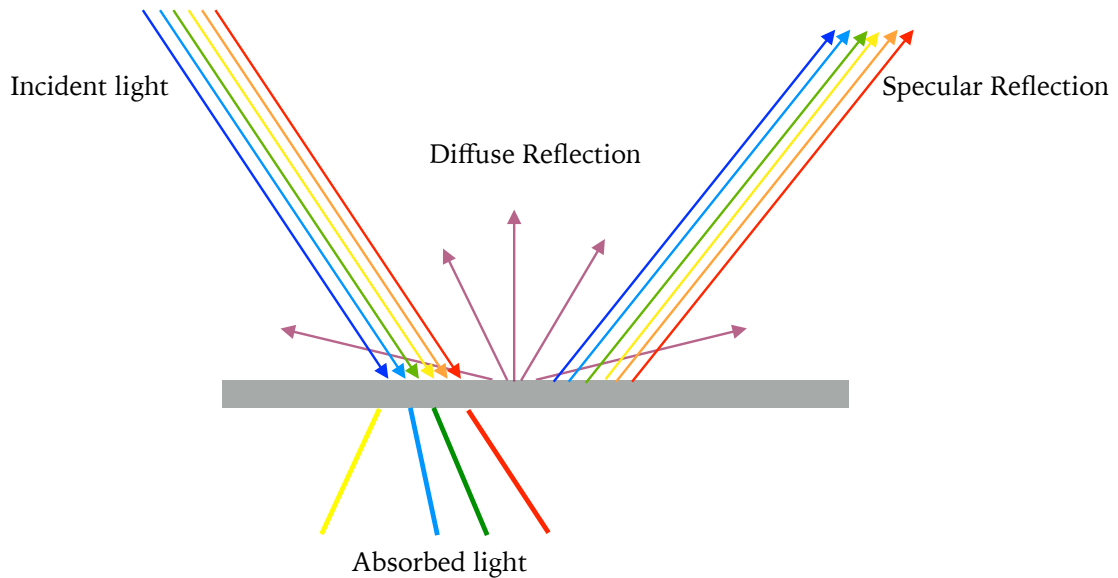


Figure 2.21. Interactions between an object's surface and the radiation of light.

Data were recorded with a Datacolor D400 spectrophotometer. Only one measure was performed for each sample as the measured area (30 mm diameter) almost corresponded to the total area of the samples. The measurement geometry was  $d/0$ , which permits to include (SCI) or not (SCE) the specular reflected radiation. The solar light was simulated using the CIE standard illuminant D65<sup>6</sup> and the 10° standard colorimetric observer was used. Differently from aluminum foils, membrane filters before exposure did not show any differences between SCI and SCE measurements, so for homogeneity only SCE measurements were considered.

---

<sup>6</sup> The D65 illuminant mimics an average daylight and has a color temperature of approximately 6500K. This is more explained in: Schanda, J. (2007) *CIE Colorimetry, in Colorimetry: Understanding the CIE System* (ed J. Schanda), « CIE illuminants and sources », John Wiley & Sons, Inc., Hoboken, NJ, USA, p.43.

### 3. RESULTS & DISCUSSION

#### 3.1. Preliminary exposure

For the analysis of substrates exposed during the preliminary exposure, only the two types of cellulose nitrate filters were considered. Indeed, at the end of the exposure, some of the light pieces of glass were found to be turned upside down or moved from their original position, probably due to a strong wind during the last part of the exposure period. This not controlled change in position could have altered the deposition process, thus glass specimens were not used for analysis and interpretation.

The distribution of samples allowed us to compare the depositions:

- between the horizontal and the vertical samples, within a DepBox and, as for horizontal samples, between DepBoxes,
- between the Whatman and Albet substrates, to observe the differences occurring because of the porosities, between DepBoxes and within a DepBox.

##### 3.1.1. PM deposition

After the exposure, samples showed a deposit of particles whose corresponding mass was determined by the difference between the mass of surrogate surfaces after and before the exposure. Figure 3.1 presents the quantity of PM collected, distinguishing among the different type of filters, horizontal and vertical substrates and the two DepBoxes.

Considering horizontal Whatman and Albet filters, both inter and intra DepBoxes, we can see that there is no significant difference in the amount of PM deposited (t-test;  $\alpha=0.05$ ). This means that both types of filter catch the

same amount of PM on their surfaces and their difference in porosity does not seem to play a major role.

Therefore, if we consider all samples independently from the type of filters, it is even more evident that samples in horizontal position in both the DepBoxes collected the same amount of PM. This observation, together with the low relative standard deviations, confirms the idea that there is a good reproducibility within and between the collectors, as presented in the PhD thesis which developed the concept of DepBox [2].

Moreover, these results suggest that the presence of vertical filters in DepBox 1 do not influence the deposition on the horizontal ones, allowing to place samples oriented in both the positions in a same DepBox.

From Figure 3.1 it is also noticeable that, as expected, a higher quantity of PM deposited on horizontal samples than on vertical samples (around 4.5 times more), due to different deposition processes.

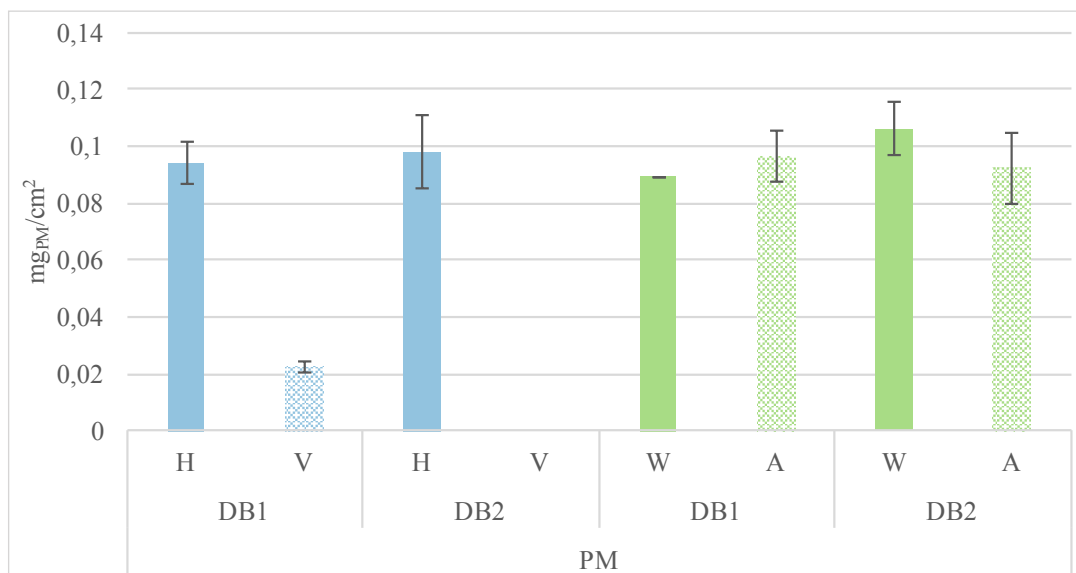


Figure 3.1. Quantity of PM deposited per surface unit of substrates (mg<sub>PM</sub>/cm<sup>2</sup>) in the two DepBoxes (DB1, DB2) on horizontal (H) and vertical (V) samples or on the different type of horizontal filters (W-Whatman, A-Albet).

### 3.1.2. Ion Chromatography (IC)

Different ions were investigated during the IC analysis: sodium ( $\text{Na}^+$ ), ammonium ( $\text{NH}_4^+$ ), potassium ( $\text{K}^+$ ), calcium ( $\text{Ca}^{2+}$ ) and magnesium ( $\text{Mg}^{2+}$ ) among the cation; chloride ( $\text{Cl}^-$ ), nitrate ( $\text{NO}_3^-$ ), nitrite ( $\text{NO}_2^-$ ) and sulfate ( $\text{SO}_4^{2-}$ ) among the anions. However, the nitrite ions were finally not taken into account as, for the large majority of samples, the concentration was below the limit of detection (LoD). However, the nitrite ions were finally not taken into account as, for a large majority of samples, the concentration was below the limit of detection (LoD).

Figure 3.2 focuses on the different ions in term of quantity per weight unit of PM, giving indication on the nature of PM deposited.

Chlorides are the major part of the anions contained in soluble salts of PM deposited on the surfaces and investigated by IC, reaching  $326 \text{ mg/g}_{\text{PM}}$  as a maximum value. The following trend is observed for the anions:

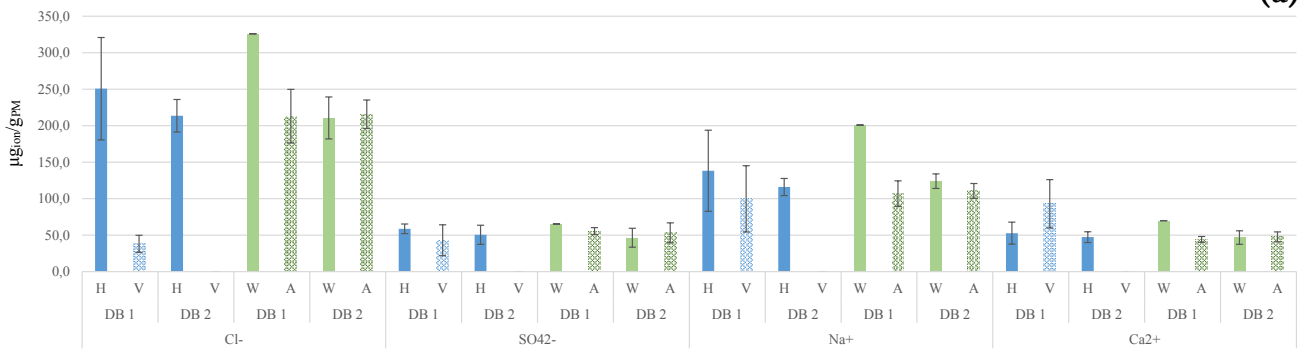
$\text{Cl}^- > \text{SO}_4^{2-} > \text{NO}_3^-$  in term of weight per gram of PM.

Sodium are the major part of the investigated cations contained in soluble salts of PM deposited on the surfaces, reaching  $201 \text{ mg/g}_{\text{PM}}$  as a maximum value. Cations were recorded as the following trend:

$\text{Na}^+ > \text{Ca}^{2+} > \text{Mg}^{2+} > \text{NH}_4^+ > \text{K}^+$  in *term of weight per gram of PM*.

The minimum value is reached by potassium (all ions considered), with around  $5 \text{ mg/g}_{\text{PM}}$  on the horizontal Whatman samples.

(a)



(b)

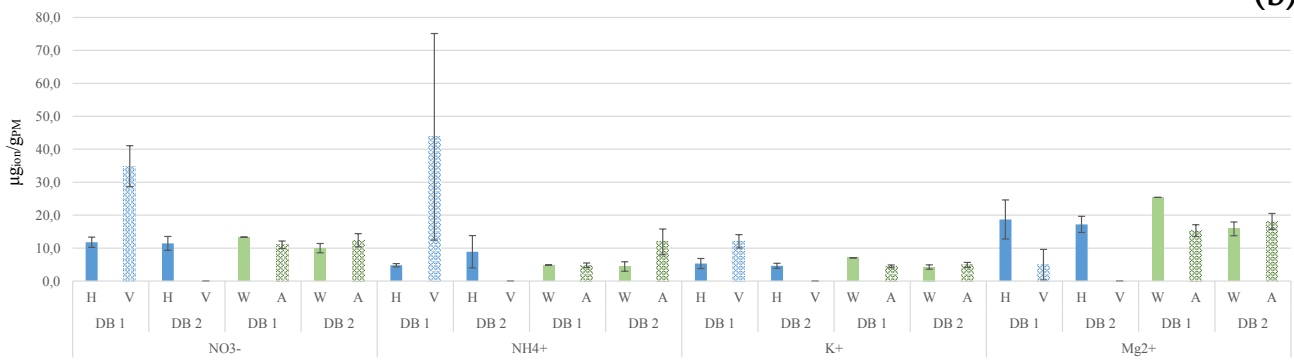


Figure 3.2. Quantity of ions per gram of PM ( $\mu\text{g}_{\text{ion}}/\text{g}_{\text{PM}}$ ) collected in the two DepBoxes (DB1, DB2) on horizontal (H) and vertical (V) samples or on the different type of horizontal filters (W-Whatman, A-Albet). IC results for the more present (a) and less present (b) ions.

Three trends about the dry deposition of soluble ions on horizontal and vertical samples can be separated:

- PM deposited on horizontal samples is richer in  $\text{Cl}^-$ ,  $\text{Mg}^{2+}$  and to a lesser extent in  $\text{Na}^+$ , than the vertical samples.
- PM deposited on vertical samples is richer in  $\text{NO}_3^-$ ,  $\text{NH}_4^+$  and to a lesser extent in  $\text{K}^+$  and  $\text{Ca}^{2+}$ , than the horizontal samples.
- PM deposited on vertical and horizontal samples contains more or less the same quantity of  $\text{SO}_4^{2-}$ . Statistically, there is no difference between horizontal and vertical samples.

As exposed in a previous work [36], the fine fraction of PM ( $\text{PM}_{2.5}$ ) represents an important fraction in the deposition mechanism occurring on vertical

surfaces. Actually the IC analysis performed shows that ions characteristics of the fine fraction, as nitrate, ammonium and potassium, were mainly found on the vertical samples; while ions characteristics of the coarse fraction, as marine chlorides, mainly deposited on horizontal samples and better hold on them. Sulfate is the element clearly identified as being part of both fine and coarse fraction, with no significant difference between its concentration among them. This result is also in accordance with measurements campaigns previously carried out in the North of Italy [37].

Figure 3.3 presents the IC results in term of quantity of ions per exposed area ( $\mu\text{g}_{\text{ion}}/\text{cm}^2$ ), giving information on the total amount of ions deposited on the filters.

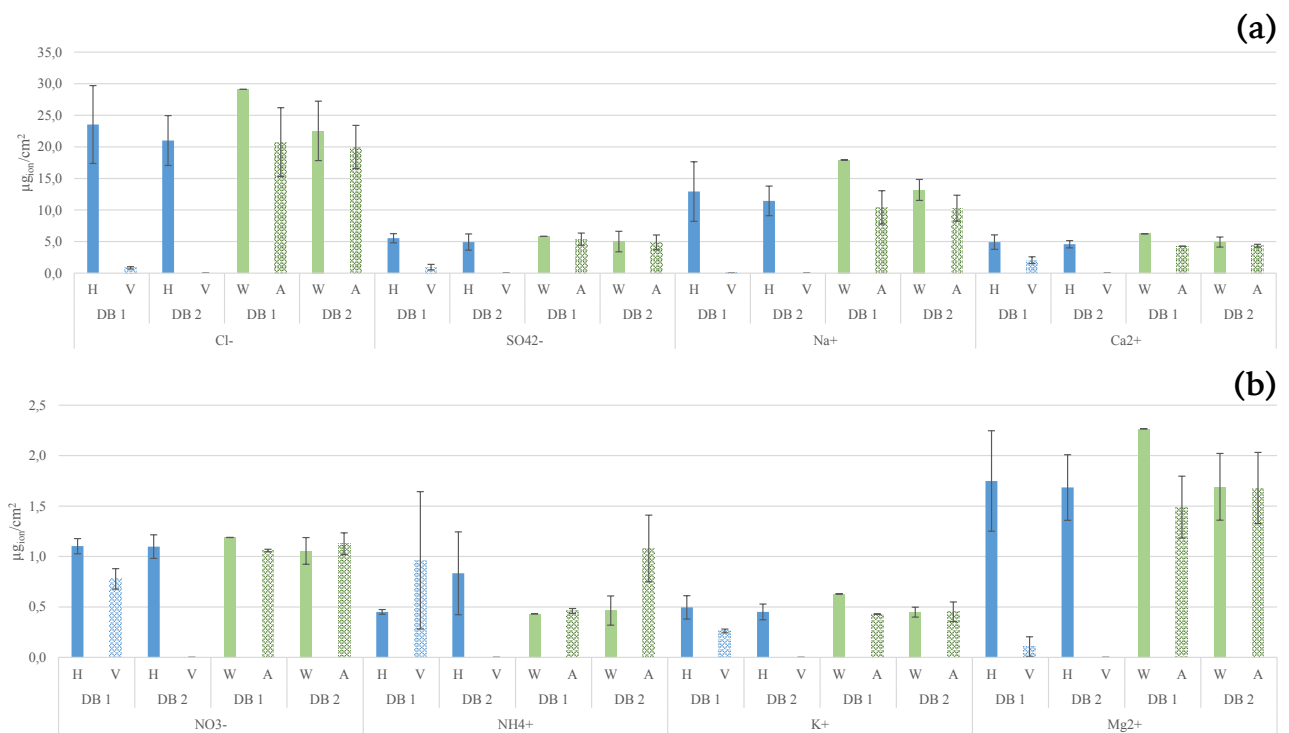


Figure 3.3. Quantity of ions deposited per surface unit ( $\mu\text{g}_{\text{ion}}/\text{cm}^2$ ) in the two DepBoxes (DB1, DB2) on horizontal (H) and vertical (V) samples or on the different type of horizontal filters (W-Whatman, A-Albet). IC results for the more present (a) and less present (b) ions.

From Figure 3.2 and 3.3 we clearly observe that PM deposited in the two DepBoxes show the same distribution and content of ions, which confirm the reproducibility of the exposure devices already observed in the previous section. Not significant difference (t-test;  $\alpha=0.05$ ) in the deposition of ions between the two types of substrates are detected and the different porosity does not seem to have any impact on the ion deposition and interaction with the surface.

By comparing the two figures, it is also interesting to notice that even if PM deposited on vertical filters is clearly richer in nitrate, the total amount of this ion on horizontal and vertical filters tend to match due to the globally higher amount of PM deposited on horizontal substrates; the same tendency is visible for ammonium and potassium

### 3.1.3. Metal Analysis by Atomic Absorption Spectroscopy (AAS)

Only two metals were investigated after the preliminary exposure, as the objective was to evaluate the possibility to detect metals in filters exposed for about one month and in which amount. Copper (Cu) and iron (Fe) are the two elements investigated here. The results for Fe are presented in Figure 3.4, and the results for Cu are shown in Figure 3.5.

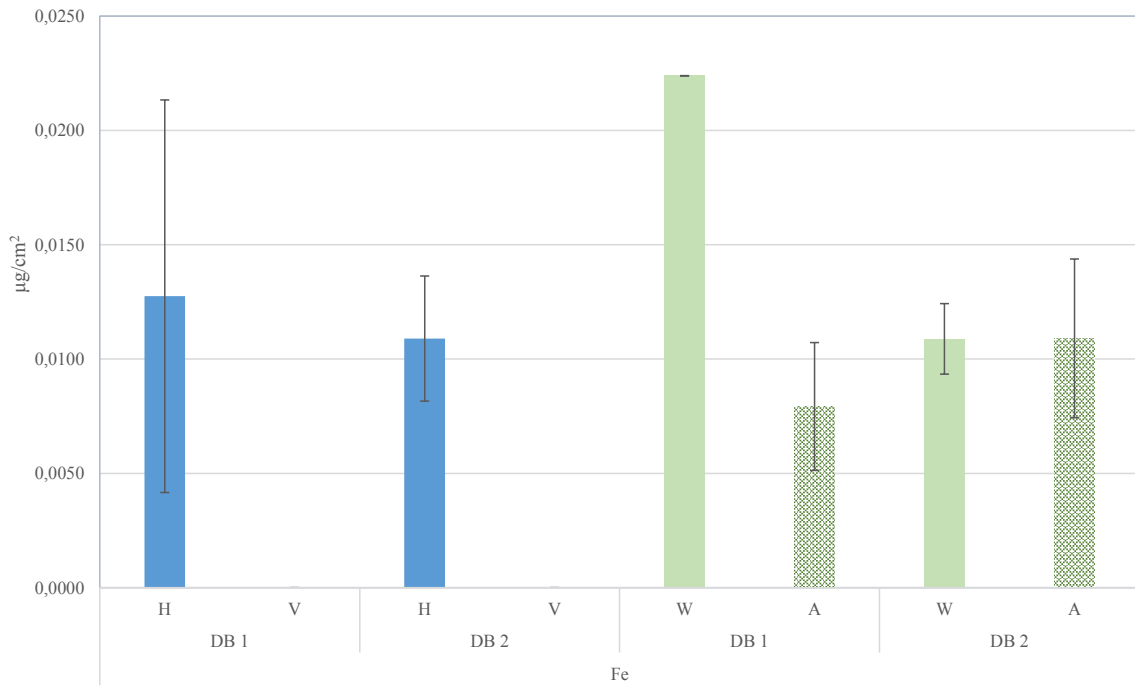


Figure 3.4. Quantity of Fe deposited per surface unit ( $\mu\text{g}/\text{cm}^2$ ). Comparison between the two DepBoxes (DB1, DB2), vertical (V) and horizontal (H) substrates and horizontal Whatman (W) and Albet (A) filters.

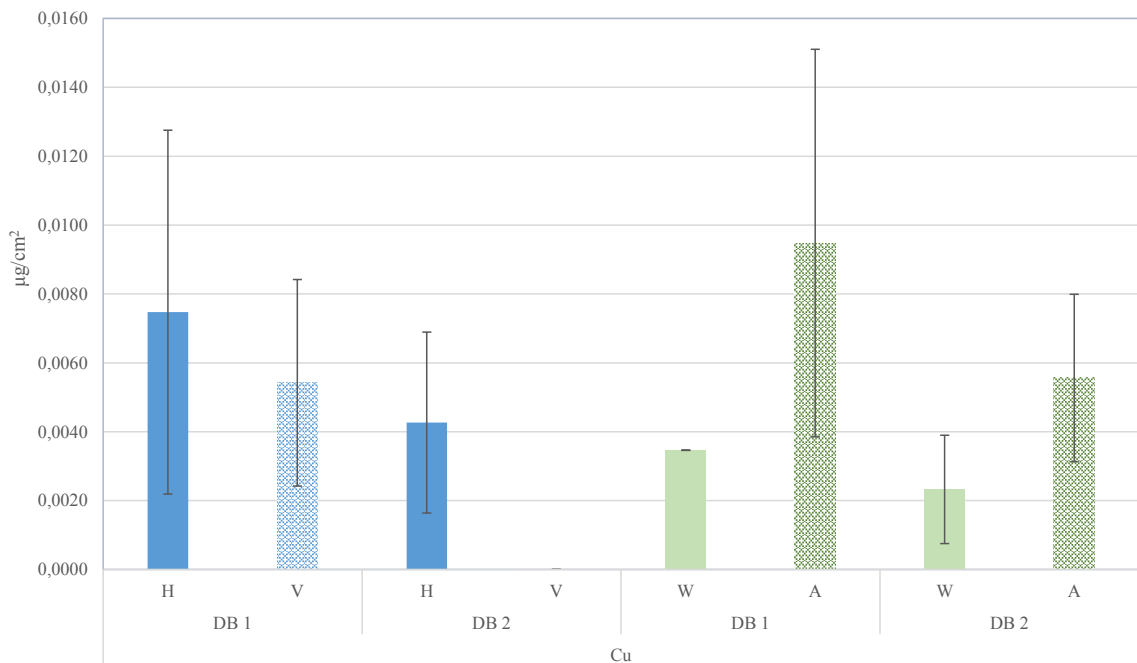


Figure 3.5. Quantity of Cu deposited per surface unit ( $\mu\text{g}/\text{cm}^2$ ). Comparison between the two DepBoxes (DB1, DB2), vertical (V) and horizontal (H) substrates and horizontal Whatman (W) and Albet (A) filters.



On Figure 3.4, we can see that the PM deposited on the vertical substrates inside the DepBox 1 (DB1) did not present a sufficient high quantity of Fe to be detected during the analysis. Iron was only identified on horizontal samples. Iron is usually more present in the coarse fraction of PM, having mainly a natural origin, and this result is consistent with the hypothesis that mainly fine PM deposits on vertical filters. On the contrary, we observe that the results are not so clear for copper on Figure 3.5. The standard deviation being quite important, we cannot consider that there is a significant difference in the Cu deposition on the horizontal and vertical samples. The origin of PM is fundamental in determining its size and Cu can have both natural and anthropogenic sources and can be present both in fine and in coarse fractions [38]. This could be the reason for this finding

Due to the relatively high standard deviations no specific different tendencies in metal depositions between the two types of filters nor between the two DepBoxes can be highlighted.

#### 3.1.4. General remarks

The preliminary exposure allowed to obtain important information in order to verify the feasibility and to set-up the effective exposure campaign. Especially the following conclusions can be drawn.

We observed and confirmed that the wet deposition process is successfully avoided when using Deposition Boxes. They are useful devices to mime the dry deposition process occurring when materials are exposed to the atmosphere.

One month seems to be the minimum time of exposure, actually a deposition of particles is clearly observed and main inorganic ions, together with some metals were identified.

There is a good reproducibility among deposits collected intra and inter DepBoxes.

It was possible to differentiate PM depositions on horizontal and vertical filters, both in term of mass and composition. Especially on vertical samples lower amount of PM deposited, but richer in ions characteristic of the fine fractions. Moreover no significant difference was determined between the two types of filters exposed, indicating that the small difference in porosity did not seem that have a major impact on the interaction between particles and surface. These results have to be confirmed or not by the analyses performed after the main campaign of exposure.

### 3.2. The main campaign.

#### 3.2.1. Visual observations.

After the 64 days of exposure, all samples were covered by a deposit of particles, and the visual aspect of the substrates was different from before the exposure campaign. Horizontal and vertical samples of each substrate were compared to a non-exposed sample, in order to characterize with the naked-eye the visual changes produced by the particles deposition. In Figure 3.6. are shown the samples appearances.

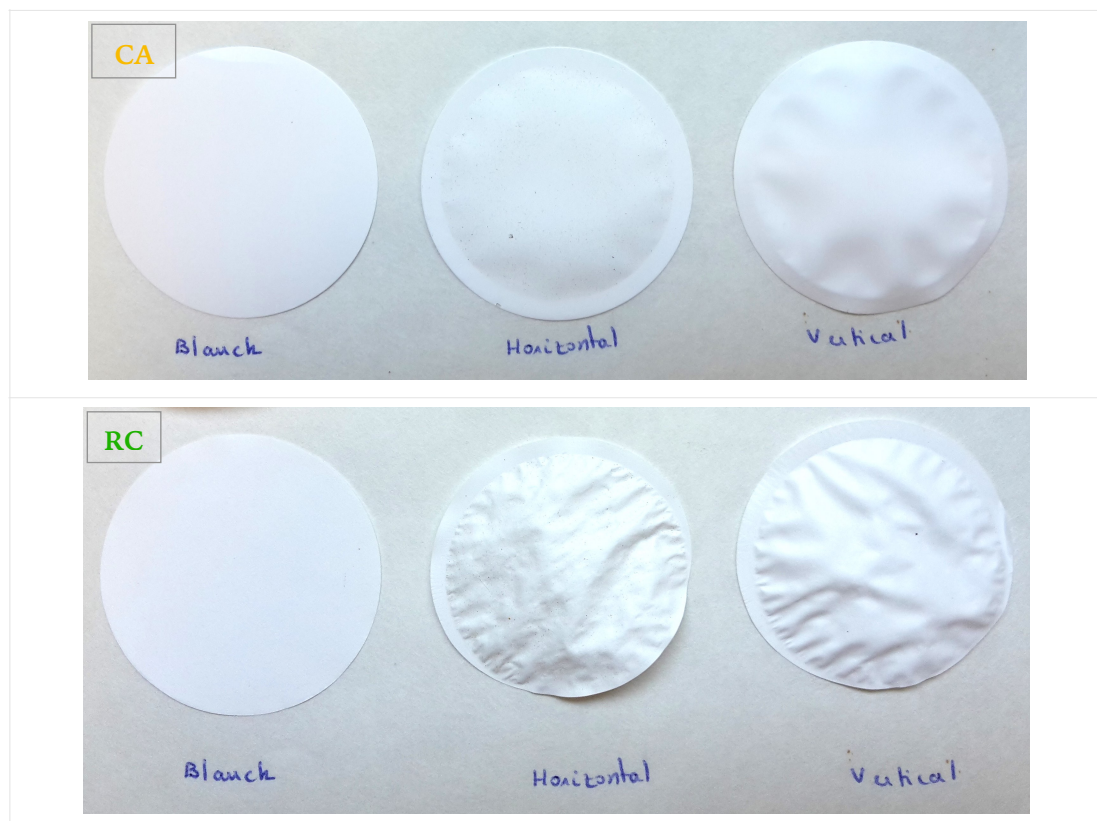


Figure 3.6. Appearance of the exposed substrates compared to the non-exposed ones.

*Follows...*

continues...

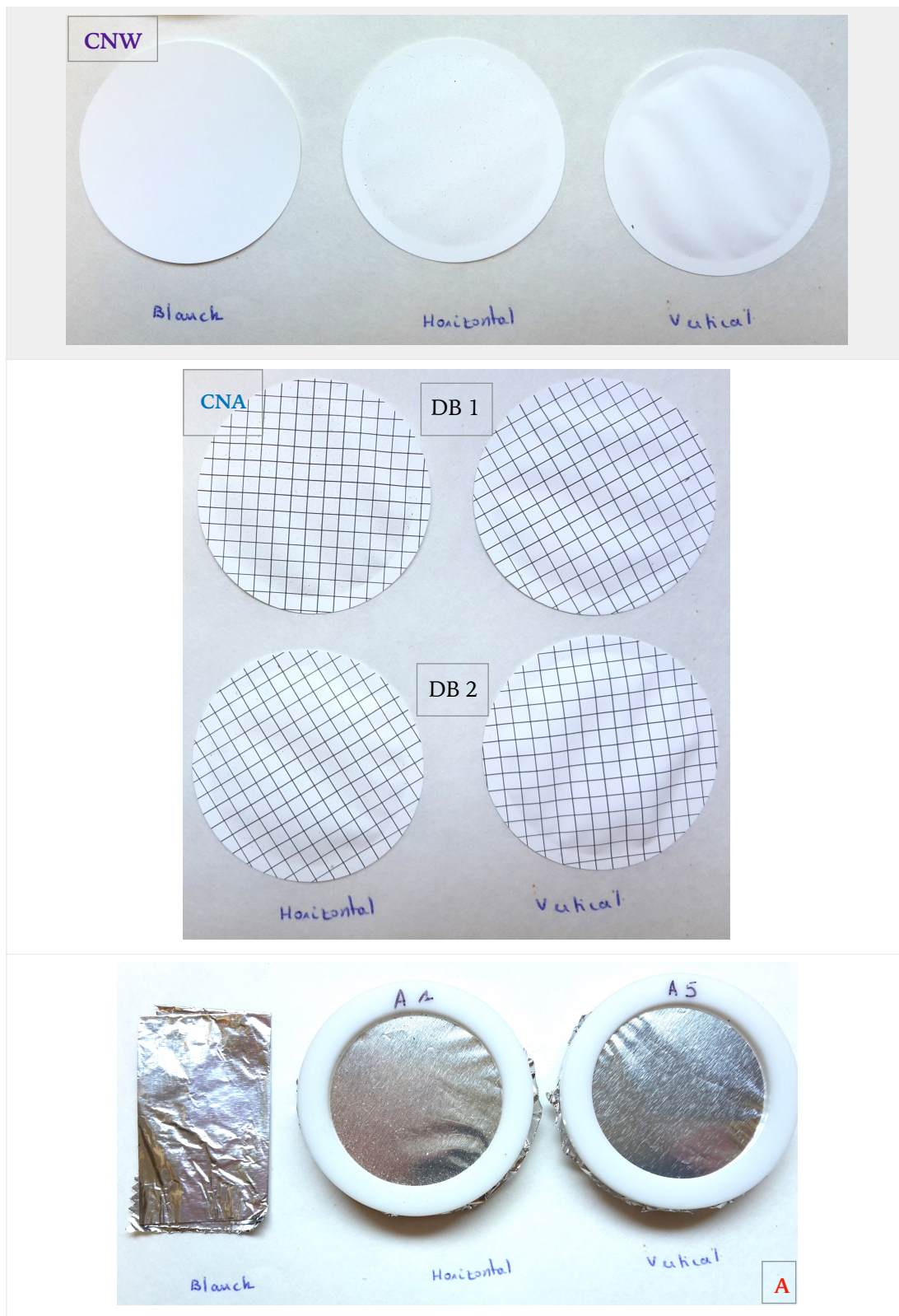


Figure 3.6. Appearance of the exposed substrates compared to the non-exposed ones. CA=Cellulose Acetate 0.45m; RC=Regenerated Cellulose 0.45m; CNW=Cellulose Nitrate 0.45m; CNA= Cellulose Nitrate 0.22m; A=Aluminum foil; DB1=DepBox1; DB2= DepBox2.

- The Sartorius Cellulose Acetate 0.45  $\mu\text{m}$  substrate (CA) exhibits a visible difference between the blank and the horizontal exposed samples. The latter ones look darker than the former ones. No visible change of colour is determined for the vertical samples.
- For the Schleicher Regenerated Cellulose 0.45  $\mu\text{m}$  substrate (RC), in term of colour, no visible change is perceptible for the vertical samples, but the horizontal ones appear darker than the blank, with the presence of reddish and yellowish zones.
- The Whatman Cellulose Nitrate 0.45  $\mu\text{m}$  (CNW) substrates do not show perceptible colour changes when vertically exposed, while the horizontally exposed ones appear darker than the blank used as reference, and a bit reddish. The visual change in colour seems to be less pronounced than the one observed for CA.
- The same general observations can be made for the samples exposed in the DepBox 1 and for the ones exposed in the DepBox 2 for the Albet Cellulose Nitrate 0.20  $\mu\text{m}$  substrates (CNA). Once more, the horizontal samples are darker than the blank, when no visible change is perceptible for the vertical ones.
- All the above-mentioned membrane substrates appear more or less wavy after the exposure, depending on the degree of atmospheric water absorption (RH data and number of precipitations events occurred during the exposure are reported in Appendix A<sup>7</sup>). According to the results of the hydrophilicity tests preliminary performed (see section 2.3.1), the waviest membranes are those in Regenerated Cellulose.

The Aluminum foils are the only samples that do not exhibit any change in the surface behavior due to the humidity present in the atmosphere. The deposit of

---

<sup>7</sup> Atmospheric data were collected from the ARPAE Emilia Romagna website (<https://www.arpae.it/>) for the period of exposure and are gathered in the Appendix A. 17 days had at least one precipitation event out of a total of 64 days of exposure.

particles is really visible on the horizontal sample and yellow big particles are easily distinguished.

Summarising, in all cases, the horizontal samples show a perceptible difference in term of colour compared to the blanks used as reference, when no surface deposit is visually perceptible on the vertical samples. The hydrophilicity behavior tested before the exposure is confirmed by the surface appearance of the substrates.

### 3.2.2. Colour measurements

The colour measurements performed give more details on the colour changes due to the atmospheric exposition. On Figure 3.7 are presented the reflectance graphs for CA, RC, CNW and CNA, respectively. The analysis was not performed for the aluminum foils to avoid any removal of particles, less trapped by this kind of surface.

For the 4 substrates, the same general trend is observed. No specific peaks are present, meaning that the different substrates reflect the light at all wavelengths. This is expected as samples appear white when not exposed. After exposure, the shapes of the curves do not change, indicating that only soiling processes and not chemical changes occurred on the substrates. Horizontal samples present a significant loss in reflectance compared to the blank, while the vertical samples present almost the same reflectance as the samples that were not exposed. The corresponding  $\Delta L$ ,  $\Delta a$ ,  $\Delta b$  and  $\Delta E$  values are given in Table 3.1.

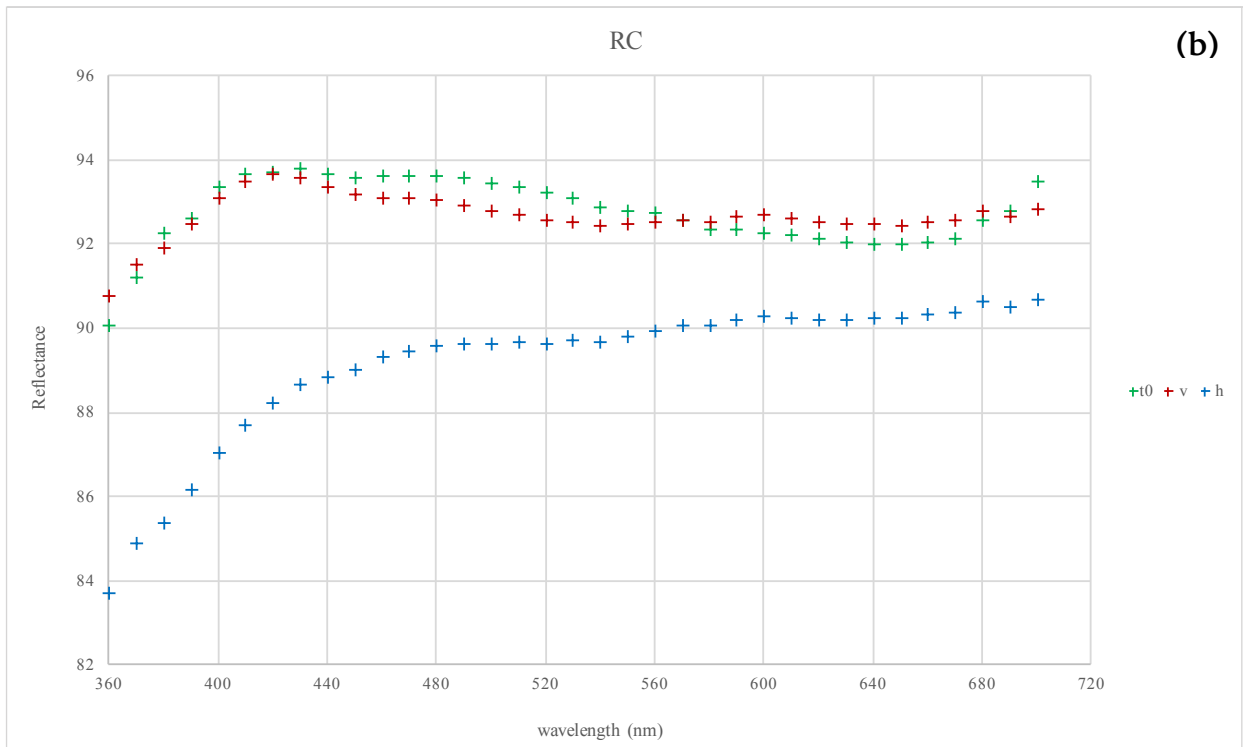
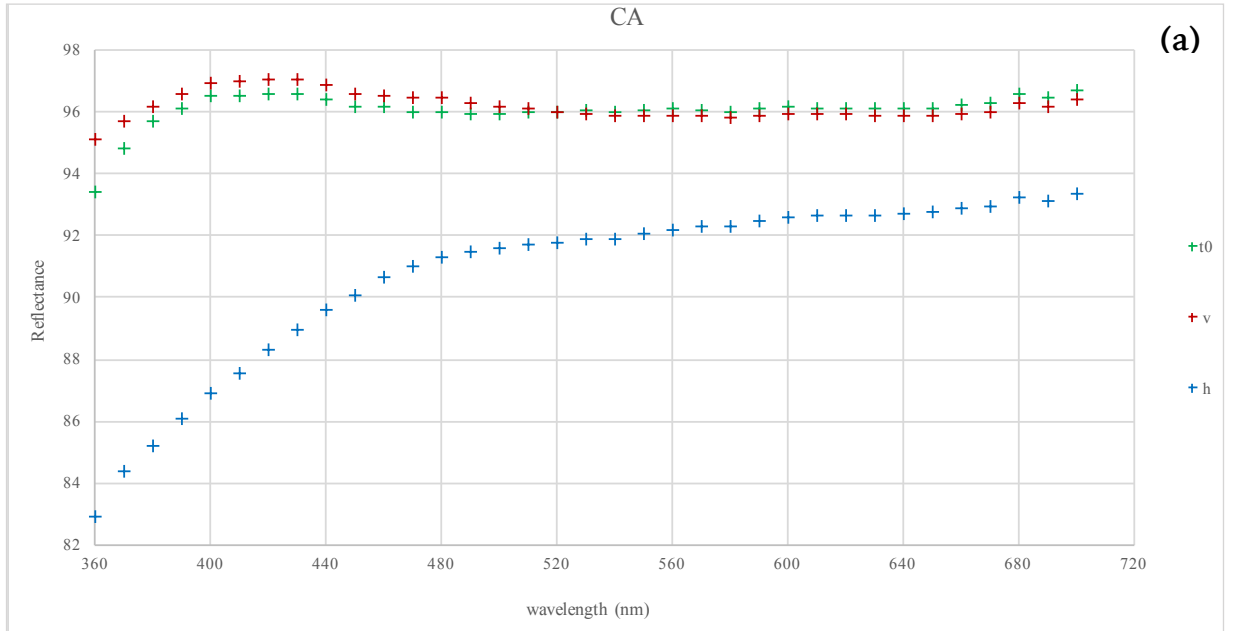


Figure 3.7. Reflectance spectra.

follows...

continues...

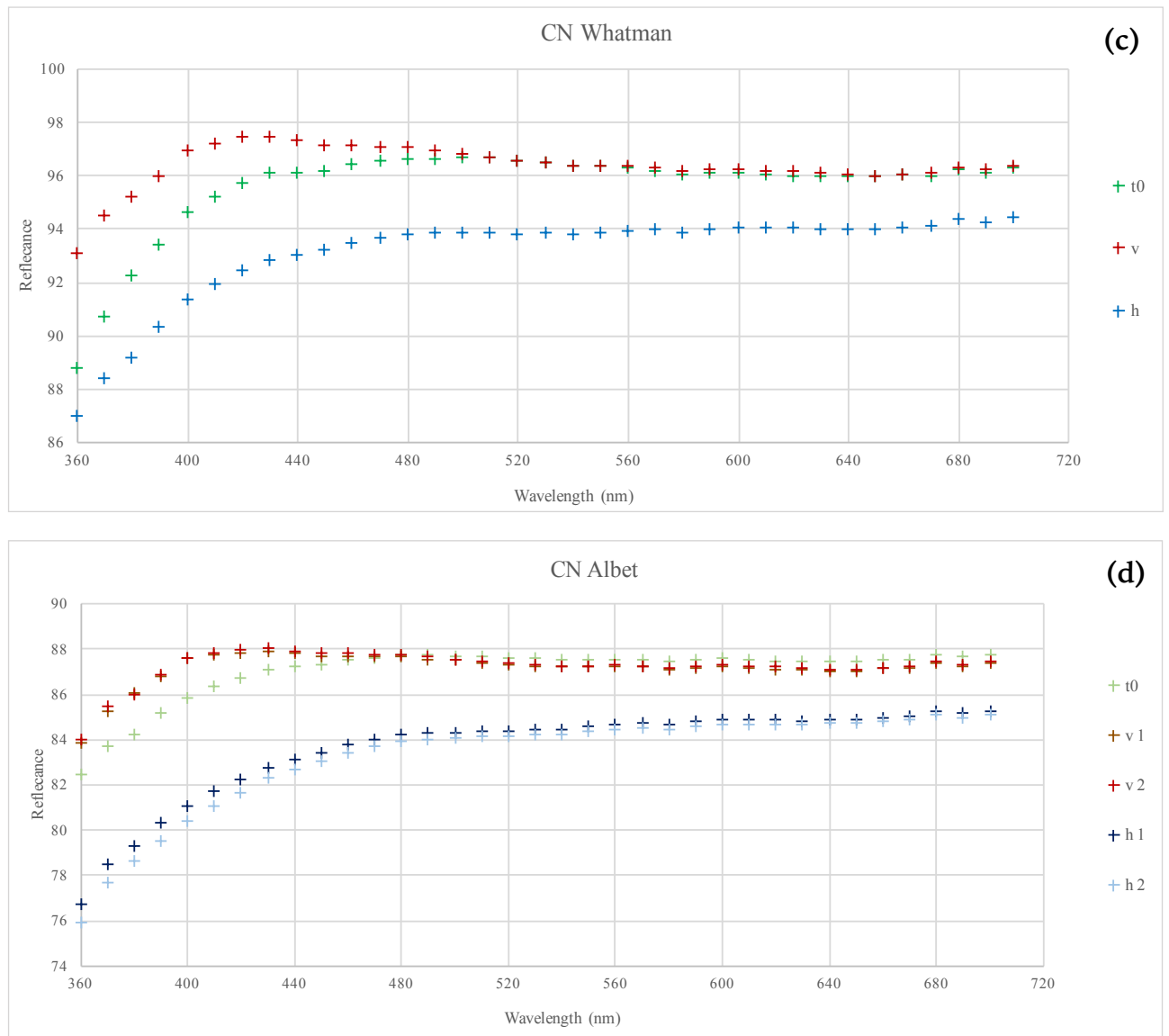


Figure 3.7. Reflectance spectra of (a) CA, (b) RC, (c) CNW and (d) CNA samples;  $+ t(0)$  = non-exposed sample;  $+ h$  = horizontally-exposed sample;  $+ v$  = vertically-exposed sample; 1 = DepBox 1, 2 = DepBox 2.



Table 3.1. Calculated  $\Delta L$ ,  $\Delta a$ ,  $\Delta b$  and  $\Delta E$  values for the different samples. *h* = horizontal; *v* = vertical; *DB* = DepBox.

Sample	$\Delta L$	$\Delta a$	$\Delta b$	$\Delta E$
CA h	-1.63	-0.29	1.51	2.24
CA v	-0.03	-0.01	-0.34	0.34
RC h	-1.21	0.34	1.16	1.71
RC v	-0.08	0.45	0.13	0.48
CNW h	-0.97	0.20	0.40	1.07
CNW v	0.05	0.28	-0.56	0.63
CNA h DB1	-1.39	-0.01	0.82	1.61
CNA h DB2	-1.29	0.02	0.69	1.46
CNA v DB1	-0.13	0.16	-0.50	0.54
CNA v DB2	-0.09	0.18	-0.52	0.56

The colour measurements confirm the general visual observations: in general, the total colour change  $\Delta E$  is not very high in absolute ( $\Delta E < 2.5$ ) but higher for the horizontal samples in every case, expressing the greater soiling effect on horizontal samples than on vertical samples. By comparing visual appearance and colour measurements, the colour variations of the surfaces result perceptible when  $|\Delta L| \geq 1$ , according to Diamanti et al [39]. We can finally notice that the values obtained for the CNA substrate, which samples were spread between the two DepBoxes, express the reproducibility of the devices.

The specific variations in colour components contributing to the total colour change are given by the  $\Delta L$ ,  $\Delta a$  and  $\Delta b$  values and presented in Figures 3.8, 3.9 and 3.10 for a better interpretation.

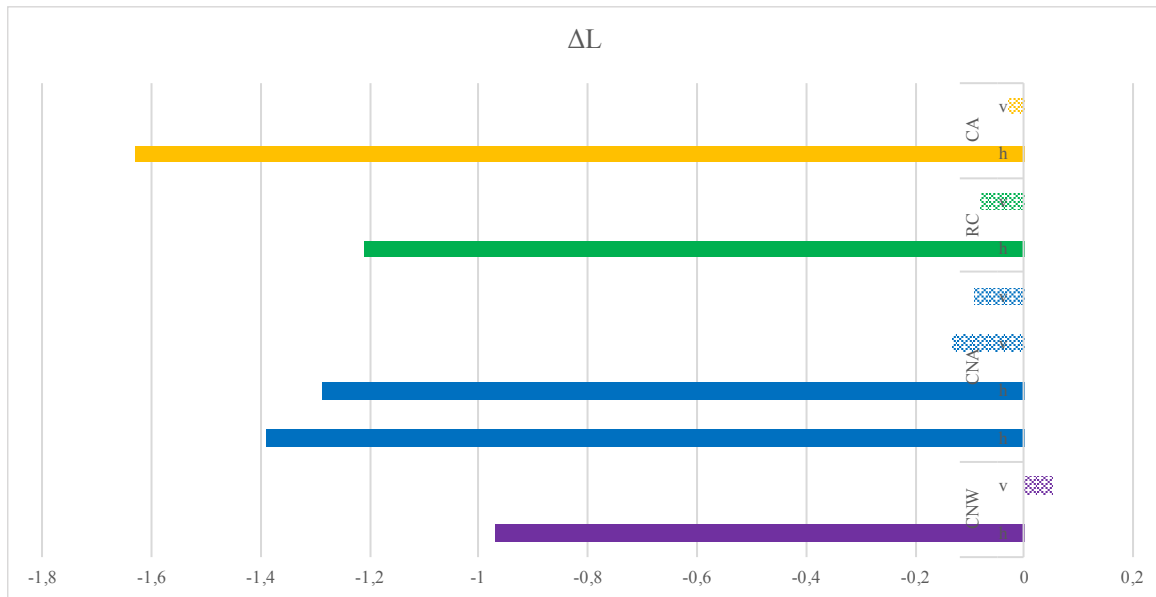


Figure 3.8.  $\Delta L$  variations for all membrane filters samples.

According to the reflectance measurements, for every substrate, the lightness value  $L^*$  decreases for both horizontal and vertical samples. Horizontal samples show  $L^*$  decreases from -0.98 (CNW) to -1.63 (CA), while vertical samples present very low decreases of  $L^*$  value ( $|\Delta L| < 0.2$ ), except for CNW v which shows a small increase.

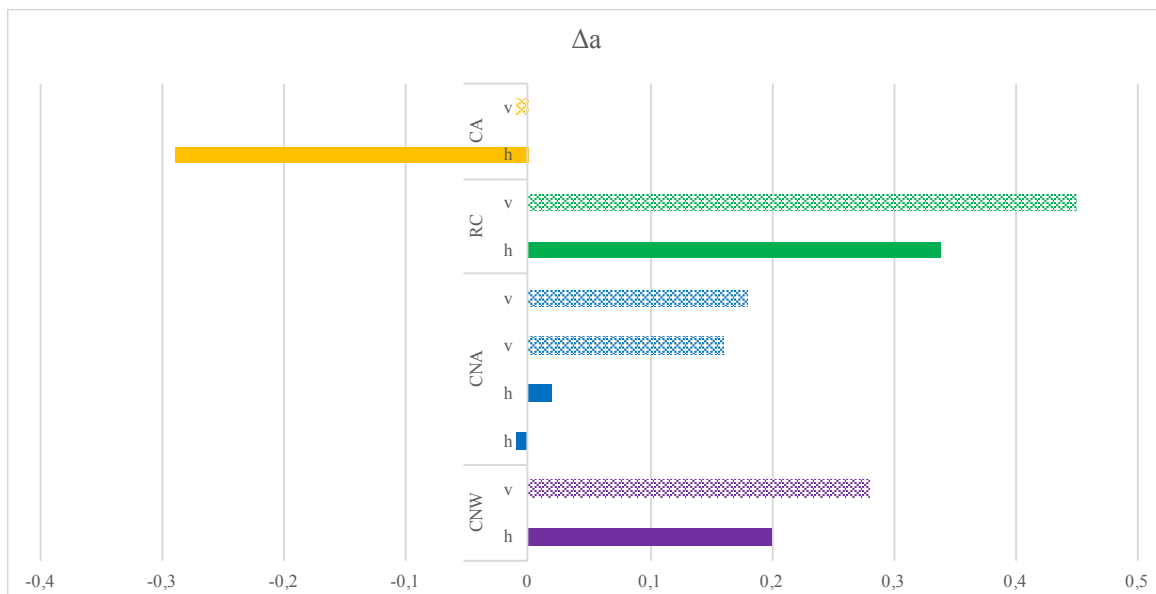


Figure 3.9.  $\Delta a$  variations for all samples.

Globally, the variation in the red-green component ( $a^*$ ) is not really significant: the maximum difference is reached by the RC vertical sample ( $|\Delta a|_{\max} = 0.45$ ). RC shows the highest difference both for horizontal and vertical samples, by having a more reddish color than the not-exposed one. This confirms the visual observation made for the horizontal sample. CNW substrate shows the same trend as RC, with lower value changes. The CNA substrate is interesting as its horizontal samples exhibit a negligible variation compared to the other substrates. CA is the only substrate which samples appear more green after the exposure.

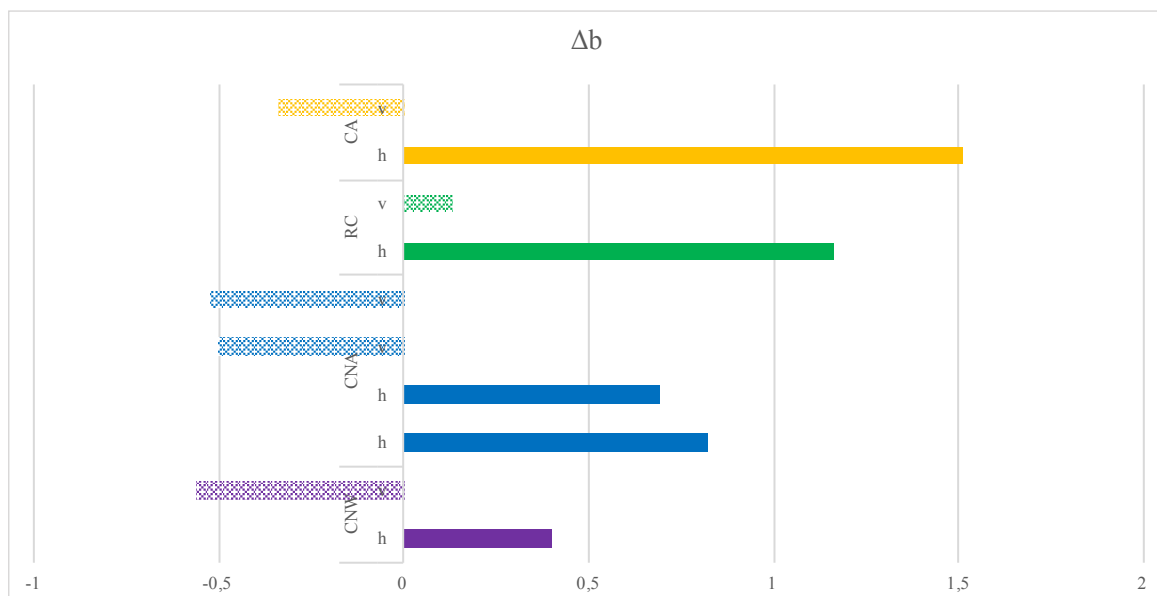


Figure 3.10.  $\Delta b$  variations for all samples.

As regards the yellow-blue component ( $b^*$ ), all substrates but RC present the same kind of variation: the horizontal samples tend to be more yellow after the exposure, as visually noticed, when the vertical samples colour is bluer. RC is the only substrate which both horizontal and vertical samples tend to be more yellow.

The colour measurements confirm the appearance changes visible to the naked-eye. The horizontal samples are the most affected by the soiling effect by showing darker surfaces than the vertical-exposed samples and the blank. The main parameter determining the total colour change is the lightness variation for all horizontal samples, when this is not true for the vertical ones, which  $\Delta E$  values are more influenced by variations in the red-green and yellow-blue components. Samples colour tend to be redder (except the CA substrate which looks greener) and more blue or yellow depending on the substrate orientation. This difference might be explained by the type of particles that get deposited on the substrates, as coarse particles due to sand or soil resuspension generally tend to be more brown/yellow and should mainly deposit on horizontal surfaces.

### 3.2.3. PM deposition

As the exposure resulted in a deposit of particles, the corresponding mass was determined, in the way exposed for the preliminary exposure: the mass of deposited particles is calculated by the difference between the mass of samples after and before the exposure.

This behavior is due to the DepBox, which has been designed to mime the dry deposition process only. Any possible particle removal mechanism is avoided. Real surfaces exposed to the atmosphere are subjected to different mechanisms, with either a positive contribution in the particles deposition, like brownian diffusion, or a negative contribution, as rain runoff. A lot of different depositional contexts thus can happen according to the place, the weather or the degree of pollution. As exposed in the original work in which the DepBox was

designed [2], the device was built to obtain repeatable samples in terms of deposited mass and to study the deposition with a seasonal time scale.

Our exposure session allowed to collect as a maximum 5,26 mg of particles on the aluminium foils, and as a minimum 0.5 mg on the vertical CNA samples, which were enough to perform chemical analyses. Figure 3.11 reports the PM masses deposited on each substrate.

Aluminum foils collected a greater quantity of particles, either considering vertical or horizontal samples (Figure 3.11 (a)). This difference is significant and can be explained by the surface properties. The metallic surfaces appear to capture and keep more particles than the studied membrane filters surfaces. This behavior of a metallic surface can be due to the electrostatic interactions between the surface and the airborne particles. Atmospheric dusts are highly charged [6], and might be attracted by the aluminum surfaces, whatever their orientations, when arriving close to them. When not considering the aluminum foils (Figure 3.11 (b)), any statistical difference is observed among the substrates: the same mass of PM was deposited on all horizontal samples, and the same observation is made for the vertical samples. However, we observe a clear distinction between the exposure orientations. All of those observations are confirmed by statistical tests (two ways ANOVA,  $\alpha = 0.05$ ). Any difference can be noticed between the Deposition Boxes (Figure 3.11 (c)) concerning the PM deposition, which definitely confirms the efficiency of DepBox to realise repeatable conditions for dry exposure.

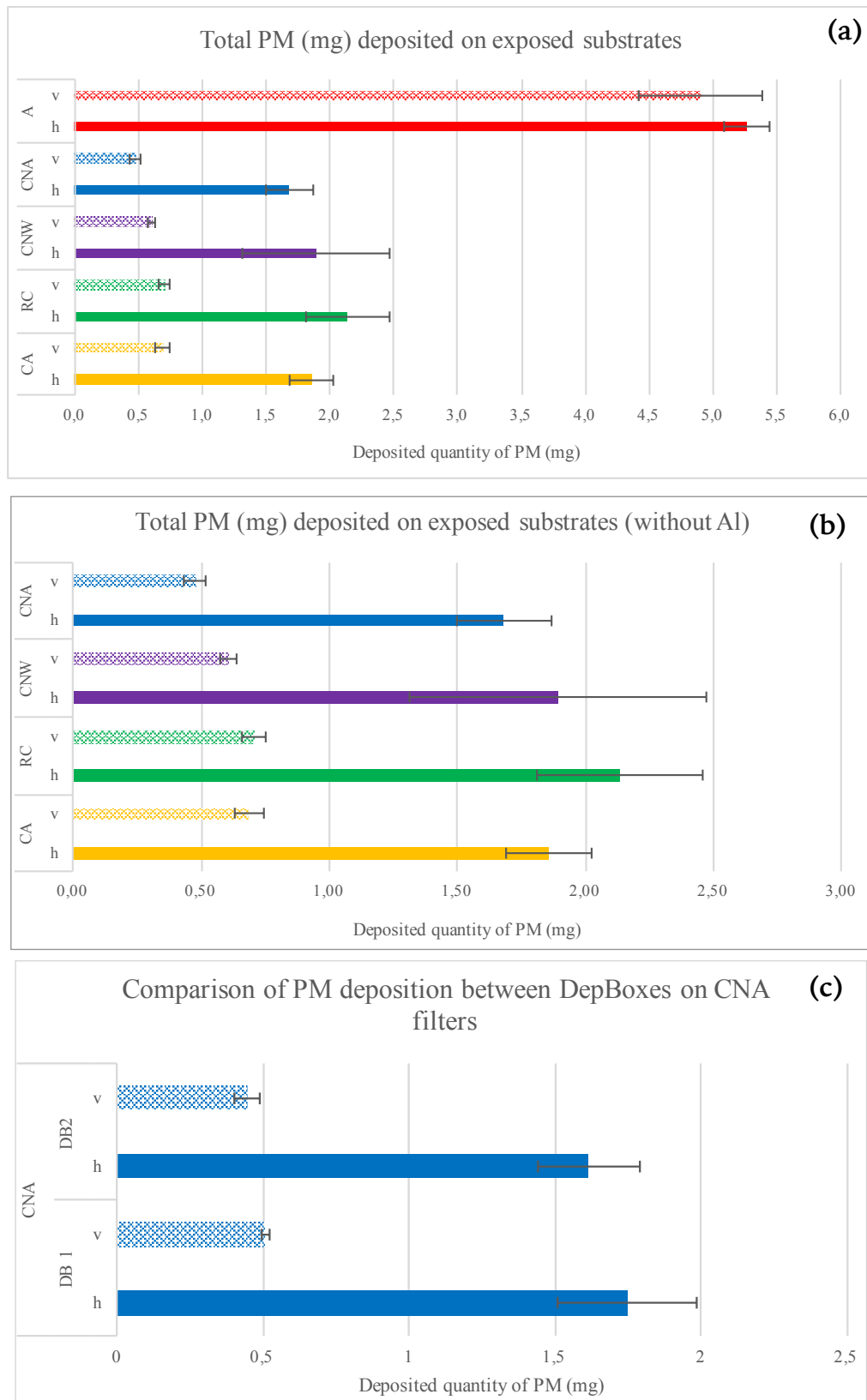


Figure 3.11. Quantity of PM (mg) deposited (a) on all substrates, (b) on all substrates but aluminium foils, (c) on the CNA substrate with a comparison between the DepBoxes (DB). Averages of at least 3 samples and relative standard deviations are reported. All the substrates had the same exposure area equal to 11.95 cm<sup>2</sup>.

### 3.2.4. Deposition rates

From the mass of deposited particles, the deposition rates were determined, according to equation 1.

$$D_{\text{rate}} = \frac{m_{\text{dep}} \cdot 1000}{A \cdot \text{days}} \cdot 30 \quad (\text{equation 1})$$

with  $D_{\text{rate}}$  = Deposition rate ( $\mu\text{g}/\text{cm}^2\text{month}^{-1}$ ),  
 $m_{\text{dep}}$  = mass of deposited particles (mg),  
 $A$  = area that collected particles ( $\text{cm}^2$ ),  
 days = days of exposure.

The deposition rates are given in Table 3.2 and represented in Figure 3.12.

*Table 3.2. Deposition rates calculated for each substrate as average of at least 3 samples. h = horizontal; v = vertical*

Substrate	CA		RC		CNW		CNA		A	
Orientation	h	v	h	v	h	v	h	v	h	v
$D_{\text{rate}}$ ( $\mu\text{g}/\text{cm}^2\text{.month}^{-1}$ )	74	27	85	28	75	24	67	19	210	195
standard deviation	7	2	13	2	23	1	7	2	7	19

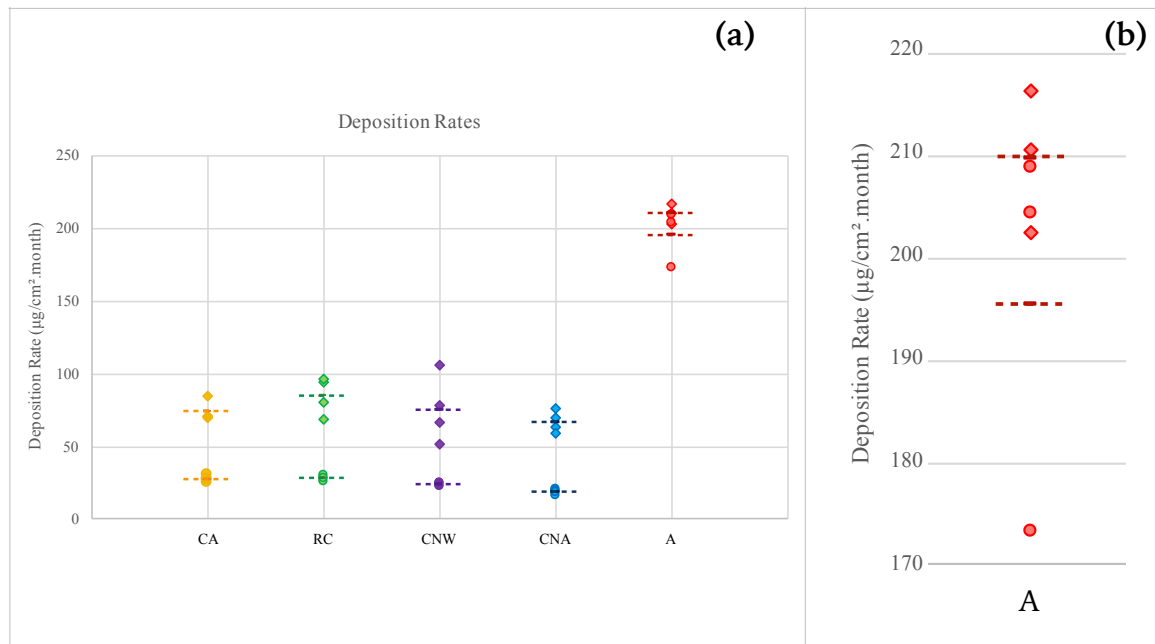


Figure 3.12. Deposition rates (a) of all exposed substrates, (b) zoom for aluminum samples. ♦ = horizontally-exposed sample, ● = vertically exposed sample; - - - = means of considered samples.

The deposition rates ranged from a minimum of  $19.0 \pm 1.7 \mu\text{g}/\text{cm}^2 \text{ month}^{-1}$  for CNA substrate in vertical position, to a maximum of  $210 \pm 7 \mu\text{g}/\text{cm}^2 \text{ month}$  for the horizontal positioned aluminium foils. The earliest conclusions about the deposition rates can be drawn by applying a two factors ANOVA test ( $\alpha = 0.05$ ) to the entire deposition rate range. It is clear that there is a difference between the different types of substrates and the different exposure orientations. However when considering only the 4 substrates, no statistical difference is noticed among the substrates when there is a noticeable difference between the horizontal and vertical samples (ANOVA,  $\alpha = 0.05$ ). As already observed, the aluminum foils are the exposed samples which present a greater deposition rates compared to the other substrates, and we can conclude that the deposition rates are not significantly different (two tails t-test,  $\alpha = 0.05$ ) for the horizontal and the vertical samples (Figure 3.12, (b)).

The results obtained for the 4 membrane filters are in accordance with previous studies. In particular, the work realised by Anaf et al. [40] consider the



difference between depositions on indoor horizontal and vertical membrane filters and the same tendency than in our case is observed. The deposition rates however appeared to be lower than ours due to the indoor exposure conditions. In the work realised by Ferm et al. [20], samples of different materials (e.g glass and stainless steel) were exposed in sheltered conditions. Here again, a clear difference is noticed between horizontal and vertical samples, but the deposition rates measured were a bit lower than during our work. This is probably due to the conditions of exposure: even if the exposed materials were sheltered under a large roof, according to the speed and the orientation of the wind and the rain, mechanisms of removal can operate. In dry deposition, fluxes can strongly depend not only on the atmospheric factors (winds, sampling height, temperature) but also by the exposure conditions of samples. Several studies highlight that relevant difference in the estimated deposition fluxes can rise as a function of both the sampling surface geometry and characteristics [41, 42, 43].

### 3.2.5. SEM-EDX analysis

The SEM-EDX analysis was supposed to be performed on selected samples and stabs that directly collected particles as described in the Experimental part (section 2.3.2 'Exposure of the substrates'). However, when removing the stabs from the Deposition Boxes, we observed a lot of volatile poplar "fluff" was deposited on them (Figure 3.13). We finally decided to not analyse them as this biological material make highly difficult the observation of the underlying particulate and, due to the vacuum applied, it could have been dispersed within the SEM chamber damaging the device.

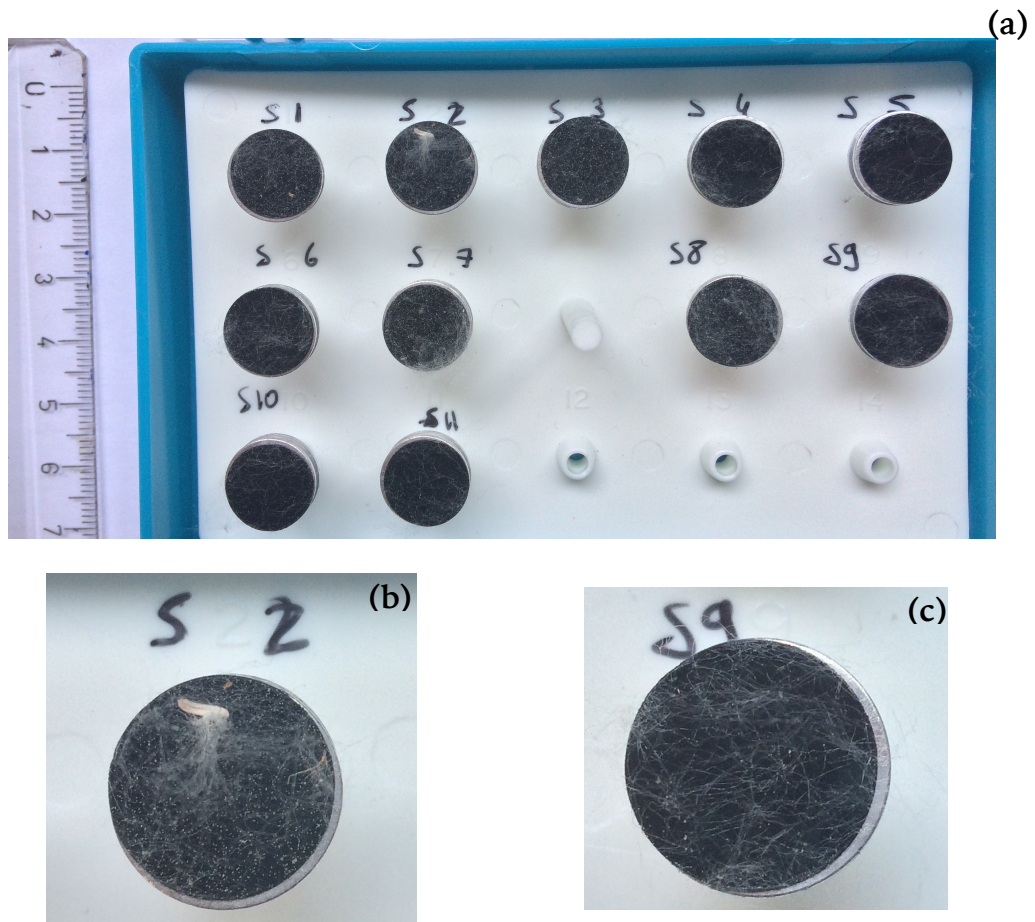


Figure 3.13. Appearance of the stubs after exposure (a) all of them, (b) one horizontally-exposed, (c) one vertically-exposed.

As expected, from a general point of view the microscopic observations reflect the general trend already pointed out by the previous analyses: a higher amount of atmospheric particles on the horizontally-exposed samples than the vertically-exposed ones, as visible on examples given in Figure 3.14. Anyway SEM-EDX analyses can provide information also on the shape, dimension, source and composition of the deposits.

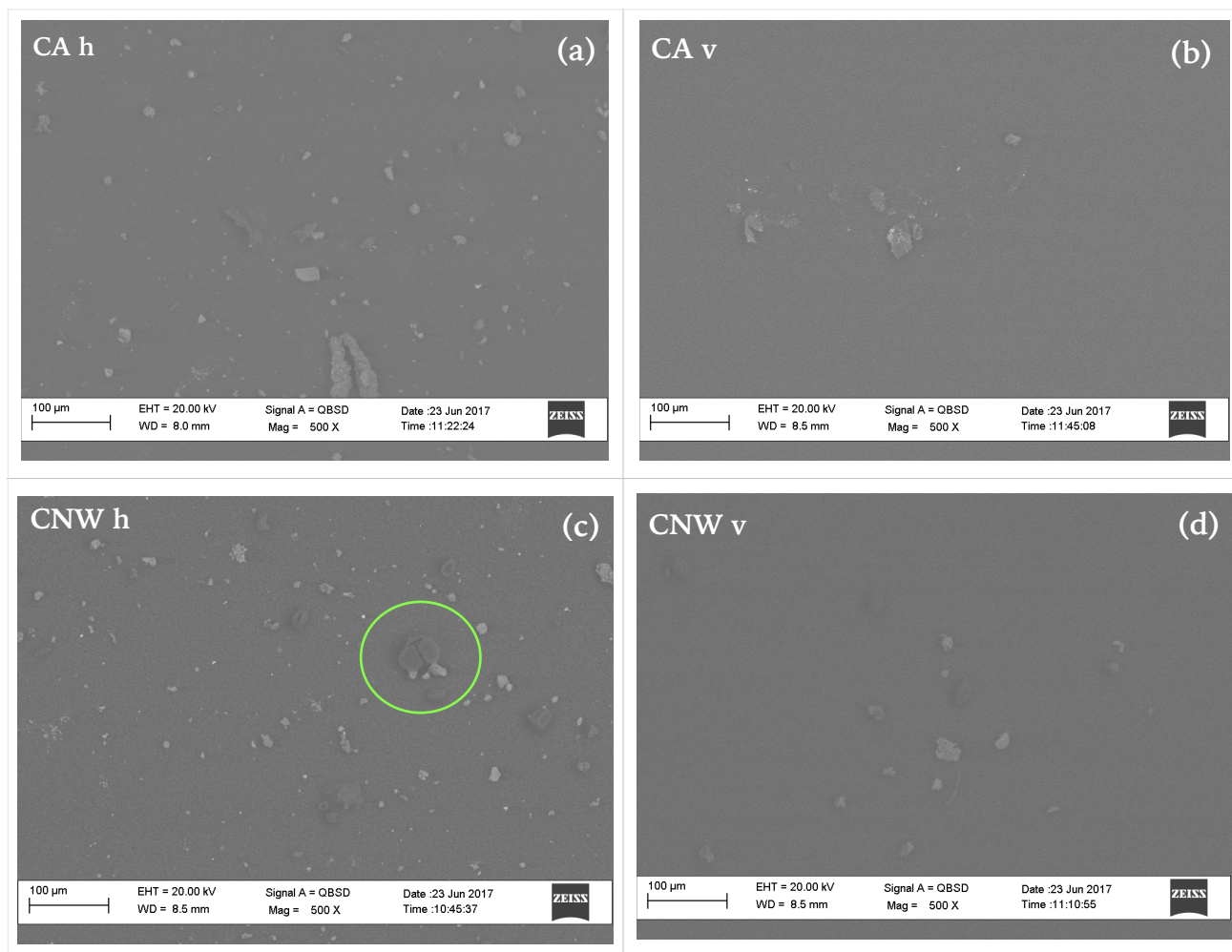


Figure 3.14. SEM images at 500X magnification for (a) horizontally-exposed CA, (b) vertically-exposed CA, (c) horizontally-exposed CNW, (d) vertically-exposed CNW. ○ = biogenic particle.

The presence of organic biogenic particles was clearly observed on the surface of each sample, especially on the horizontal ones, as the one in the green circle that can be seen on Figure 3.14 (c). As the exposure process occurred during spring, characterized by pollen being carried out a lot by the wind, their presence is expected.

Silicates were found on all of the horizontally exposed samples with a weight % between 0.13 (CNW & RC) and 1.54 (CA). Other crustal elements such as Al and Ca were also detected. Their proportions are given in Table 3.3.

Table 3.3. Weight % of some crustal elements found on the horizontal samples (from EDX maps at 500X magnification).

		Si K				
		CA h	RC h	CNW h	CNA h	A h
Weight %		1.54	0.13	0.13	0.31	0.43
$\sigma$		0.06	0.01	0.01	0.01	0.02
		Al K				
		CA h	RC h	CNW h	CNA h	A h
Weight %		0.4	0.05	0.15	0.08	70.88
$\sigma$		0.06	0.01	0.01	0.01	0.42
		Ca K				
		CA h	RC h	CNW h	CNA h	A h
Weight %		2.15	0.15	0.21	0.38	0.25
$\sigma$		0.06	0.01	0.01	0.01	0.01

Specific kind of particles were identified during the observation and characterized by recording EDX spectra, as can be seen, as an example, on Figure 3.15 for the CA horizontal sample.

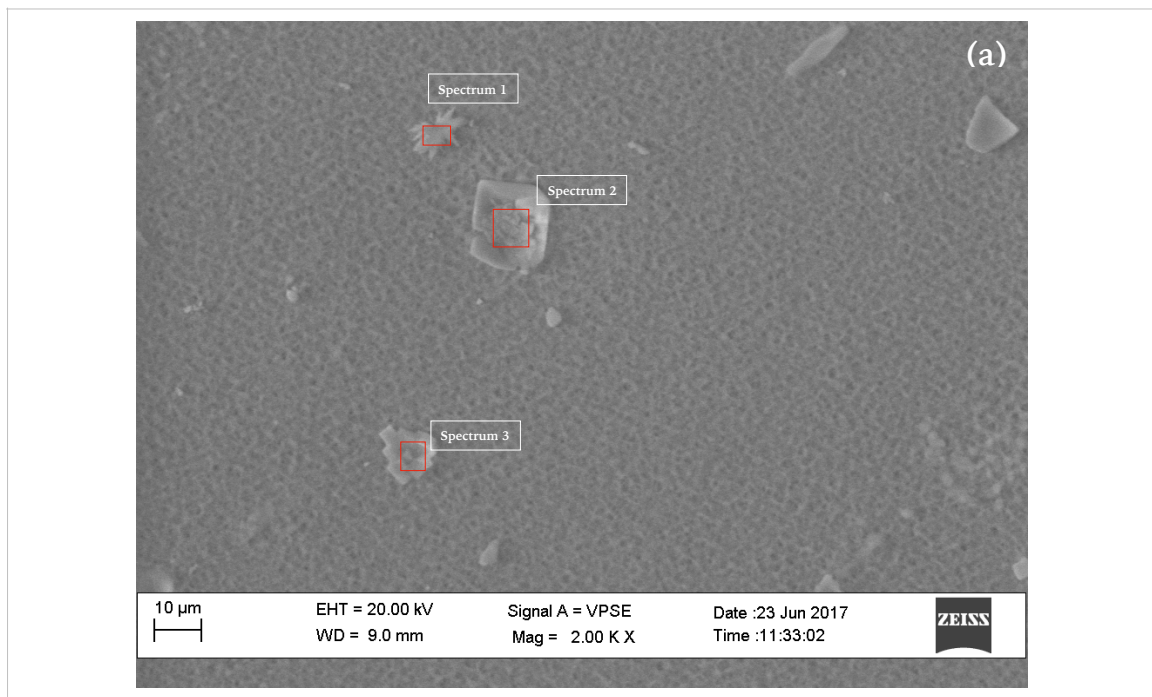


Figure 3.15

follows...

... continues

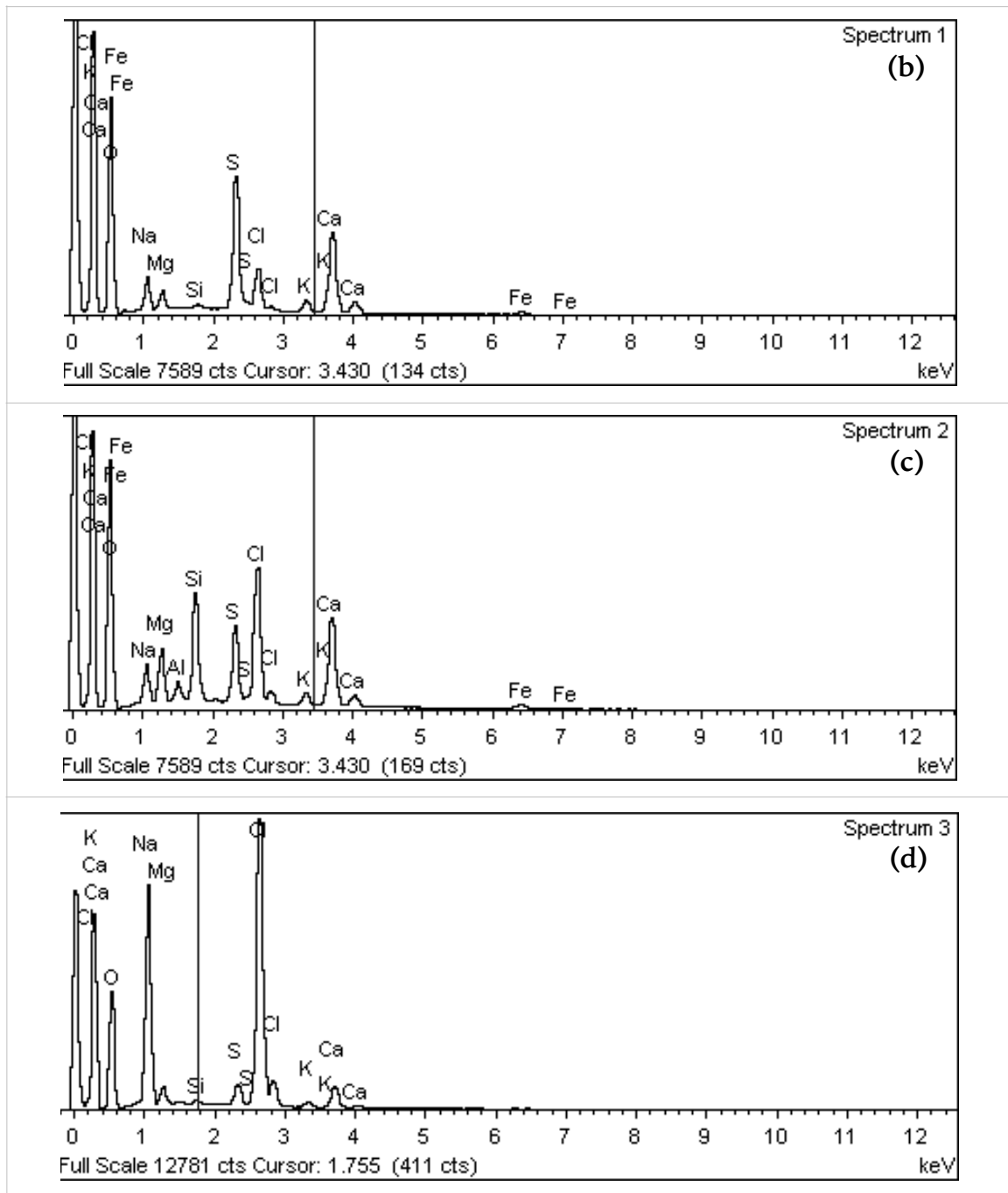


Figure 3.15. (a) SEM image of CA horizontal sample with location of specific spectra recorded. (b) corresponding EDX spectrum 1, (c) corresponding EDX spectrum 2, (d) corresponding EDX spectrum 3. The elements identified by EDX and their corresponding weight % are given in Appendix B.

The particles from which the spectrum 3 was taken correspond to NaCl aggregated crystals. Its characteristic pattern was identified in previous studies [44]. Pósfai et al. [45] studied marine aerosols and observed that sulfates of Na and Ca with minor K and Mg can form on NaCl crystals. This observation may correspond to the gathered particles analysed as spectrum 2. Mixed-cations sulfates have a long shape, appearing in the form of needles as exposed in the work of Pósfai et al. [46]. The deposited particles analysed as spectrum 1 correspond to this shape and the elemental composition confirms this idea.

Identified elements on the samples indicate that a significant amount of particles seem to originate from the sea, in agreement with the main direction of the winds during the exposure period (Figure 3.16).

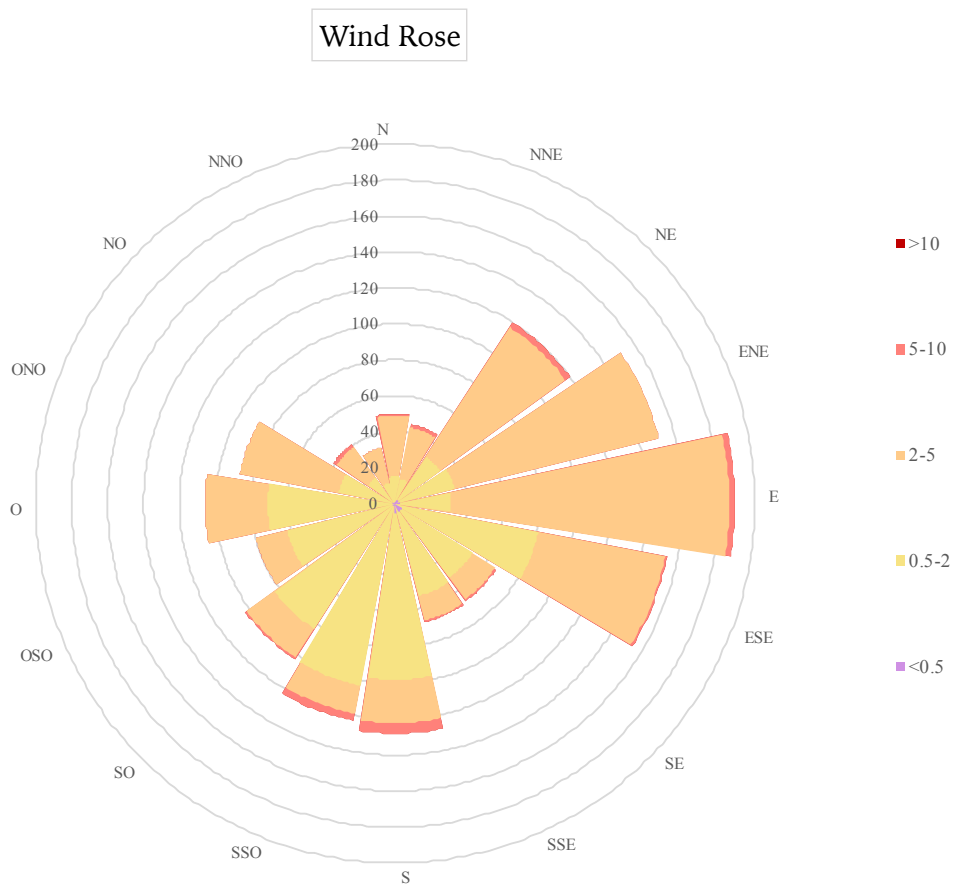


Figure 3.16. Wind rose based on ARPAE atmospheric data recorded during the exposure period. The wind speeds (m/s) are shown in different colors.

The wind originated mainly from East (ENE, E, ESE), which corresponds to the direction of the sea, and had a speed included between 2 and 5 m/s. We notice that winds also originated from the South direction (S, SSO), which correspond to an urban area, with a general slower speed (0.5-2 m/s). An interesting particle was clearly identified on the horizontal CNW sample, as presented in Figure 3.17.

The EDX spectrum allowed us to identify the particle as being iron oxide (FeO). The particular spherical shape of the particle is indicative of any high-temperature process, including combustion or smelting [47]. This is the only one observed on the selected CNW sample, and indicates the presence of some particles also from anthropogenic sources.

Summarising, the SEM-EDX analysis reveals the presence of big biogenic particles, which present characteristic shape and form. Crustal elements such as Si, Ca, Al were identified, as well as element originating from the marine aerosols (Na, Cl). Aggregates of NaCl crystals have been found on different substrates as well as the presence of mixed-cation sulfates. Other elements and more specifically metals were also identified (e.g. K, Cu, Fe) that can originate from both natural and anthropogenic sources: an anthropogenic part of particle was testified during the analysis with the clear identification of anthropogenic FeO.

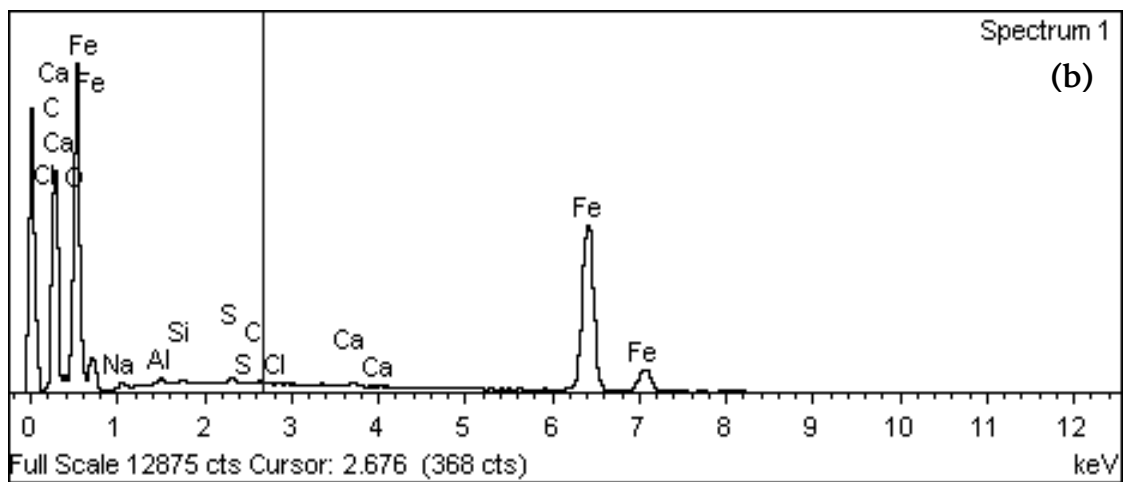
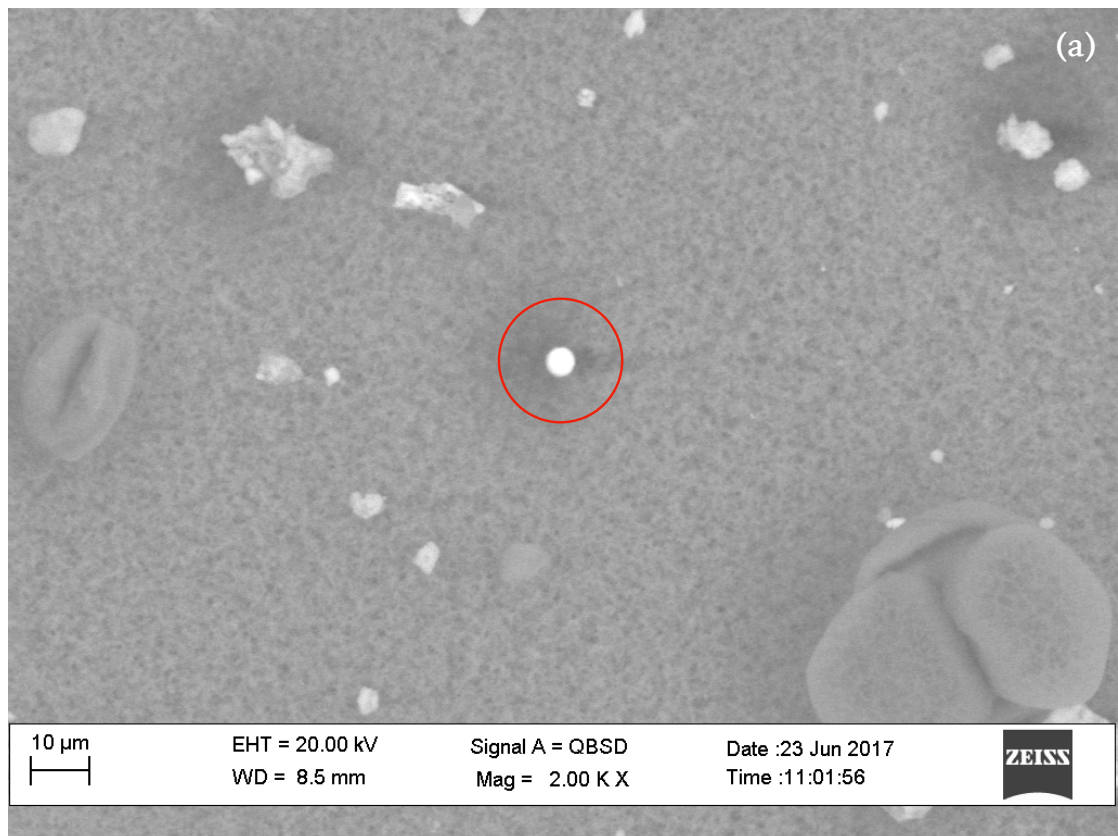


Figure 3.17. SEM image of horizontally-exposed CNW. (a) Iron oxide particle (inside the red circle) and (b) its corresponding EDX spectrum.



### 3.2.6. Treatment of SEM images by Image J

SEM images were processed through the free software Image J. The particles have been separated from the matrix by means of a lightness threshold value, and the particles were counted as a function of the area of their visible side with the use of the 'Analyse particles' plugin (Figure 3.18). An estimation in term of geometrical equivalent diameter was also given, on the basis of the area of the visible side of the particles and by assimilating them to spherical particles.

The Image J software allows us to count precisely the number of particles, and also to determine their visible area. Data obtained from one representative SEM image (500X) per substrate are gathered in Table 3.4.

By comparing data, we observe that more particles deposited on the horizontal selected zones (with a mean of 231 particles, all substrates considered) than on the vertical selected ones (with a mean of 65 particles, both substrates considered). The areas of the visible side of particles vary in a quite big range, from  $0.3 \mu\text{m}^2$  for vertical CA to  $5627.2 \mu\text{m}^2$  for horizontal CNW. The particles deposited on the horizontal surfaces can reach bigger sizes than the ones on the vertical surfaces.

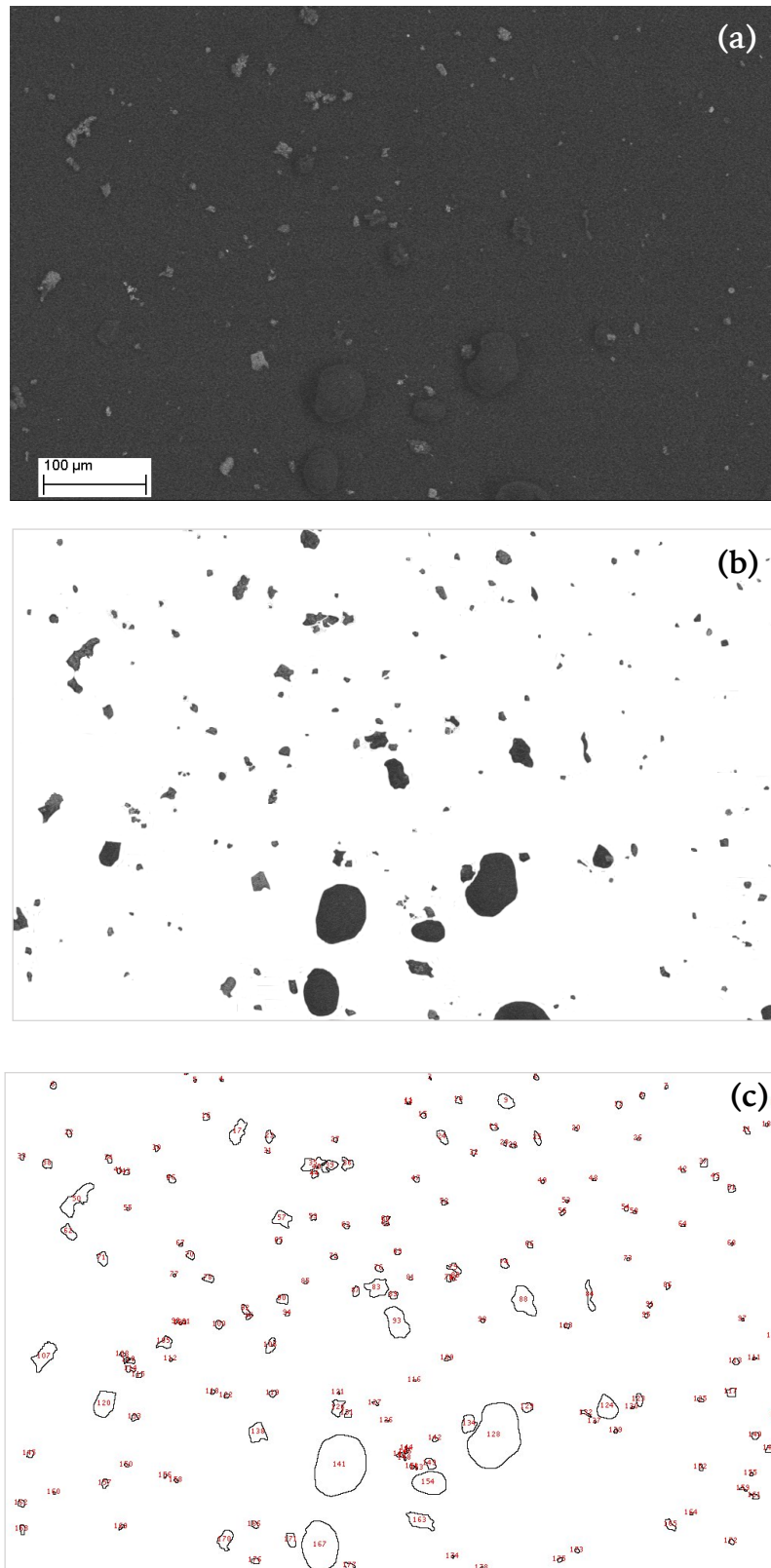


Figure 3.18. Example of SEM image processed through the Image J software. (a) Original SEM image of horizontal RC sample (BSE, 500 x), (b) removal of the background, (c) image analysed with particles counted.

Table 3.4. Number (Nb particles) and visible areas (A,  $\mu\text{m}^2$ ) of particles on selected zones of the substrates (500X magnification), calculated through Image J software.

Horizontal samples					
Filter	CA 3	RC 2	CNW 2	CNA 1	A2
Zoom	500x	500x	500x	500x	500x
Nb particles	283	179	228	224	239
mean A ( $\mu\text{m}^2$ )	52.5	85.3	172.7	92.6	87.7
max A ( $\mu\text{m}^2$ )	2153.1	2353.5	5627.2	4266.3	1509.6
min A ( $\mu\text{m}^2$ )	0.6	0.5	1.1	0.5	0.6
Vertical samples					
Filter	CA 6		CNW 5		
Zoom	500x		500x		
Nb particles	80		47		
mean A ( $\mu\text{m}^2$ )	48.7		84.3		
max A ( $\mu\text{m}^2$ )	1084.5		562.3		
min A ( $\mu\text{m}^2$ )	0.3		2.2		

To give an indication of the dimensional distribution of the collected particles, the calculated visible areas were counted and divided into four ranges (Figure 3.19). As range limits, the visible areas corresponding to particles with aerodynamic diameters values usually adopted to classify PM were used.

Actually, PM can be classified in 4 categories according to the aerodynamic diameter ( $D_a$ ):

- ultra-fine particles ( $PM_{<0.1}$ ), which particles are lower than 0.1  $\mu\text{m}$  in  $D_a$ ,
- fine particles ( $PM_{0.1-2.5}$ ), with  $D_a$  ranging from 0.1 to 2.5  $\mu\text{m}$ ,
- coarse particles ( $PM_{2.5-10}$ ), which particles  $D_a$  range from 2.5 to 10  $\mu\text{m}$ ,
- ultra-coarse particles ( $PM_{>10}$ ), with  $D_a$  higher than 10  $\mu\text{m}$ ,

corresponding to the following ranges in term of “visible area” ( $A_v$ )

- ultra-fine particles:  $A_v < 0.031 \mu\text{m}^2$ ,
- fine particles:  $0.031 \mu\text{m}^2 \leq A_v < 19.6 \mu\text{m}^2$ ,
- coarse particles:  $19.6 \mu\text{m}^2 \leq A_v < 314.2 \mu\text{m}^2$ ,
- ultra-coarse particles:  $A_v \geq 314.2 \mu\text{m}^2$ .

Particle size distribution trends to appear similar for horizontal surfaces, with coarse and fine particles being the most represented classes. Not relevant differences between these two classes can be observed as for CNW, CNA and A, fine particles were the majority of recorded particles, for RC more or less the same number of both fine and coarse particles was obtained and for CA the greater amount was that of coarse particles. In any case, for a given substrate, the difference in number between fine and coarse particles is always not higher than 40. Considering that the differences among substrates results are not so high even if only one SEM image per substrate has been elaborated with Image J at the moment, we can expect the number and the dimensional distribution of the particles observable with SEM to be similar when considering more samples. Trends vary for vertical surfaces, that are clearly enriched in fine PM. None ultra-fine particle was identified for any substrate independently from the orientation, because the visible area corresponding to the instrumental detection limit related to the resolution of SEM images acquired has been estimated in  $0.4 \mu\text{m}^2$ .

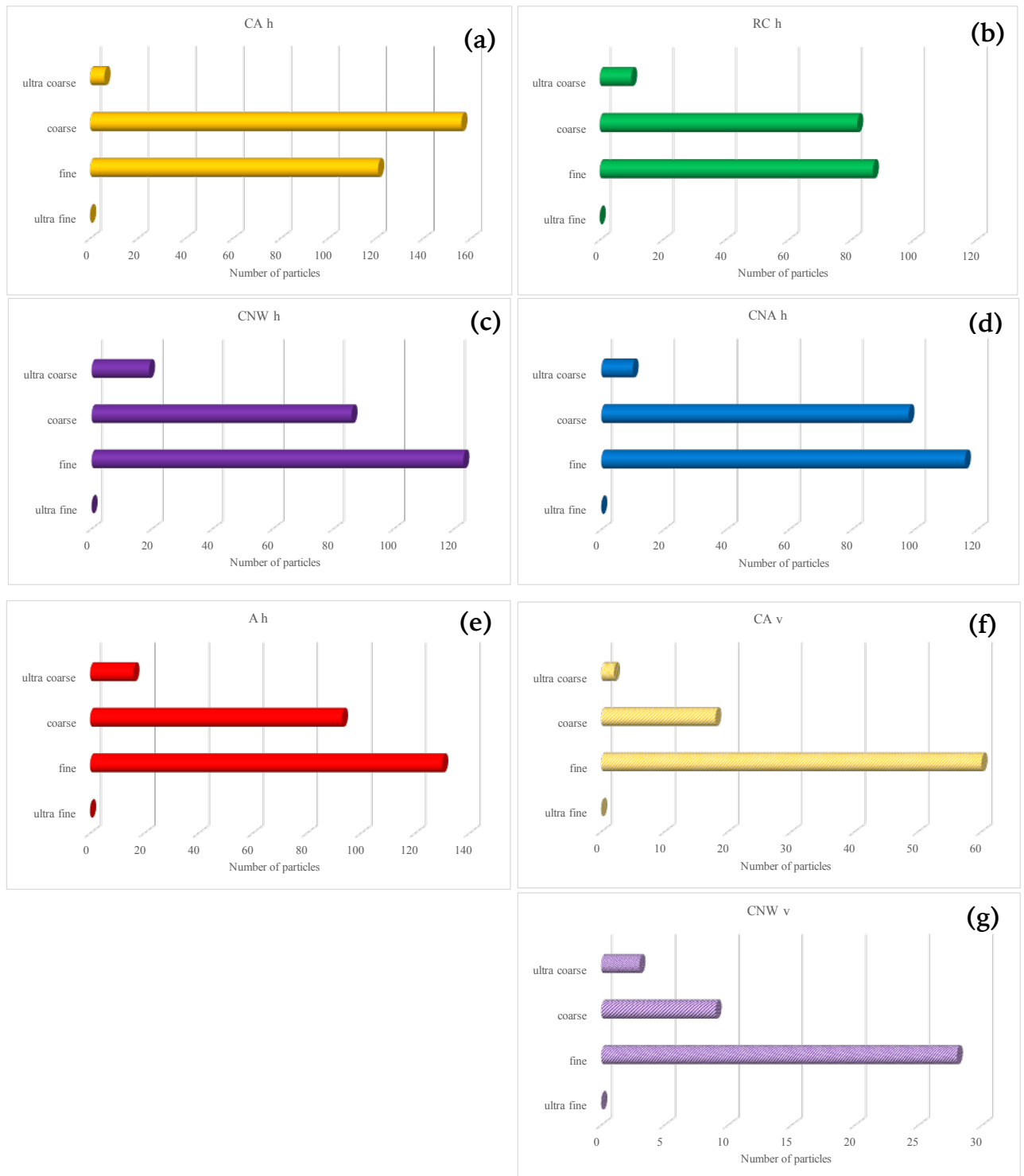


Figure 3.19. Particles distribution according to their visible area ( $\mu\text{m}^2$ ) for: (a) horizontal CA, (b) horizontal RC, (c) horizontal CNW, (d) horizontal CNA, (e) horizontal A, (f) vertical CA, (g) vertical CNW.

Overall, the treatment of SEM images by Image J software shows that a higher number of particles deposit on horizontal substrates. Fine particles can deposit either on vertical or horizontal samples. However, bigger particles, being part of the coarse and, in a lesser extent, extra coarse fractions mainly deposit on horizontal surfaces. Very small differences in term of number of particles and their distribution can be noticed between the substrates exposed with the same orientation, which may be attenuated with the time of exposure. These findings tend to confirm that main mechanisms of deposition are different between the two exposure orientations. Gravitational settling, mainly acting on the deposition of coarse particles, is one of the mechanisms occurring for horizontal surfaces when this process does not have considerable effect for vertical surfaces.

### 3.2.7. Ionic composition of the PM soluble-fraction

The same ions as the ones analysed during the preliminary exposure were investigated: Cl<sup>-</sup>, NO<sub>2</sub><sup>-</sup>, NO<sub>3</sub><sup>-</sup>, SO<sub>4</sub><sup>2-</sup> among the anions, and Na<sup>+</sup>, NH<sub>4</sub><sup>+</sup>, K<sup>+</sup>, Ca<sup>2+</sup>, Mg<sup>2+</sup> among the cations. Nitrites were not taken into account in the following discussion as the concentration was below the limit of detection for a majority of samples.

- Anions

In term of weight, the major part of the anions contained in soluble salts of PM deposited on the surfaces and investigated by IC is represented by nitrates, reaching  $48 \pm 13$  mg/g<sub>PM</sub> as a maximum value on vertical substrates. The following general trend is observed (Figure 3.20):



The relative amount of the considered anions for all the substrates are reported in Appendix C.

The investigated anions exhibit different trends:

- PM deposited on vertical surfaces is richer in  $\text{NO}_3^-$  than PM deposited on horizontal surfaces (except for aluminium foils). Furthermore, the two ways ANOVA test ( $\alpha = 0.05$ ) allows to highlight no statistical difference on nitrate deposition in term of  $\text{mg/g}_{\text{PM}}$  among the membrane filters, but significant difference between horizontal and vertical samples. Aluminum foils exhibit a different behaviour, with  $\text{NO}_3^-$  being much less present on the deposited particles, either on horizontal or vertical samples, and appear being more present in PM deposited on horizontal aluminum surfaces. In term of absolute amount of nitrate desposit, we can observe higher amount on horizontal surfaces.
- PM deposited on horizontal surfaces is richer in  $\text{Cl}^-$ , as confirmed by two ways ANOVA ( $\alpha = 0.05$ ), and we can see on Figure 3.20 (b) that the total amount of this ion deposited per surface unit is also higher on horizontal surfaces. Furthermore, no chloride was found on vertical RC samples. As chloride is usually more present on coarse particles from sea spray, this finding suggests that coarse particles mainly deposit on horizontal surfaces, which confirms the first observation made by elaborating SEM images through the Image J software. No statistical difference on chloride deposition in term of  $\text{mg/g}_{\text{PM}}$  is noticed among the substrates (ANOVA test and t-test,  $\alpha = 0.05$ ).
- As regards  $\text{SO}_4^{2-}$ , the two ways ANOVA test ( $\alpha = 0.05$ ) allows to highlight no statistical difference on sulfate deposition in term of  $\text{mg/g}_{\text{PM}}$  between the exposure orientations, and in general, there is no difference among the depostion on membranes filters (only CNW exhibit a higher amount than the other membrane filters on vertical samples). PM deposited on Aluminum

foils, contains a much less important concentration in sulfate than the membrane filters. These behaviours are clearly observable on Figure 3.20 (a).

The IC analysis performed after the main exposure campaign confirms the first observations made after the preliminary results. Chloride, characteristic of the coarse fraction of PM was mainly found on horizontal samples and better hold on them; while nitrate, characteristic of the fine fraction, mainly deposited on vertical samples. Sulfate did not show significant difference in its concentration in PM deposited on horizontal and vertical samples suggesting that it could be part of both fine and coarse fraction. In absolute value, it deposited more on horizontal surfaces.

Compared to the membrane filters, the aluminum foils showed that the investigated anions were not so concentrated, considering both the PM composition and the total amount per surface unit, as it would have been expected on the basis of gravimetric measurements (see section 4.2.3 'PM deposition'). One explanation can be the presence of extra big particles, visible by the naked-eye, on the aluminum foils surfaces. The deposition of yellow biogenic particles was one of the first thing characterising those surfaces after exposure (see 4.2.1 'Visual observations'). The big particles have a greater proportion in the deposited mass and can explain the difference between the aluminum foils and the membrane filters.



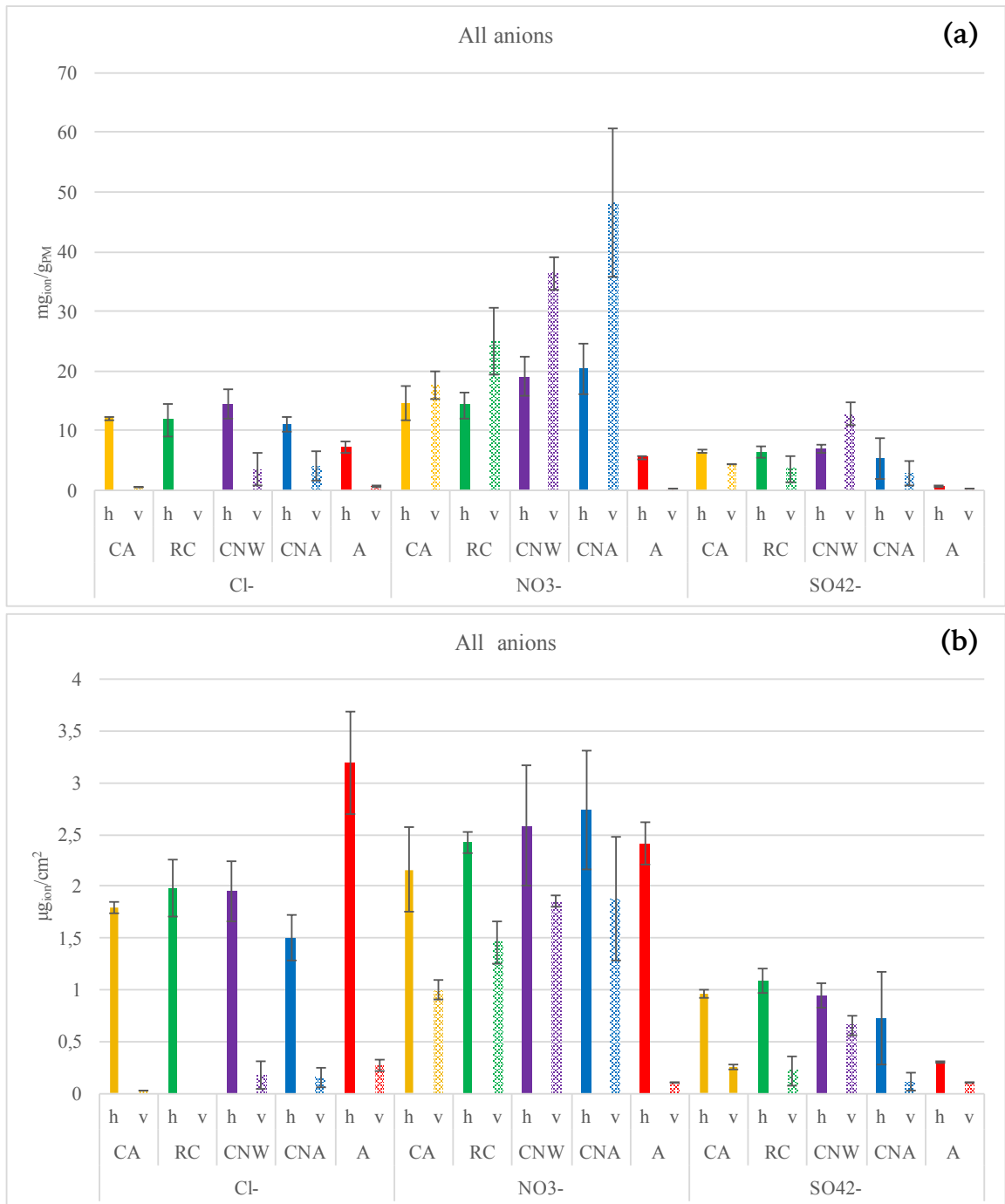


Figure 3.20. Quantity of ions per gram of PM ( $mg_{ion}/g_{PM}$ ) on (a) horizontal and (b) vertical samples and quantity of ions deposited per surface unit ( $\mu g_{ion}/cm^2$ ) on (c) horizontal and (d) vertical samples.

- Cations

Two months of exposure to dry deposition processes to collect amount of all selected cations are suitable to be analysed by IC.

In term of weight, Calcium represents the major part of the investigated cations contained in soluble salts of PM deposited on the surfaces, reaching  $26 \pm 3 \text{ mg/g}_{\text{PM}}$  as a maximum value on horizontal samples. Cations were recorded as the following general trend:

$$\text{Ca}^{2+} > \text{Na}^{+} > \text{NH}_4^{+} > \text{K}^{+} > \text{Mg}^{2+} \text{ in term of weight per gram of PM.}$$

Figure 3.21 shows the amount of cations found on the different substrates both in  $\text{mg}_{\text{ion}}/\text{g}_{\text{PM}}$  and  $\mu\text{g}_{\text{ion}}/\text{cm}^2$ .

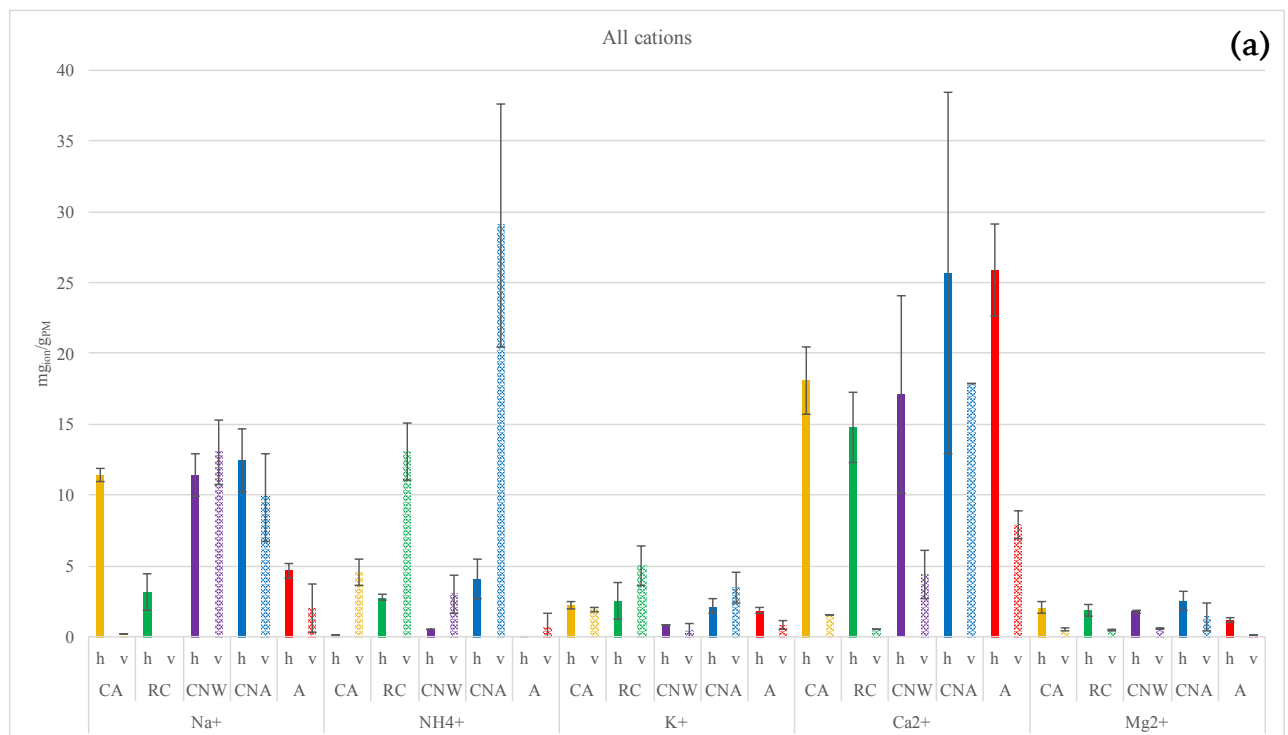


Figure 3.21. Quantity of ions per gram of PM ( $\text{mg}_{\text{ion}}/\text{g}_{\text{PM}}$ ) on horizontal -h- and vertical -v- samples(a) and quantity of ions deposited per surface unit ( $\mu\text{g}_{\text{ion}}/\text{cm}^2$ ) on horizontal -h- and vertical -v- samples (b)

follows...

continues...

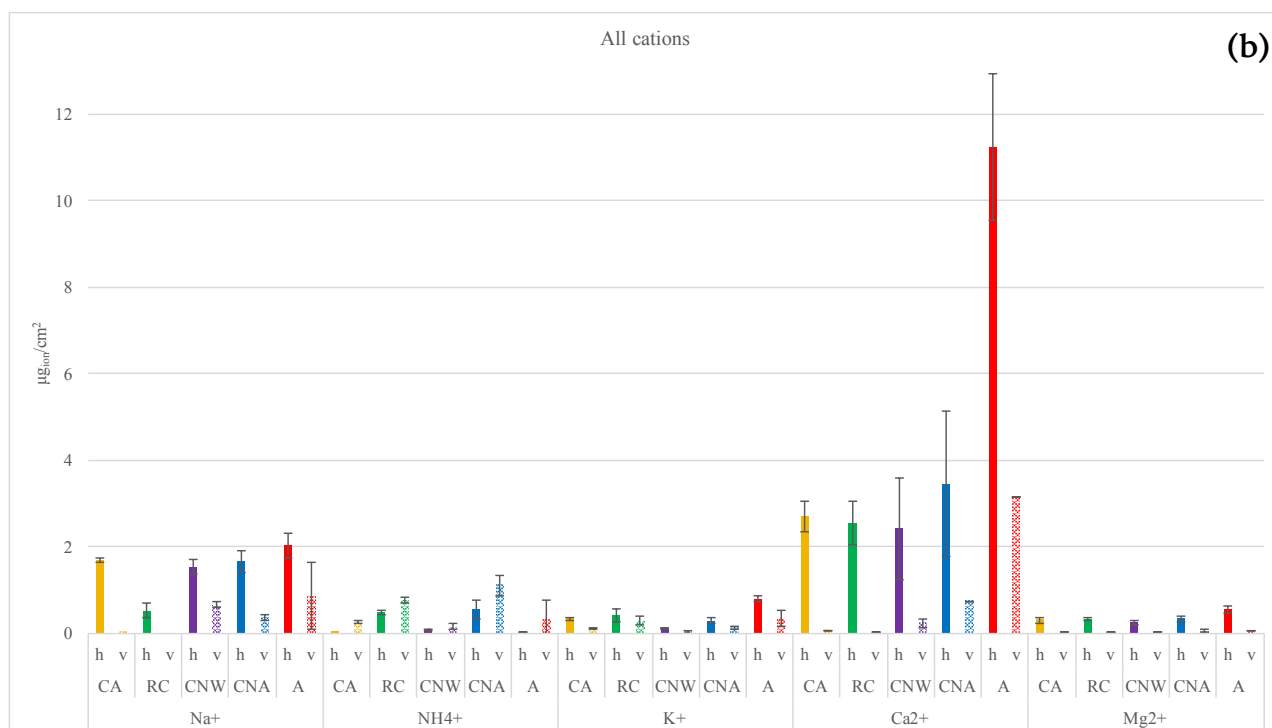


Figure 3.21. Quantity of ions per gram of PM ( $mg_{ion}/g_{PM}$ ) on horizontal -h- and vertical -v- samples (a) and quantity of ions deposited per surface unit ( $\mu g_{ion}/cm^2$ ) on horizontal -h- and vertical -v- samples (b).

As for anions, different trends are recognisable:

- PM deposited on vertical sample is richer in ammonium, and in a lesser extent in potassium. As those cations are characteristic of PM fine fraction, this indicates that fine particles mainly deposited on vertical surfaces. Statistical difference is observed between the exposure orientations and among the substrates, for both ions (two ways ANOVA,  $\alpha = 0.05$ ). Going deeper, when considering the cellulose nitrate membrane filters (CNW, 0.45  $\mu m$ , and CNA, 0.20  $\mu m$ ), we see that the filters with low porosity tend to collect greater amount of ammonium and potassium: PM deposited on CNA horizontal surfaces is 8 times richer in  $NH_4^+$  and 3 times richer in  $K^+$ , when

the PM deposited on CNA vertical surfaces is 10 times richer in  $\text{NH}_4^+$  and 7 times richer in  $\text{K}^+$  than the corresponding CNW surfaces. When different type of membrane filters having the same porosity ( $0.45 \mu\text{m}$ ) are compared, we notice that RC, the more hydrophobic, collects a greater amount, than CA and CNW, hydrophilic filters. Porosity and hydrophilicity seem to play a role in the deposition of fine particles enriched in ammonium and potassium. In term of absolute amount of  $\text{NH}_4^+$  desposit, we can observe higher amount on vertical surfaces.

- PM deposited on horizontal surfaces is, as expected, richer in calcium and magnesium. Not any difference is relevant among the substrates, when the exposure orientations show significant differences (two ways ANOVA,  $\alpha = 0.05$ ). We can also see on Figure 3.21 (b) that the total amount of this ions is also higher on horizontal surfaces. Calcium is usually found inside coarse particles [36, 37], when magnesium can be present in various fractions. The presence of those elements on horizontal surfaces confirms the fact that coarse particles mainly deposit on horizontal surfaces through gravitational processes.
- Sodium was detected on every horizontal sample, but on vertical samples only on 3 substrates in significant amounts: the CN membrane filters and the aluminum foils. Focusing on CNA and CNW membranes filters, not significant difference is observed, among the samples and between the exposure conditions (two tails t-test,  $\alpha = 0.05$ ). Looking at the other membrane filters, CA and RC, it is clear that PM deposited on horizontal filters is richer in  $\text{Na}^+$  than PM deposited on vertical filters. Aluminum foils finally shows almost the same concentration of  $\text{Na}^+$  on the horizontally deposited as on the vertically deposited particles. We can also notice on Figure 3.21 (b) that the total deposited amount of this ion is also higher on all horizontal surfaces.

The IC analysis allowed to differentiate PM depositions on horizontal and vertical substrates, in term of composition. On vertical samples PM deposited is richer in ions characteristic of the fine fraction, namely nitrates, ammonium and potassium; while ions characteristic of the coarse fraction, as calcium and chloride, were mainly found on the horizontal samples and better hold on them. Sulfate, being part of both fine and coarse fractions, did not show significant difference between its concentration among them. Except for ammonium, potassium and sodium no significant difference was noticed between the different substrates for the analysed ions.

### 3.2.8. Metals analysis

Different metals were investigated after the main campaign of exposure: Cu, Cr, Cd, Pb, Al, Fe and Mn.

Considering the PM composition, cadmium is the less present metal investigated, reaching as a maximum  $0.83 \pm 0.02 \mu\text{g/g}_{\text{PM}}$  for vertical CNW, and iron is the most concentrated metal, reaching  $5.4 \pm 0.6 \text{ mg/g}_{\text{PM}}$  for horizontal CNA. The following general trend is observed (Figure 3.22):

$\text{Fe} \approx \text{Al} \gg \text{Cr} > \text{Mn} > \text{Cu} > \text{Pb} \gg \text{Cd}$  *in term of weight per gram of PM.*

For all metals, except for Al and Fe, the concentrations found were quite low, especially for Cd and Cu, that in some samples were found at the same levels as the blank. Moreover, the variability among the different samples of a same substrate was higher than for main ions, therefore specific different tendencies in metal depositions are difficult to determine.

However, we can observe from Figure 3.22 that the PM deposited on the horizontal membrane filters tends to be richer in Fe and Mn, and the PM deposited on the vertical membrane filters tends to be richer in Cr. The difference between the exposure orientation is not so clear for the other metals, namely Al, Cu, Pb and Cd. To confirm or not these observations from a statistical point of view, ANOVA tests (two ways,  $\alpha = 0.05$ ) were performed among the results and the following conclusions were made:

- for Al, Fe, Pb, Cd, Cr and Cu: no significant difference is observed among the substrates and between the orientation exposure;
- for Mn: no significant difference is observed among the substrates, when a significant difference is observed between vertical and horizontal samples;

Considering the total amount of each metal deposited on the surfaces (Figure 3.22 (b), (d), (f)), in general a higher amount tends to be observed on horizontal substrates, even if statistically significant differences are noticeable only for Mn, which amount is higher on horizontal membrane filters than on the vertical ones.

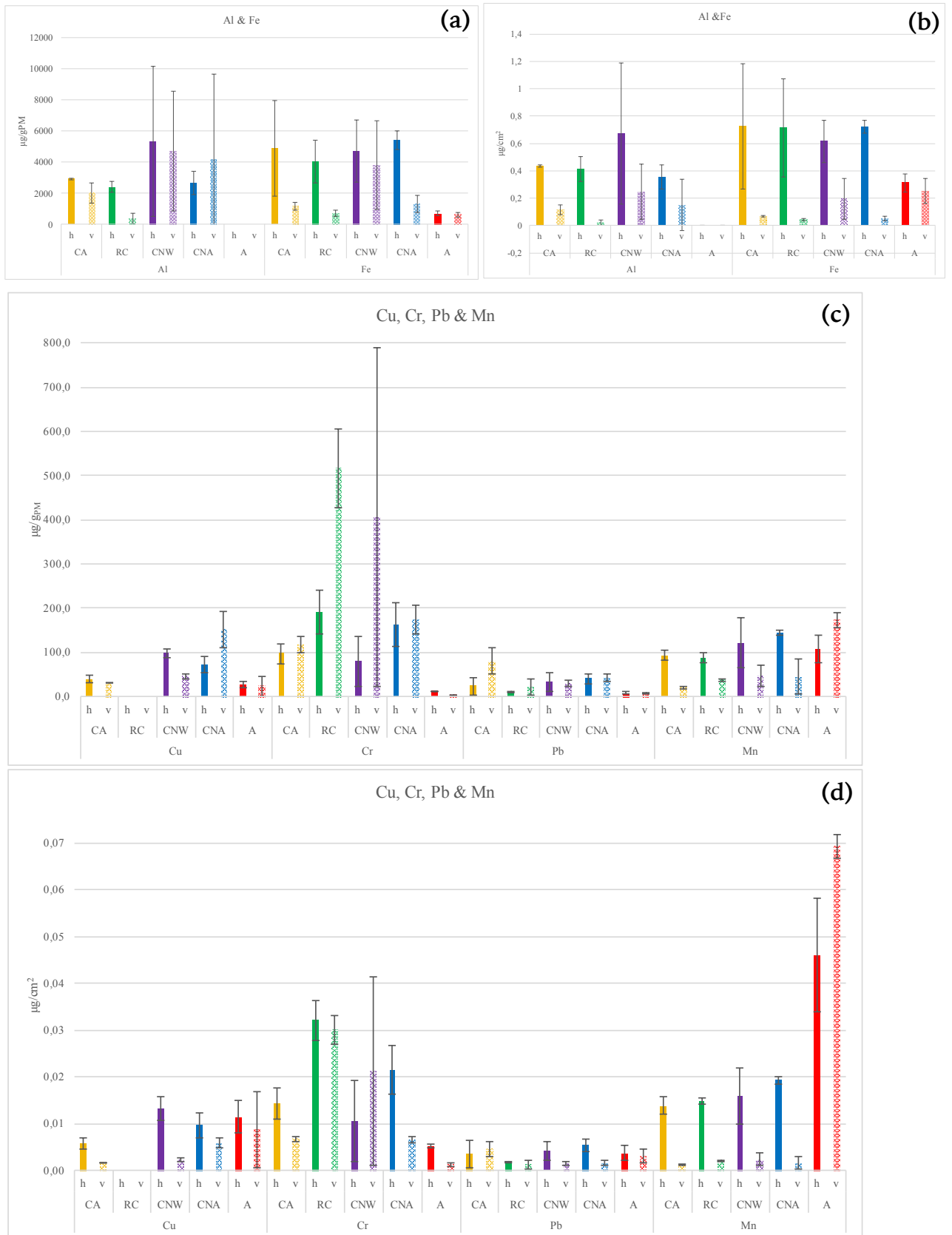


Figure 3.22. Quantity of metal per gram of PM ( $\text{mg}_{\text{ion}}/\text{g}_{\text{PM}}$ ) (a), (c), (e) and quantity of metal deposited per surface unit ( $\mu\text{g}/\text{cm}^2$ ) (b), (d), (f)

follows..

continues...

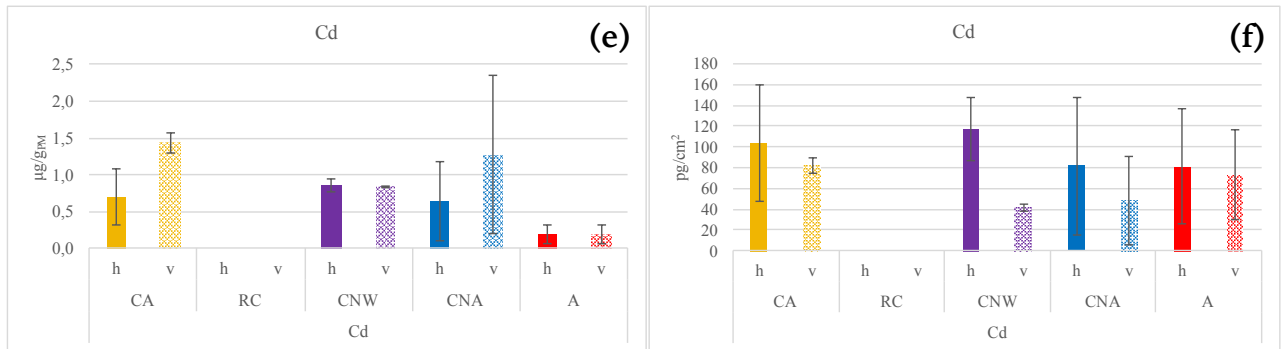


Figure 3.22. Quantity of metal per gram of PM ( $mg_{ion}/g_{PM}$ ) for (a) Al and Fe, (c) Cu, Cr, Pb and Mn, (e) Cd.

Quantity of metal deposited per surface unit ( $\mu g/cm^2$ ) for (b) Al and Fe, (d) Cu, Cr, Pb and Mn (f) Cd. h = horizontal substrates, v = vertical substrates.

- Enrichment factor

From the data obtained for metal analysis, enrichment factor (EF, equation 2) have been calculated, in order to evaluate the crustal or anthropogenic contribution to the deposited metals.

$$EF = \frac{\left(\frac{[Me]}{[Al]}\right)_{sample}}{\left(\frac{[Me]}{[Al]}\right)_{crust}} \quad (\text{equation 2})$$

with  $[Me]$  = concentration of metal, either from the deposited particles on the sample or from the earth upper crust;

$[Al]$  = concentration of aluminum, either from the deposited particles on the sample or from the earth upper crust.

The enrichment factors of the investigated metals were calculated by assuming Al as totally originating from the crust and using, for the upper crust



composition, reference values given by Rudnick and Gao [48]. On the basis of the literature, we may assume that metals with  $EF > 100$  are mainly of anthropogenic origin, while metals with  $EF < 10$  are mainly of crustal origin [49]. They were calculated for each metal, considering all the samples gathered or the horizontal and vertical samples separated, according to the results obtained from the statistical tests performed. The results obtained for the EF are given in Table 3.5.

*Table 3.5. EF calculated for the investigated metals.*

Metal	Cu	Cr	Cd	Pb	Al	Fe	Mn
EF	< 0.01	< 0.003	> 150	< 0.005	1	< 3.5	< 4

We observe that the EF are low, being lower than 4 for each metal, except for Cd that is higher than 100. This suggests that Cd deposited on our samples originate mainly from anthropogenic sources, which is in accordance with previous works focusing on this metal [11, 50]. On the contrary the other metals show a clear natural origin and probably come from soil resuspension.

The metal analysis performed by AAS reveals that Al and Fe were the most concentrated metals in the PM deposited on the samples, reaching about 5 mg/g<sub>PM</sub> when the other metals were present in µg/g<sub>PM</sub> as order of magnitude. All the investigated metals shown a crustal origin except for Cd was mainly from anthropogenic sources. In general really significant differences in metal deposition among different substrates or orientation were not highlighted both in term of PM composition than of absolute metal deposition.

### 3.2.9. TOC results.

Total Organic Carbon (TOC) contained in the PM soluble fraction was obtained by subtracting Total Inorganic Carbon (TIC) value to Total Carbon (TC) value, as presented in section 2.4.4. The amount of PM collected during two months of spring exposure was, in general, not enough for determining TOC in the soluble fraction. Actually for most of the water-extracted samples, the TC and TIC contents were not different from blanks. Only for three samples, two horizontal ( $RC_h$  and  $CNW_h$ ) and one vertical ( $CNW_v$ ) it was possible to detect significant amounts of soluble organic carbon ranging from 40 ( $CNW_h$ ) to 130 ( $RC_h$ ,  $CNW_v$ ) mg/g<sub>PM</sub>, representing from 30 up to 95% of the total soluble carbon. These few results do not allow to outline any specific trends.

## 4. CONCLUSION

This master thesis work is part of a project that aims to better understand the role and contribution of particulate matter in building and heritage materials decay. The specific objective was to collect and analyse PM dry depositions on surrogate materials exposed outdoor with different orientations, by eliminating the variability induced by environmental removal mechanisms. To this aim, four surrogate materials (three types of membrane filters and Al foils), exhibiting different surfaces features, were exposed in the urban-marine site of Rimini for 63 days in horizontal and vertical positions within a Deposition Box device. The collected deposits were investigated through various analytical techniques and the following conclusions can be drawn.

- The Deposition Box has been confirmed to be an efficient field exposure device to isolate the dry deposition processes and to collect homogeneous,

representative and reproducible PM deposits on different materials: for every kind of substrate, a very good reproducibility in term of deposited mass was observed both inter and intra Deposition Boxes.

- Due to PM atmospheric concentrations and composition, a higher exposure time was required in spring than in winter to collect a quantity of PM sufficient for analytical measurements: about two months were found to be the minimum time needed for spring exposure in order to perform analytical characterizations.
- From gravimetric measurements, a clear difference was noticed between the two exposure orientations, with higher deposition rates on horizontal than on vertical substrates, as also evident by visual, colorimetric and SEM analyses. Actually, while no colour changes were perceptible on the vertical substrates, horizontal surfaces appeared darker and more yellow than the corresponding not exposed substrates. This increase in the yellow component can be related to the type of particles that get deposited on the horizontal surfaces, in fact SEM-EDX analyses showed a higher presence of coarse particles rich in crustal elements such as Si, Ca, Al. Other kind of coarse particles with a natural origin were identified by SEM-EDX mainly on horizontal substrates, such as aggregates of NaCl crystals and mixed-cation sulfates from marine aerosols, or big biogenic particles. The presence of anthropogenic particles was also demonstrated by the clear identification of spherical FeO particles. Among metals analysed by AAS, Cd shown a clear anthropogenic origin, as demonstrated by the calculation of the Enrichment Factors.
- Two dimensional fractions were mainly identified on the substrates through SEM images elaborations: fine and coarse particles, presenting specific depositions processes. Fine particles were found either on vertical and horizontal samples, when bigger particles mainly deposited on horizontal surfaces.

- The ionic elements analysed in the PM soluble-fraction enabled to identify which species preferentially deposits according to the surface orientation and, at the same time, to confirm the previous observation from a chemical point of view. Chloride and calcium, with a prevalent natural origin and characteristic of the coarse fraction of PM, were mainly found on horizontal samples and better hold on them; while PM deposited on vertical surfaces was richer in compounds mainly with an anthropogenic origin and characteristic of the fine fraction, such as nitrate, ammonium and potassium. Sulfate, found on both parts of PM, did not show significant difference between its concentration among vertical and horizontal surfaces.
- The differences highlighted above demonstrate that through the Deposition Box it is possible to discriminate the main mechanisms involved in the PM depositions on vertically and horizontally oriented substrate. Brownian diffusion is the deposition mechanisms that more affects fine particles that have a longer residence time in atmosphere than the bigger particles; the small particles are almost not conditioned by the viscosity of the medium, and thus easily cross the laminar layer and impact on the surfaces. This process enable the interaction also with surfaces not horizontally oriented and was the main mechanism involved in the deposition on vertical surfaces. The gravitational effect is particularly efficient for particles having a diameter greater than 2  $\mu\text{m}$  and is observed for bigger and heavy particles, so both Brownian diffusion and gravitational settlings played a role in the deposition on horizontal surfaces.
- Considering the different kind of substrates, they do not exhibit noticeable different behaviours among them, except for Aluminum. Al foils collected a greater quantity of particles than the membrane filters, either considering vertical or horizontal samples. This behaviour can be due to the electrostatic interactions between the metallic surface and the airborne particles. Charged

atmospheric dusts might be attracted by the aluminum surfaces, whatever their orientations, when arriving close to them.

The work realised during this master thesis allowed to discriminate the mechanisms responsible of the dry deposition of atmospheric particles on surfaces with different nature and orientation and to determine which chemical species, and in which amount, tend to preferentially deposit on them. Different soiling effects were then identified, according to the exposure orientation of the surfaces: the effect is more visible on horizontal surfaces, more affected by corrosive species like chlorides, when the vertical surfaces tend to be less aesthetically affected, even if higher concentrations of secondary aggressive species like nitrates were found on them.

This work could be widened by increasing the time of exposure of surrogate surfaces, in order to see if the differences in mass and composition of deposited PM noticed between the orientations exposure can be smoothed or increased over time, and by performing exposure seasonal campaign to characterize deposits representative of different periods of the year. Results here obtained will be fundamental to extend this kind of exposure also to materials actually used for building construction or artworks, in order to perform controlled and reproducible field investigation on their decay due to dry depositions.

## 5. BIBLIOGRAPHY

[1] G. Hanrahan, *Key concepts in environmental chemistry*, « Chapter 6 The Atmosphere and Associated Processes », Academic Press, Oxford, UK, 2012, pp. 181-182.

[2] Marco Casati, PhD Thesis, *Interactions Between Atmospheric Particulate Matter And Stone Surfaces By Means Of Laboratory And In Field Studies*, « Effect of Particulate Matter on Stone Material », Università Degli Studi Di Milano, 2015, pp.5-9.

[3] Sabbioni, C., *Contribution of Atmospheric Deposition to the Formation of Damage Layers*, *Sci. Total Environ.* 1995, **167**, pp. 49–55.

[4] C. Leygraf, I. O. Wallinder, J. Tidblad, T. Graedel, *Atmospheric Corrosion*, 2nd Edition, « Chapter 1. The Many faces of Atmospheric Corrosion », « Chapter 8. Corrosion in Outdoor Exposures », « Chapter 9. Aerosol and Air Quality », John Wiley & Sons, New York, 2016.

[5] Kucera, V., “Chapter 6, Influence of Acid Deposition on Atmospheric Corrosion of Metals: a Review”, in *Materials Degradation Caused by Acid Rain*, edited by R. Baboian, ACS Symposium Series; American Chemical Society, Washington, DC, 1986, pp104-118.

[6] D. Camuffo, *Microclimate for cultural heritage, Conservation, Restauration and Maintenance of Indoor and Outdoor Monuments*, « Chap. 8 Dry deposition of airborne Particulate Matter: Mechanisms and Effects », 2nd Edition, Elsevier Science, USA, 2014, pp.235-292.

[7] P. J. Creighton, P. J. Lioly, F. H. Haynie, T. J. Lemmons, J. L. Miller, J. Gerhart, *Soiling by atmospheric aerosols in an urban industrial area*, *Journal of Waste Management Association* 1990;40(9), pp.1285–9.

[8] F. H. Haynie, *Theoretical model of soiling of surfaces by airborne particles. Aerosols*, Boca Raton: Lewis Publishers, 1986. pp. 951–9.

- [9] C.M. Grossi et al., *Soiling of building stones in urban environment*, Building and Environment, 2003, **38**, pp.147–159.
- [10] « Health Aspects of Air Pollution with Particulate Matter, Ozone and Nitrogen Dioxide », Report on the World Health Organisation (WHO), Bonn, Germany, 2003. Available at: [http://www.euro.who.int/\\_\\_data/assets/pdf\\_file/0005/112199/E79097.pdf](http://www.euro.who.int/__data/assets/pdf_file/0005/112199/E79097.pdf) (Access: 12/04/2017).
- [11] C. Hueglin, R. Gehrig, U. Baltensperger, M. Gysel, C. Monn and H. Vonmont, *Chemical characterisation of PM<sub>2.5</sub>, PM<sub>10</sub> and coarse particles at urban, near-city and rural sites in Switzerland*, Atmospheric Environment **39** (2005) pp. 637–651.
- [12] Pathak, R.K., Louie, P.K.K., Chan, C.K. (2004). *Characteristics of aerosol acidity in Hong Kong*, Atmospheric Environment, 38(19), 2965–2974.
- [13] Perrone, M.G., Larsen, B., Ferrero, L., Sangiorgi, G., De Gennaro, G., Udisti, R., Zangrando, R., Gambaro, A. and Bolzacchini, E., *Sources of High PM<sub>2.5</sub> Concentrations in Milan, Northern Italy: Molecular Marker Data and CMB Modelling*, Sci. Total Environ. 2012, **414** pp.343– 355.
- [14] Yao, X., Fang, M., Chan, C.K., *Size distribution and formation of dicarboxylic acids in atmospheric particles*, Atmospheric Environment, 2002, **36**, pp.2099–2107.
- [15] Tsai, Y. I., Hsieh, L.-Y., Weng, T.-H., Ma, Y.-C., & Kuo, S.-C., *A novel method for determination of low molecular weight dicarboxylic acids in background atmospheric aerosol using ion chromatography*, Analytica Chimica Acta, 2008, **626(1)**, pp.78–88.
- [16] Saiz-Jimenez, C., *Deposition of Airborne Organic Pollutants on Historic Buildings*, Atmos. Environ. Part B, 1993 (**27**), pp.77–85.
- [17] McAlister, J.J., Smith, B.J. and Török, A., *Transition Metals and Water-soluble Ions in Deposits on a Building and Their Potential Catalysis of Stone Decay*, Atmos. Environ., 2008, **42**, pp.7657–7668.

- [18] Maro, D., Connan, O., Flori, J.P., Hébert, D., Mestayer, P., Olive, F. and Solier, L., *Aerosol Dry Deposition in the Urban Environment: Assessment of Deposition Velocity on Building Facades*, *J. Aerosol Sci.*, 2014, **69**, pp.113–131.
- [19] Urosevic, M., Yebra-Rodríguez, A., Sebastián-Pardo, E. and Cardell, C., *Black Soiling of an Architectural Limestone during Two-year Term Exposure to Urban Air in the City of Granada (S Spain)*, *Sci. Total Environ.*, 2012, **414**, pp.564–575.
- [20] Ferm, M., Watt, J., O’Hanlon, S., De Santis, F. and Varotsos, C., *Deposition Measurement of Particulate Matter in Connection with Corrosion Studies*, *Anal. Bioanal. Chem.*, 2006, **384**, pp.1320–1330.
- [21] P. Pesava, R. Aksu, S. Toprak, H. Horvath, S. Seidl, *Dry deposition of particles to building surfaces and soiling*, *The Science of the Total Environment*, 1999, **235**, pp.25-35.
- [22] T. Ihara, B. P. Jelle, T. Gao, A. Gustavsen, *Accelerated aging of treated aluminum for use as a cool colored material for facades*, *Energy and Buildings*, 2016, **112**, pp. 184–197.
- [23] Simona Raffo, « The influence of the environment on the atmospheric corrosion of weathering steel: field and laboratory studies », PhD Thesis in Chemistry, Alma Mater Studiorum - Università di Bologna, 2016.
- [24] Judith C. Chowa, , John G. Watsona, Sylvia A. Edgertonb, Elizabeth Vega, *Chemical composition of PM<sub>2.5</sub> and PM<sub>10</sub> in Mexico City during winter 1997*, *The Science of the Total Environment*, 2002, **287**, pp.177-201.
- [25] Somporn Chantara, *PM<sub>10</sub> and Its Chemical Composition: A Case Study in Chiang Mai, Thailand*, *Air Quality - Monitoring and Modeling*, Dr. Sunil Kumar (Ed.), 2012.
- [26] Jorge Herrera, Susana Rodriguez and Armando P. Baez, *Chemical Composition and Sources of PM<sub>10</sub> Particulate Matter Collected in San José, Costa Rica*, *The Open Atmospheric Science Journal*, 2009, **3**, pp.124-130.



- [27] P. S. Zhao, F. Dong, D. He, X. J. Zhao, X. L. Zhang, W. Z. Zhang, Q. Yao, and H. Y. Liu, *Characteristics of concentrations and chemical compositions for PM<sub>2.5</sub> in the region of Beijing, Tianjin, and Hebei, China*, *Atmos. Chem. Phys.*, 2013, 13, pp. 4631–4644.
- [28] P. R. Hadad, P. E. Jackson, , *Journal of Chromatography Library*, 1990, 46.
- [29] Raffo, I. Vassura, C. Chiavari, C. Martini, M. C. Bignozzi, F. Passarini, E. Bernardi, *Weathering steel as a potential source for metal contamination: Metal dissolution during 3-year of field exposure in a urban coastal site*, *Environmental Pollution*, 2016, 213, pp. 571-584.
- [30] M. B. Sperling, B. Welz, *Atomic Absorption Spectrometry*, Weinheim, Wiley-VCH, 1999, 3rd éd.
- [31] Image originating from Shimadzu Company website. [Online]. Available at: <http://www.shimadzu.com/an/toc/lab/toc-l4.html> (Access 08/08/2017).
- [32] Picture originating from ‘Scanning electron microscopy. Working principle.’ [Online]. Available at: <http://www.utu.fi/fi/yksikot/sci/yksikot/fysiikka/laboratoriot/materiaali/materiaalitieede/tutkimusmenetelmat/sem/Sivut/home.aspx> (Acces 15/05/2017).
- [33] Picture originating from ‘Various modes of electron emissions from incident x-rays or electrons.’ [Online]. Available at: <https://sites.ualberta.ca/~ccwj/teaching/microscopy/> (Acces 15/05/2017).
- [34] Picture originating from ‘Scanning Electron Microscope.’ [Online]. Available at : <https://www.purdue.edu/ehps/rem/rs/sem.htm> (Access 15/05/2017).
- [35] C. Chiavari, A. Balbo, E. Bernardi, C. Martini, M. C. Bignozzi, M. Abbottoni, and C. Monticelli, *Protective silane treatment for patinated bronze exposed to simulated natural environments*, *Mater. Chem. Phys.*, 2013, vol. 141, no. 1, pp. 502–511.

- [36] Nava, S., Becherini, F., Bernardi, A., Bonazza, A., Chiari, M., García-Orellana, I. and Vecchi, R., *An Integrated Approach to Assess Air Pollution Threats to Cultural Heritage in a Semi-confined Environment: The Case Study of Michelozzo's Courtyard in Florence (Italy)*, *Sci. Total Environ.*, 2010, **408**, pp.1403–1413.
- [37] G.M. Marcazzan, G. Valli & R. Vecchi, *Composition of coarse and fine fractions of particulate matter at an urban and a conurban site in Northern Italy*, *Transactions on Ecology and the Environment*, WIT Press, 2001, vol 47, pp.243-252.
- [38] X. Wang, T. Sato, B. Xing, *Size distribution and anthropogenic sources apportionment of airborne trace metals in Kanazawa, Japan*, *Chemosphere* 65 (2006), pp.2440–2448.
- [39] M.V. Diamanti, S. Aliverti, M.P. Pedferri, *Decoupling the dual source of colour alteration of architectural titanium: Soiling or oxidation?*, *Corrosion Science* 72 (2013), pp.125–132.
- [40] W. Anaf, L. Bencs, R. Van Grieken, K. Janssens, K. De Wael, *Indoor particulate matter in four Belgian heritage sites: Case studies on the deposition of dark-colored and hygroscopic particles*, *Science of the Total Environment* 506–507 (2015) pp.361–368.
- [41] P. López-García, M.D. Gelado-Caballero, D. Santana-Castellano, M. Suárez de Tangil, C. Collado-Sánchez, J.J. Hernández-Brito, *A three-year time-series of dust deposition flux measurements in Gran Canaria, Spain: A comparison of wet and dry surface deposition samplers*, *Atmospheric Environment*, 2013, **79**, pp.689-694.
- [42] Shannigrahi, A.S., Fukushima, T., Ozaki, N., *Comparison of different methods for measuring dry deposition fluxes of particulate matter and polycyclic aromatic hydrocarbons (PAHs) in the ambient air*, *Atmospheric Environment* **39** (4), 2005, pp.653-662.
- [43] Huang, J., Liu, Y., Holsen, T.M., *Comparison between knife-edge and frisbee-shaped surrogate surfaces for making dry deposition measurements: wind tunnel experiments and computational fluid dynamics (CFD) modeling*, *Atmospheric Environment* **45** (25), 2011, pp.4213-4219.

[44] Mészáros A. and Vissy K., *Concentration, size Distribution And Chemical Nature of Atmospheric Aerosol Particles In remote Oceanic Areas*, Aerosol Science, 1974, Vol. 5. pp.101-109.

[45] Pósfai M., Anderson J.R., Buseck P.R., Shattuck T.W., and Tindale N.W., *Constituents of a Remote Pacific Marine Aerosol: a TEM Study*, Atmospheric Environment Vol. 28. No 10, 1994, pp. 1747-1756.

[46] Pósfai M., Anderson J.R., Buseck P.R., and Sievering H., *Compositional variations of sea-salt-mode aerosol particles from the North Atlantic*, Journal of Geophysical Research, Vol. 100, 1995, pp.23063-23074.

[47] Willis R.D., Blanchard F.T., and Conner T.L., « Chapter 5: Examples of Research Applications », *Guidelines for the Application of SEM/EDX Analytical Techniques to Particulate Matter Samples*, National Service Center for Environmental Publications (NSCEP), Exposure Research Laboratory, September 2002, pp. 45-53

[48] Rudnick, R.L., Gao, S., 2003. « Composition of the Continental crust ». In: Rudnick, R.L. (Ed.), *The Crust*, vol. 3, pp.1-64 of *Treatise on Geochemistry*, Holland, H.D.,Turekian, K.K., (Eds.). Elsevier-Pergamon, Oxford.

[49] E. Padoan, M. Malandrino, A. Giacomino, M.M. Grosa, F. Lollobrigida, S. Martini and O. Abollino, *Spatial distribution and potential sources of trace elements in PM<sub>10</sub> monitored in urban and rural sites of Piedmont Region*, Chemosphere 145 (2016), pp.495-507.

[50] B.J. Alloway and E. Steinnes, « Chapter 5. Anthropogenic addition of cadmium to soils », from M.J. McLaughlin and B.R. Singh, *Cadmium in soils and plants*, Kluwer Academic Publishers, 1999.

## APPENDICES

### APPENDIX A. Atmospheric data.

Atmospheric data recorded by ARPAE Emilia Romagna, at their monitoring sites depending on data (Rimini Urbana, Rimini Ausa & Rimini Marrecchia).

*Table A. Atmospheric data recorded during the exposure campaign.*

*T = Temperature; RH = Relative Humidity; PE = Precipitation Event; PM = Particulate Matter; TOW = Time of wetness.*

Date	T (°C)			RH (%)			Number of PE	PM (µg/m <sup>3</sup> )		TOW (hours/day)
	mean	min	max	mean	min	max		2.5	10	
10/04/2017	15,7	13,5	17,2	74,8	72,0	79,0	0	13	19	0
11/04/2017	16,3	11,6	19,2	60,1	45,0	84,0	0	15	21	1
12/04/2017	15,1	12,1	16,6	72,3	62,0	84,0	0	8	16	4
13/04/2017	16,6	12,1	20,7	62,0	46,0	80,0	0	14	23	0
14/04/2017	16,7	13,2	18,9	59,9	46,0	70,0	0	13	25	0
15/04/2017	16,5	14,4	19,2	71,4	53,0	87,0	2	11	19	6
16/04/2017	15,7	12,8	18,5	75,8	50,0	92,0	2	11	18	10
17/04/2017	13,5	11,8	14,9	65,4	53,0	86,0	1	2	9	2
18/04/2017	10,1	6,4	16,4	72,8	48,0	84,0	1	4	12	5
19/04/2017	9,6	4,6	13,9	50,2	22,0	84,0	1	4	12	5
20/04/2017	9,5	4,9	12,5	47,2	31,0	75,0	0	12	18	0
21/04/2017	9,4	5,6	12,0	44,3	30,0	67,0	0	13	19	0
22/04/2017	11,9	4,0	16,2	50,7	21,0	69,0	0	13	24	0
23/04/2017	13,8	10,1	15,9	66,1	56,0	79,0	0	10	22	0
24/04/2017	14,3	10,0	17,1	69,7	54,0	83,0	0	9	18	3
25/04/2017	17,2	11,1	21,5	51,4	36,0	73,0	0	8	13	0
26/04/2017	17,8	14,5	20,7	52,1	37,0	71,0	0	11	21	0
27/04/2017	18,5	14,7	20,4	64,3	53,0	84,0	4	6	24	3
28/04/2017	15,4	11,5	19,3	48,5	24,0	89,0	1	3	11	4
29/04/2017	11,8	8,8	14,8	61,5	46,0	89,0	1	4	13	1
30/04/2017	12,1	6,6	16,1	57,2	33,0	78,0	0	3	14	0
01/05/2017	14,3	7,8	20,7	54,2	34,0	72,0	0	11	22	0

Date	T (°C)			RH (%)			Number of PE	PM (µg/m³)		TOW (hours/year)
	mean	min	max	mean	min	max		2.5	10	
02/05/2017	13,0	8,4	15,6	70,7	60,0	81,0	0	7	15	1
03/05/2017	14,7	10,6	17,5	68,7	51,0	81,0	0	7	12	1
04/05/2017	14,5	12,3	16,8	76,3	62,0	89,0	2	6	12	6
05/05/2017	14,7	11,5	17,3	74,8	65,0	88,0	0	8	15	7
06/05/2017	14,9	11,6	17,1	82,9	72,0	91,0	4	7	17	16
07/05/2017	15,0	12,0	17,8	77,5	57,0	92,0	2	0	4	12
08/05/2017	16,6	11,8	20,0	66,3	47,0	82,0	1	5	8	3
09/05/2017	13,8	10,6	15,8	82,1	66,0	94,0	1	2	7	13
10/05/2017	14,5	9,2	17,3	77,6	66,0	89,0	1	4	14	12
11/05/2017	16,7	13,2	18,5	80,9	74,0	88,0	0	12	24	13
12/05/2017	19,6	16,1	22,7	66,4	48,0	88,0	0	11	26	5
13/05/2017	20,5	17,6	24,3	52,8	34,0	64,0	0	9	13	0
14/05/2017	20,3	16,5	22,7	54,1	46,0	64,0	0	11	16	0
15/05/2017	19,3	16,9	21,6	64,6	54,0	77,0	0	12	19	0
16/05/2017	19,8	16,0	23,4	58,1	35,0	82,0	0	11	18	1
17/05/2017	20,3	15,9	23,7	50,5	36,0	65,0	0	7	16	0
18/05/2017	19,3	14,5	21,7	67,1	53,0	79,0	0	9	14	0
19/05/2017	22,7	16,7	27,6	49,4	26,0	77,0	0	8	15	0
20/05/2017	17,6	14,6	19,1	68,9	53,0	86,0	3	6	12	3
21/05/2017	18,4	14,4	22,1	59,8	36,0	87,0	1	4	8	5
22/05/2017	20,2	14,6	24,0	54,5	40,0	71,0	0	9	16	0
23/05/2017	22,1	16,1	25,9	54,0	35,0	76,0	0	11	20	0
24/05/2017	22,3	19,0	25,2	62,6	47,0	74,0	0	13	18	0
25/05/2017	19,4	15,1	21,4	61,5	35,0	87,0	1	3	15	3
26/05/2017	18,8	13,4	22,6	50,3	29,0	68,0	0	4	14	0
27/05/2017	20,4	14,6	24,6	49,5	35,0	64,0	0	7	20	0
28/05/2017	21,4	16,0	25,1	53,8	42,0	66,0	0	8	16	0
29/05/2017	21,4	15,4	24,7	56,6	44,0	70,0	0	no data	12	0
30/05/2017	23,0	18,1	25,4	58,5	47,0	71,0	0	15	20	0

Date	T (°C)			RH (%)			Number of PE	PM (µg/m <sup>3</sup> )		TOW (hours/year)
	mean	min	max	mean	min	max		2.5	10	
31/05/2017	24,6	20,0	27,3	48,0	36,0	66,0	0	13	20	0
01/06/2017	23,6	19,7	26,6	49,4	30,0	70,0	0	10	17	0
02/06/2017	23,7	20,2	26,9	42,8	28,0	57,0	0	10	17	0
03/06/2017	24,2	19,1	27,1	45,8	37,0	58,0	0	10	18	0
04/06/2017	23,9	19,6	28,1	54,0	36,0	69,0	0	8	20	0
05/06/2017	23,3	20,2	25,7	64,0	49,0	76,0	0	7	19	0
06/06/2017	24,2	20,5	28,1	50,7	32,0	73,0	0	8	16	0
07/06/2017	23,2	18,6	26,2	44,9	25,0	74,0	0	8	20	0
08/06/2017	20,4	16,2	22,0	47,0	34,0	69,0	0	3	16	0
09/06/2017	20,4	14,3	23,8	45,2	26,0	62,0	0	7	15	0
10/06/2017	22,2	18,0	25,6	49,5	27,0	62,0	0	11	23	0
11/06/2017	22,7	17,8	25,7	53,5	40,0	66,0	0	8	17	0
12/06/2017	22,5	18,0	26,9	47,5	34,0	58,0	0	10	18	0

APPENDIX B. Weight % of identified elements in SEM-EDX analysis.

Here are gathered the weight percentages of identified elements from the spectra 1, 2 and 3 recorded on the CA horizontal sample analysed by SEM-EDX (section 3.2.5, Figure 3.17).

*Table B. Identified elements and their weight %.*

Spectrum	Elements										
		O K	Na K	Mg K	Al K	Si K	S K	Cl K	K K	Ca K	Fe K
1	weight %	66.15	4.45	/	/	1.74	11.19	4.29	1.25	9.84	0.16
	weight % $\sigma$	0.36	0.17	/	/	0.11	0.17	0.11	0.08	0.91	0.11
2	weight %	60.06	3.69	3.68	1.04	6.09	4.75	10.36	1.01	8.33	0.98
	weight % $\sigma$	0.34	0.13	0.11	0.07	0.11	0.1	0.14	0.06	0.13	0.1
3	weight %	41.29	23.16	1.92	/	0.26	1.59	28.42	0.59	2.76	/
	weight % $\sigma$	0.36	0.21	0.09	/	0.05	0.06	0.22	0.05	0.07	/

APPENDIX C. Relative amounts of considered ions for analysed substrates during the main campaign.

In this appendix are given the percentage distribution of the analysed anions calculated on the basis of the ion concentration per gram of PM ( $\text{mg}/\text{g}_{\text{PM}}$ ).



*Figure C. Percentage distribution of the analysed anions calculated on the basis of the ion concentration per gram of PM ( $\text{mg}/\text{g}_{\text{PM}}$ ) for the samples (a) exposed in horizontal position (b) exposed in vertical position.*

*follows...*



... continues

(b)

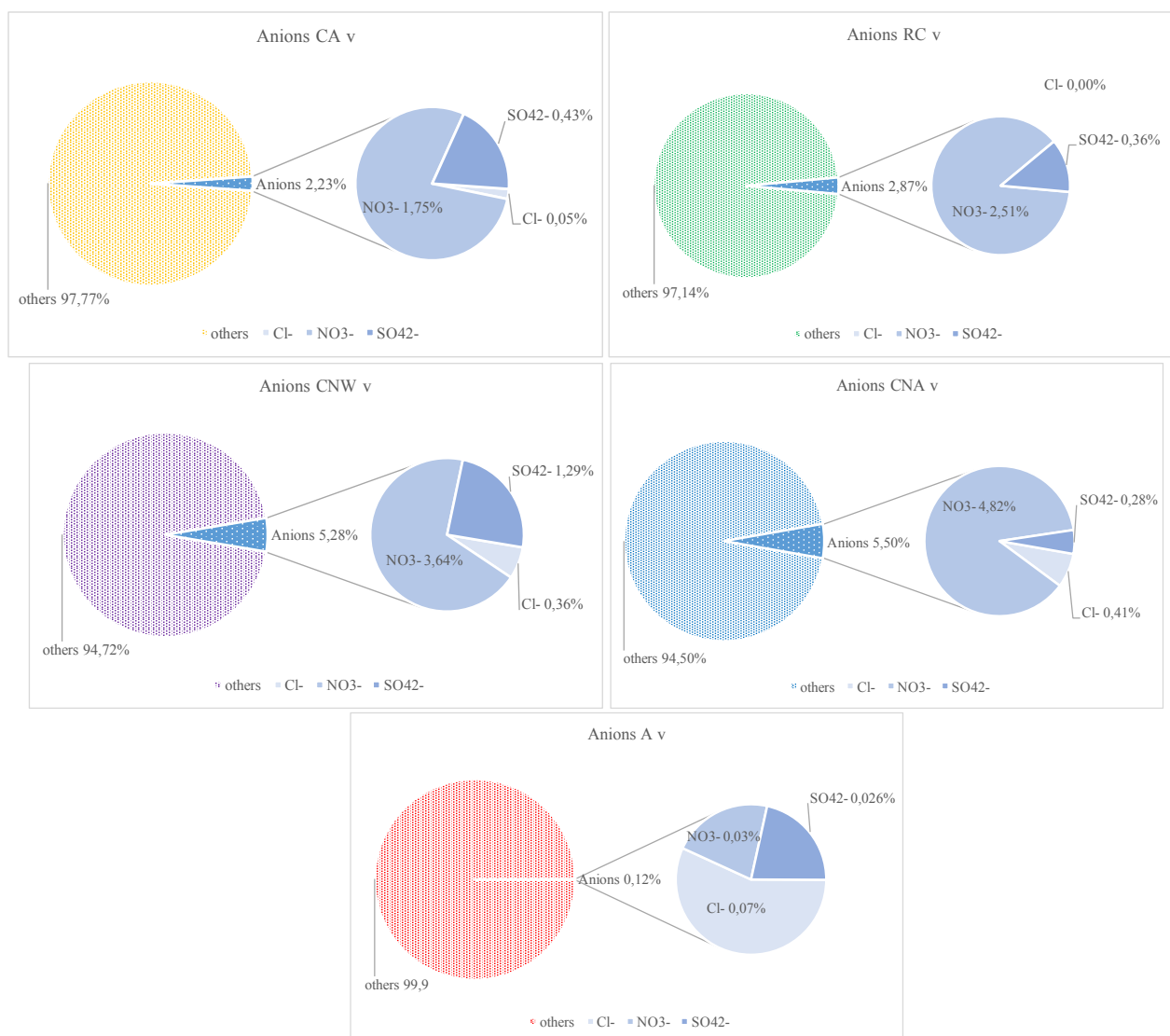


Figure C. Percentage distribution of the analysed anions calculated on the basis of the ion concentration per gram of PM ( $\text{mg}/\text{g}_{\text{PM}}$ ) for the samples (a) exposed in horizontal position (b) exposed in vertical position.